1974

The variation of the Neel temperature as a function of solute concentration for several antiferromagnetic alloys of alpha-manganese

Willie Williams Jr.
Iowa State University

The variation of the Neel temperature as a function of solute concentration for several antiferromagnetic alloys of alpha-manganese

by

Willie Williams, Jr.

A Dissertation Submitted to the
Graduate Faculty in Partial Fulfillment of
The Requirements for the Degree of
DOCTOR OF PHILOSOPHY

Department: Professional Studies
Major: Education (Higher Education)

Approved:

Signature was redacted for privacy.

In Charge of Major Work

Signature was redacted for privacy.

For the Major Department

Signature was redacted for privacy.

For the Graduate College

Iowa State University
Ames, Iowa
1974

TABLE OF CONTENTS

INTRODUCTION

Alpha-Mn is in many respects one of the most unique of all the transition metals. Of particular interest is the antiferromagnetic transition that occurs at 95 K. With the exception of Cr, Alpha-Mn is the only transitional metal that orders in this fashion.

Extensive work has been done on the Cr system, making particular use of neutron diffraction and electrical resistivity measurements. These approaches have provided results that give a fairly good understanding of the antiferromagnetic nature in this system.

This study, prompted in part by the Cr studies, was undertaken to provide some quantitative results on the antiferromagnetic transition in Mn. The Neel temperature should be a measure of the strength of the ordering interaction, though not necessarily in any simple way. Thus, the variation of the Neel temperature as a function of the shifted Fermi level should provide some useful insights. By alloying small percentages of impurity elements into alpha-Mn, the Fermi level can be shifted. By assuming that the rigid band approximation holds, which is a reasonable assumption for small percentages of impurity in a host metal, one may treat the alloys as having energy bands and a density of states curve very similar to pure alpha-Mn.

Like Cr, alpha-Mn shows anomalous behavior in its electrical resistivity at the onset of antiferromagnetic ordering. The resistivity exhibits a minimum at the Neel temperature. This anomalous behavior provides a superior method for determining the Neel temperature, since other transport properties do not show as sharp a transition and because the measurement itself is not as sophisticated as some other transport measurements.

Earlier work by Bellau and Coles (1) and Williams and Stanford (2) has shown that a systematic trend might be present in the alloys of the Mn system. They observed an increase in the Neel temperature for impurity elements to the right of Mn and a decrease for those to the left. It then becomes desirable to do an extensive study of many alloy systems of alpha-Mn to verify this apparent trend. Thus this work undertakes the study of some half-dozen additional Mn-alloy systems, with the hope of providing further insight into the antiferromagnetic transition.

BACKGROUND

To fully understand and make qualitative remarks about the behavior of a metal like Mn, one needs detailed results on quantities like the density of states, N(E) and the Fermi surface from both a theoretical and experimental point of view. Presently, there is very little detailed work of this nature. At best there are only bits and pieces of information on various properties. Of course, this lack of information is due in part to the complicated crystal structure of Mn and the difficulty of growing large single crystals of Mn (3-6).

Mn crystallizes in four different crystal structures. The four crystallogical phases of Mn are summarized in Table I (7,8). Earlier work by Bradley and Thewlis (9) established the existence of four inequivalent atom sites in the crystal. The basis of the whole arrangement is a simple body-centered cubic lattice, with each lattice point being associated with a cluster of 29 atoms. Figure 1 shows one such cluster of atoms around the central atom of the unit cell.

Around each type 1 atom (site I) is an octahedron of type 4 atoms (site IV). The opposite sides of the octahedron are of a different size so that the symmetry is tetrahedral. The four type 2 atoms (site II) are somewhat further from the center of the group and are arranged tetrahedrally about the

Table I. Summary of the four phases of Mn.

Phase	Atom per Cell	A° 300 K	Atomic Volume 300 K	Magnetic Structure	Phase Range
α(cubic)	58	8.894	12.09	AFM	0-100 K
β(cubic)	20	6.300	12.50	PAR	1000-1369 K
γ(fcc) *	4	3.715	12.80	AFM	1364-1410 K
δ(bcc)	2	2.978	13.15	AFM	1410-1450 K

*Tetragonal at room temperature c/a = 0.950.

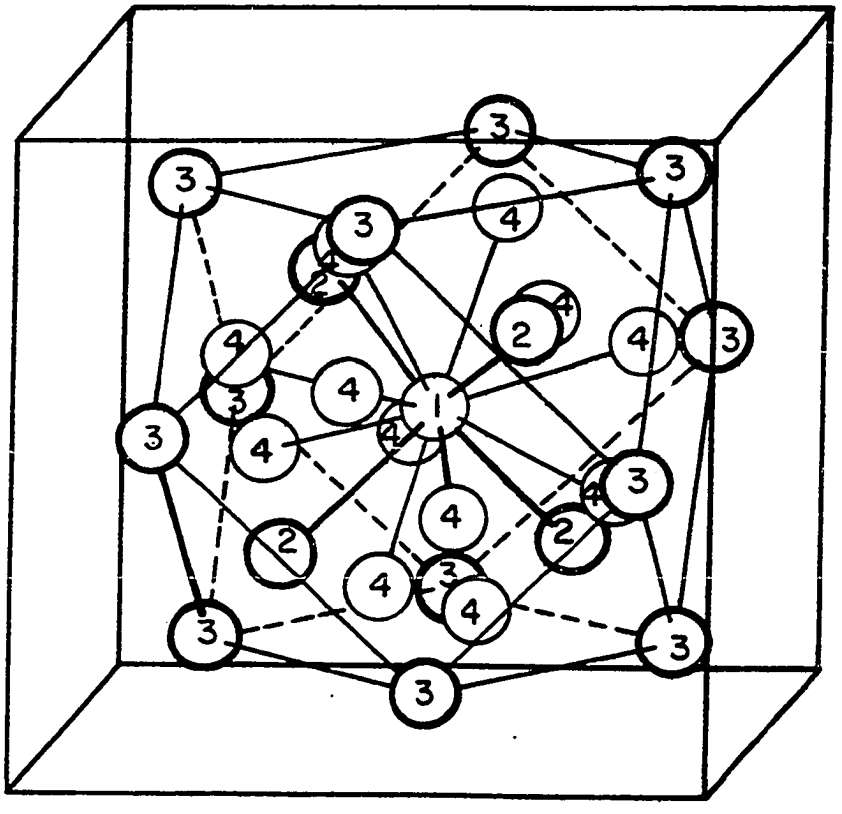

Figure 1. One half of the unit cell of alpha-manganese. The nearest neighbors of type 1 atoms are shown. This group of 29 atoms is repeated at each corner and body-centered position in the cubic lattice

center. The twelve outer-most type 3 atoms (site III) comprise a polyhedron having cubic and octahedral faces. The whole cluster has symmetry which is tetrahedral, as is that of the crystal as a whole. The relative position of atoms is summarized in Table II (9,10,11).

Thus, the complex nature of the crystal structure makes the application of many of the techniques that are applicable to less complex structures unusable in the case of α-Mn. Much more extensive work has been done on the simpler phases, β and γ. In fact, a preliminary calculation has been done for the Fermi surface of γ-Mn (12). Weiss and Tauer (8) have pointed out that the complex structure (α) at lower temperatures results as an avoidance of having one electron in a doubly degenerate d-orbital. The gain in intra-atomic exchange energy by having two electrons in the doubly degenerate orbitals more than compensates for the distortional energy that is invclved in going from a simple structure to a ccmplex one. Table III summarizes various other properties of the four phases of Mn.

Thus Mn, like other elements of the first transitional period, will be expected to have an incompletely filled 3-d shell (and probably very complex in the case of Mn) which has a high density of states and a low mobility. This should

Table II. The crystallographic parameters of Mn.

Site	# of atoms	coordinate
I	2	0 0 0, 1/2 1/2 1/2
II	8	aaa, etc. 1/2+a 1/2+a 1/2+a, etc.
II	24	bbc, etc. 1/2+b 1/2+b 1/2+c, etc.
IV	24	dde, etc. 1/2+d, 1/2+d 1/2+e, etc.

	Bradley and Thewlis Ref. 9	Gazzara et al. Ref. 11	Kunitomi et al. Ref. 10
a	0.31	0.316	0.317
b	0.35	0.356	0.356
c	0.04	0.034	0.034
d	0.08	0.089	0.089
e	0.27	0.282	0.282

be demonstrated by a large electronic specific heat, high electrical resistivity and a strong paramagnetic susceptibility.

Table III. Several physical properties of the four phases.

Phase	Θ K	γ X10⁴	S_{mag}	T_N K	H_{mag}	$(H_0 - H_0^{\alpha})$ cal/mole
α	460	25.3	1.071	95	105	-
β	422	22.5	1.38	0	0	724.5
γ	355	11.2	2.35	580*	1210	1137.8
δ	370	22.5	1.38	627	990	863.5

*640 K for fct.

Note Θ, γ, S_{mag}, T_N, H_{mag}, $(H_0 - H_0^{\alpha})$, represents the Debye temperature, electron specific heat coefficient, total magnetic entropy, magnetic critical temperature, total magnetic enthalpy, and the total energy difference at absolute zero relative to α-Mn respectively.

Magnetic Properties

Owing to the uniqueness of the physical make up of Mn, it might be expected that the associated magnetization would

have a certain uniqueness about it. Since in 3-d transitional metals and alloys much of the magnetization is carried by quasi-free electrons or itinerant electrons, the crystal structure will determine in a large part the nature of the magnetization. That is to say, the crystal symmetry, inter-atomic distance, etc., will be important in determining the nature of the magnetization.

The occurrence of AFM ordering in Mn was first reported by Shull and Wilkinson (4) from neutron diffraction work on a powdered sample. They observed paramagnetic scattering at temperatures well above the Neel temperature (95 K). The temperature dependence of the intensity suggested the possibility of short range ordering with a paramagnetic moment of $0.5\mu_B$ per atom at 450 K. A later analyses by Kasper and Roberts (5) showed that the atoms in inequivalent sites carried different moments. They proposed two collinear models for the assignment of moments to the respective sites. Their assignment along with two others are reported in Table IV. Oberteuffer et al. (13) report an increasing moment associated with sites I, II, and III as the temperature is decreased below the Neel temperature. Rather extensive theoretical and experimental work by Yamada et al. (14,15) has recently shown that a non-collinear model is more appropriate for assigning the moments to respective sites. The larger moments are associated with the sites which have the largest

atomic volume.

Sato and Arrott (]6), have suggested a nearly free electron approach to the magnetization in Mn. They propose a Jones zone surrounded by planes having $h^2+k^2+l^2 = 54$ and attribute the onset of magnetization to the additional energy gaps which are introduced in the Fermi surface. A spin density wave is chosen in the (641) direction and allowed to span the Fermi surface. This wave was suggested by Arrott and Coles to be incommensurate with the lattice (6). However, recent research has shown that the magnetization has a q = (1,0,0) (14,17) rather than deviating in a (641) direction. Also, only one wave vector was detected. This does not rule out the possibility of spin wave, however.

There is no observed change in the magnetic or crystal structure as the temperature is lowered from 60 K to 4.2 K, although there is an increase in the thermal expansion and atomic volume (18,19) in the ordered region. Finkel (18) has alluded that this increase in the atomic volume is attributed to an appreciable contribution of the spin waves to the thermal expansion. The anomaly in the linear expansion, $\alpha(T)$ at the Neel temperature is of the negative λ type suggesting a second order phase transition. From the change in $\alpha(T)$ Finkel determined, $dT_N/dp = -1.64$ deg/k bar. There is a marked change in the expansion coefficient at the T_N. The change in the lattice constant below the Neel temperature is

Table IV. The magnetic moment at each site.

Site	Moments*			
	Collinear Model			Non-collinear Model
	A	B	Ref. 13	Ref. 14
I	1.54	2.50	1.71	1.9
II	1.54	2.50	1.46	1.7
II	3.08	1.70	1.11	0.6
IV	0.0	0.0	0.02	0.2

* Moments are in units of Bohr Magneton.

represented by equation 1 (19),

$$\Delta a/a = -(1.61 \pm .0911) \times 10^{-6} T^2 \qquad (i)$$

It is interesting that such a simple form would represent the expansion coefficient, since the net result is the difference between a positive lattice contribution and a negative mag-

netic contribution.

The actual occurrence and magnitude of the magnetic moment on the various sites have been suggested to depend on the number of surrounding atoms, the coordination number and the inter-atomic distances (20-22,5). It would seem that the greater the number of surrounding neighbor atoms, the more the localization of the moments is suppressed. Kasper and Roberts (5) have pointed out that for very small separations of Mn atoms (≤ 2.37 A°) there is a tendency for spin coupling. Both Kasper and Roberts and Yamada et al. (14) suggest that the coupling coefficient J, for near-neighbor distances is positive. This would suggest AFM coupling between adjacent atoms. For immediate ranges of distances (2.49 to 2.82 A°) the coupling is anti-parallel and for long distances (≥ 2.82 A°) parallel coupling occurs.

Several NMR studies (22-27) has been conducted on α-Mn and its alloys. These studies have shown a negative Knight shift K, for α-Mn. The nuclear spin-spin relaxation time T_2 shows a discontinuity at the Neel temperature. Now the degree of order in the electrons spin system is reflected by the amplitudes of the fluctuating local field produced at the nuclear sites. The fluctuation in the electronic system near T_N is reflected in the nuclear magnetic relaxation time, T_2. Thus, T_2 gives an indication of the order of the spin system. Above T_N, T_2 is proportional to $(T_N-T)^{1/3}$ and below T_N it is

proportional to $(T_N-T)^{2/3}$. Very similar behavior of T_2 is observed for several Mn-alloys. The experimental values of T_1, the spin-lattice relaxation time and T_2 are 30±5 msec. and 270±10 sec. respectively. T_1 is a measure of the rate of exchange of energy between the spin system and the rest of lattice. T_1 is determined by the interaction of conduction electrons and nuclear spins.

The internal fields at the Mn sites have been reported to have values as low as 10 kOe (23) and as high as 90 kOe (28,29) for each site. A more recent study has in part, reconciled these studies by reporting different internal fields for each of the sites. Masuda and Taki (26) report internal fields of 261 kOe, 196 kOe, 9 kOe and 1 kOe for sites I, II, III and IV respectively. These values are in good agreement with values reported from a Mossbauer study (30) on several Mn-Fe alloys. They also reported small internal fields associated with sites III and IV.

A much more recent NMR study by Kohara and Asayama (22,31) has identified NMR signals of 200, 151, 31, and 5 MHz for sites I, II, III and IV respectively. From the observation of these frequencies, they have been able to trace the positioning of impurities in the Mn structure. They determined that impurities to the right of Mn enter sites III and IV resulting in an increase in the magnetic moment on site I, while impurity elements to the left of Mn enter sites I and

II causing a reduction in the moments on these sites. These findings are in agreement with the above Mossbauer study and the work of Kasper (32) on a series of Mn-Fe alloys.

Several measurements of the susceptibility (16,33) have shown no ancmalous effect in the susceptibility at the Neel temperature. There is a wide flat maximum in the region of 125 K to 145 K. The positive maximum in $d\chi/dt$ nearly corresponds to the Neel temperature. The lack of an anomalous behavior in the susceptibility probably reflects that the susceptibility is little affected by the ordering at the T_N. Similar effects are observed in Mn-alloys. One interesting result (34,35) from measurements of the susceptibility of Mn alloys is the consistency of impurity elements to the right of Mn (Fe and Co) to have susceptibilities lower than pure-Mn, while those to the left (V,Cr) show higher values. The density of states at the Fermi level in Mn is one of the highest among metals. Also, it may have a rather rapidly varying density of states at the Fermi level (35,36). Thus based on the above observations, the density states of Mn, may look something like that shown in Figure 2. This is not unreasonable in light of the fact that to the lowest approximation the density states is proportional to the susceptibility as can be seen from equation 2 (37).

$$\chi = 2\mu^2 N(E)[1+\pi^2/6k^2T^2\{(1/N)d^2N/dE^2-((1/N)dN/dE)^2\}] \quad (2)$$

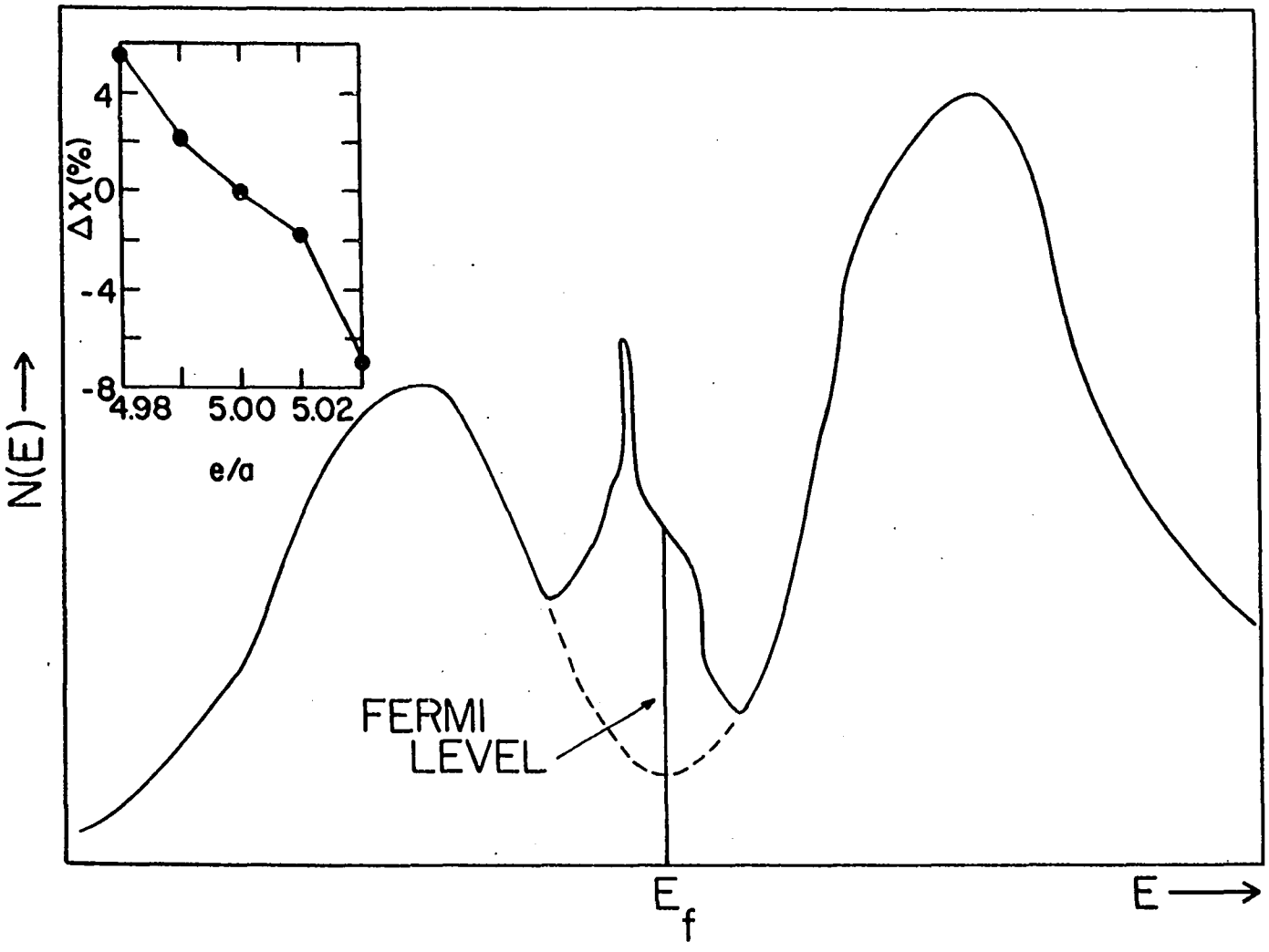

Figure 2. A hypothetical density of states curve for alpha-manganese

Thus, as the Fermi level is increased, the density states may drop.

The actual nature of the magnetization in Mn is not obviously localized or itinerant in nature. In some respects, it appears to be localized (moment above the Neel temperature), and in other respects itinerant (negative expansion coefficient and sensitivity to the number of d-electrons). Probably the actual situation is a combination of localized magnetic moments on the atoms and itinerant magnetism introduced by cooperative mechanism below T_N.

Transport Properties

Because the magnetic properties have a profound effect on some of the transport properties, the transport properties have been used to infer information about the magnetic properties. Such measurements as the Hall coefficient, electrical and magnetoresistance and specific heat measurements have provided some information on the nature of the magnetic ordering in Mn.

Specific heat measurements have been conducted by a number of researchers (38-42). A peak is observed in the specific heat at the Neel temperature. Tauer and Weiss (41) report the electron specific heat coefficient, γ to be 28×10^{-8} cal/mole/deg. This would suggest that Mn has a high density of states at the Fermi surface. Tauer and Weiss separated

the magnetic part of the specific heat and found that it increased with decreasing temperature. At T_N, there is a peak in the magnetic specific heat and it decreases to 0 with decreasing temperature. They deduced a Debye temperature, Θ_D of 460 K. This compares well with Θ_D= 485 K deduced from elastic module measurements (43).

The Hall coefficient has been determined by Meaden and Pelloux-Gervais (33). The coefficient is reported to decrease with decreasing temperature and become negative at 230 K and remain so until 8 K is reached. There is no observed anomaly at the Neel temperature. However, there is a minimum in the 40 to 45 K region. Based on a one band model they reported 0.9 positive carriers per atom at room temperature and 0.9 negative carriers at 192 K. In order to explain the positive Hall coefficient, a two band model was suggested with a nearly full 4-s band overlapping a nearly empty 3-d band. They further showed that if the Fermi level occurs near the top of the 4-s band, conduction would be by highly mobil 4-s band holes.

The thermoelectric power has been measured by Griffiths and Coles (44). They report a negative value above the Neel temperature, that becomes positive surprisingly close to T_N. They account for the change in sign by the introduction of new Brillouin zone planes of magnetic orgin below T_N. A mark peak occurs in the thermoelectric power for pure Mn at lower

temperatures. This has been observed in the rare earth metals. Also, several Mn-Cr and Mn-Fe alloys were considered in this study. These alloys showed very similar behavior to that of pure Mn. The same authors also reported measurements of the magnetoresistance. Mn shows a very steeply increasing magnetoresistance below T_N. It changes by 4 orders of magnitudes between 100 K and 2 K. This behavior is attributed to the Brillouin effect mentioned above. Based on the structure of their results, they pointed out the possibility that the electronic structure of the AFM state is not fully established until about 20 K. They observed only negligible field induced reduction in the spin-disorder above 100 K in a field of 15 kilogauss.

One final transport property is the electrical resistivity. Mn shows one of the largest values of all the transitional metals. At 295 K, it is 144.0 μohm-cm (45). This large value of the resistivity has been suggested to be caused by spin-disorder above the T_N (1). The magnetic ordering has anomalous effect on the resistivity. At the Neel temperature a minimum occurs. The occurrence of this minimum in the resistivity has been used by several researchers in determining the Neel temperature in Mn alloys (1,2,46). It has been shown by such measurements that the introduction of elements to the right of Mn into the Mn crystal causes an increase in T_N, while those to the left cause a decrease in T_N.

This method will be used in the present work to extend the observation of the change in Neel temperature due to alloying to several other Mn alloys.

EXPERIMENT

Apparatus

The apparatus used in this experiment is shown in Figure 3. A Leeds and Northrup K-5 potentiometer was used to measure the voltage across the samples. The K-5 has a resolution of .02μv and is rated to have less than 0.1μv transient thermal emfs, while operating switches and slide wire. A Keithley 155 Null detector was used in conjunction with the K-5 to complete the measuring circuit. The Null detector has a sensitivity of 0.1μV and is rated to have less than 0.1μv per °C drift. Since it was desirable to measure several samples at once, the potentiometer was wired through a Leeds and Northrup low-thermal ten-pole double-pole-double-throw (DPDT) rotary selector switch. The switch is rated to have less than 1.0μv thermal emf and contact resistance of 0.001±0.0005 ohm. The switch was wired to provide voltage reversal for the K-5 detector, while also providing a means of selecting one of several samples. A mini-box was used to encase the switch and protect it from thermal variation.

A copper anchor block was used to connect the various sample voltage leads to the selector switch leads. The anchor consisted of two small copper bars (1.00 in. X 0.50 in. X 0.44 in.) mounted with a screw to a terminal strip. The two bars were arranged so as to sandwich the two leads

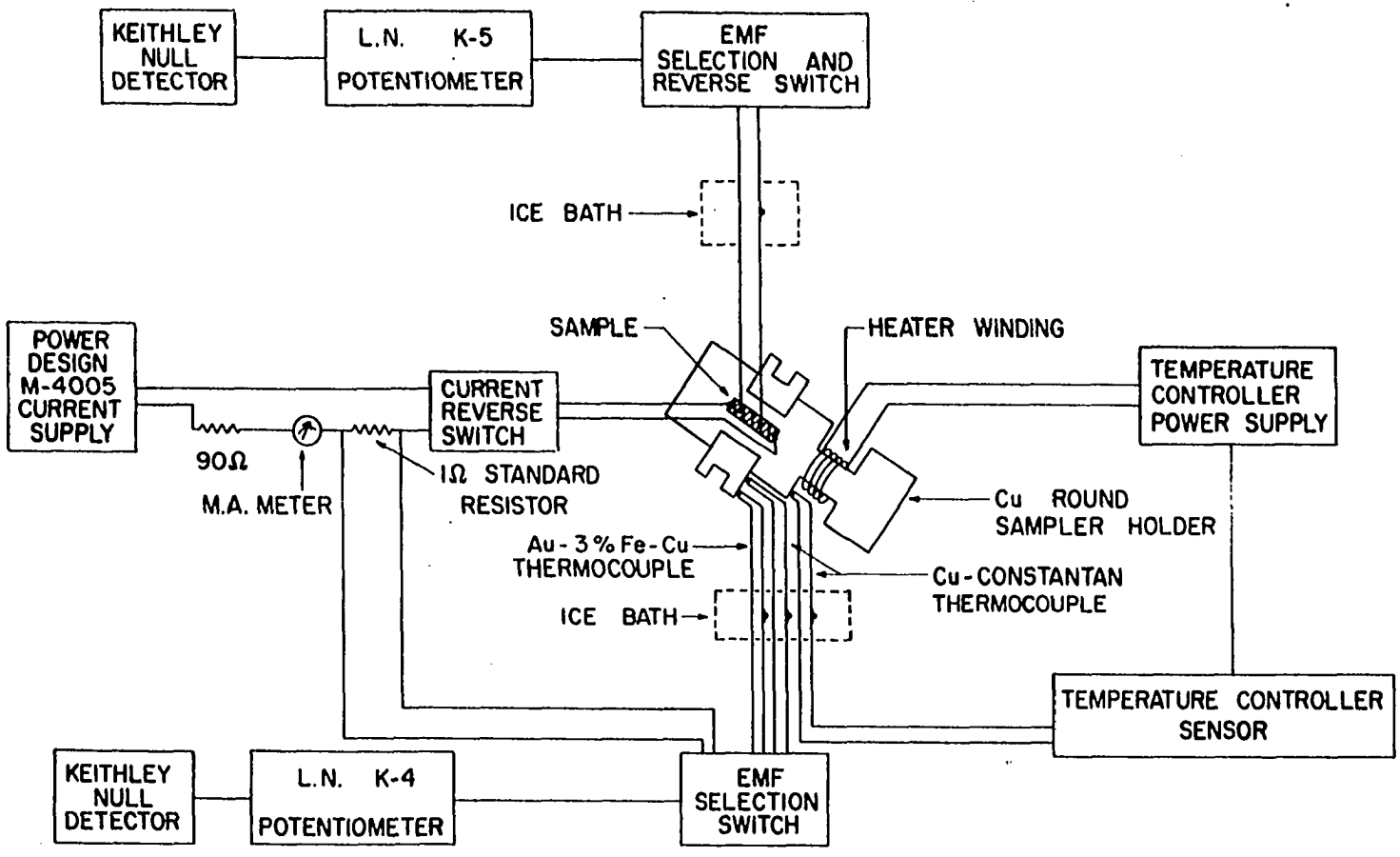

Figure 3. Block diagram of the apparatus used in resistivity measurements

between them, by tightening the screw. This was also mounted in a mini-box to shield the anchors from thermal variation.

The temperature of the sample was monitored by use of thermocouples. A copper-constantan thermocouple was used for high temperature readings and a gold-iron thermocouple was used for low temperature readings. The thermocouples were glued with GE #7031 varnish into special recesses in the sample holder. The copper-constantan thermocouple was calibrated by taking voltage readings at three known temperatures. These temperatures were liquid helium (4.2 K), liquid nitrogen (77.7 K) and room temperature (296.7 K). The data from these readings were fed into a special computer program that fitted the specific emfs to the known shape of the copper-constantan emf versus temperature curve. From this fit, a corresponding table of emf versus temperature (per 0.1 of a degree) was generated for the copper-constantan thermocouple.

The gold-iron thermocouple was calibrated against a standard emf table by Finnemore et al. (47) for gold-iron thermocouples. A voltage reading at helium temperature was taken and compared to the table value. All other table values were subsequently adjusted by the difference observed in the table value and the emf reading at helium temperature.

Both thermocouples were connected to a second Leeds and Northrup low thermal selector switch. The connections were

made through the special copper anchor block described above. This provided the advantage cf being able to switch between thermocouples at the appropriate temperature without the need for a mechanical change over. This same selector switch was used in connection with current measurements as will be described below. The leads from the selector switch were connected to either a Leeds and Northrup K-4 potentiometer or a Data Technology Corporation (DTC) 350 digital multimeter. The K-4 potentiometer has a resolution of .05μv and is rated to have less than 0.1μv transient thermal emfs, when operating switches and slide wire. The DTC-350 has a resolution of 1μv and is rated to have less than 400 ms settling time. A second Keithley 155 Null detector was used inconjunction with the K-4. Although the DTC-350 was less accurate than the K-4, it provided the advantage of a digital read-out while still meeting the minimum accuracy.

The voltage and thermocouple leads were continuous leads that passed from the sample holder to an ice bath. From the bath larger wires were used to connect the thermocouple and voltage leads to the measuring apparatus. The bath was used to provide a constant reference temperature for the thermocouples, as well as for the voltage leads. The current was measured across a standard 1 ohm (0.9995) resistor. The resistor was placed in series and before a low thermal Guildline Instrument (GI) 4-pole double-pole-double-throw

(DPDT) push button selector switch. The switch was rated to have a maximum generation of thermal emf of less than 0.01 microvolt. This switch served both as an off-on control and a current reversal control. Since the standard resistor was in series with the samples, the current through the samples could be calculated by monitoring the voltage across the resistor. The voltage leads from the standard resistor was connected through the second Leeds and Northrup low thermal rotary selector switch. This allowed the same detector to be used in measuring the temperature and the voltage across the standard resistor.

The current was supplied by a Power Design (PD) model 4005 power supply. The PD 4005 was rated to have less than 10 mv drift per 24 hours. A 100 milliammeter was also incorporated into the circuit to provide a coarse indication of the current flowing in the circuit.

Since it was desirable to take measurements over a large temperature range, it became necessary to provide a means of controlling the temperature. This was achieved by use of a temperature controller. It consisted of a sensing element and a power supply. A copper-constantan thermocouple was used as the temperature sensor which fed information into the sensing element. The thermocouple voltage was compared to a preset adjustable reference voltage. The sensing element would seek a null between the thermocouple voltage and the

reference voltage by supplying power to the heater. The sensing element would control the power supply output to the heating element, thus maintaining the system at any preset temperature. The temperature could be controlled to within about 1 K. The power was adjustable and had a maximum output of 200 ma. It could be operated in an automatic mode as described above or a manual mode, which supplied continuous power to the heater.

The actual heater consisted of 120 ohms of manganin wire. The wire was doubled and twisted before being wrapped around a specially machined copper base. This was done to reduce transient voltages from being induced in the measuring circuit. This base was drilled and tapped to receive the copper sample holder described below. The heater windings were glued in place with GE #7031 varnish.

This experiment was conducted over the temperature range between liquid helium (4.2 K) and room temperature (300 K). A glass dewar system was used to contain the cryogenic fluids. The dewar system consisted of a double-wall outer dewar (see Figure 4). This was evacuated and sealed. A smaller second double-wall dewar, which could be mechanically evacuated, was placed inside the outer dewar. The inner dewar was used to contain a helium bath, while the outer dewar contained a nitrogen bath. The inner dewar was mounted in an aluminum collar for support. The collar was attached

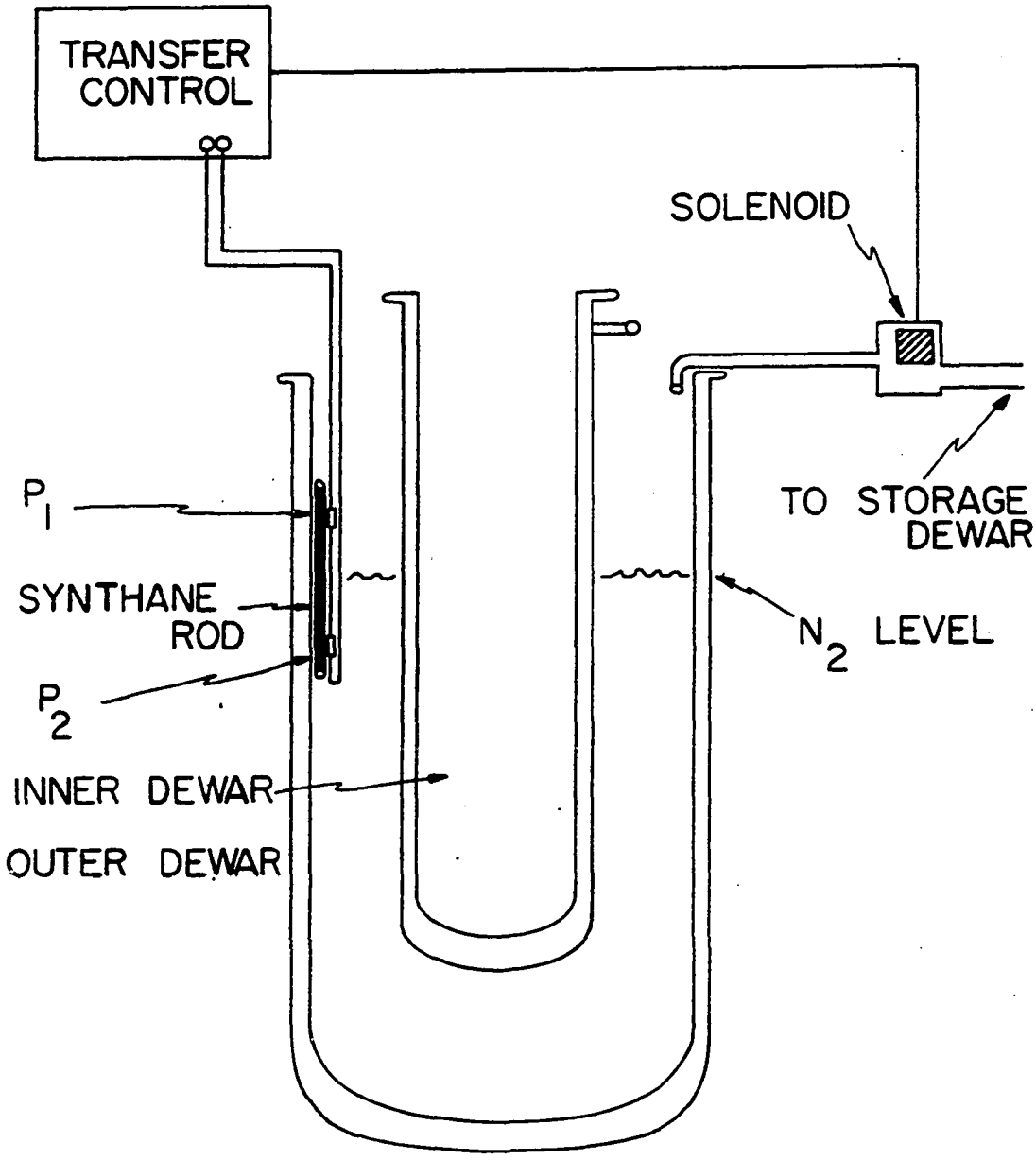

Figure 4. The dewar system showing transfer sensors

to a steel plate mounted in an angle-iron frame. The outer dewar was provided with a metal base and stand. It could be slipped over the inner dewar and supported by its base from a shelf mounted in the angle-iron frame.

Since it was desirable to minimize the thermal cycling of samples, it was necessary to maintain the samples at liquid nitrogen temperatures ordinarily. This was accomplished by constructing an automatic nitrogen transfer system (48). The circuit is shown in Figure 5. Two carbon resistors (470 ohms) were mounted on a synthane rod approximately 8 inches apart (see Figure 4). These resistors served as sensors and controlled the transfer of nitrogen. The two sensor resistors provided the controlling current to trigger the two silicon controlled rectifiers (SCR's). When both sensors were out of the nitrogen bath, both SCR's were conducting. The current was large enough to activate the relay, which opened a solenoid valve to a pressurized liquid nitrogen dewar. Once both sensors were within the nitrogen bath, the SCR's were turned off and the relay opened, stopping the transfer of liquid nitrogen.

The sample holder assembly consisted of a (5.5 in. diameter) brass plate. The plate was mounted with a pumping line, a feed-through for the voltage and thermocouple leads, and an opening for helium transfer and recovery. The pumping line consisted of a (0.25 in.) copper line mounted on top of

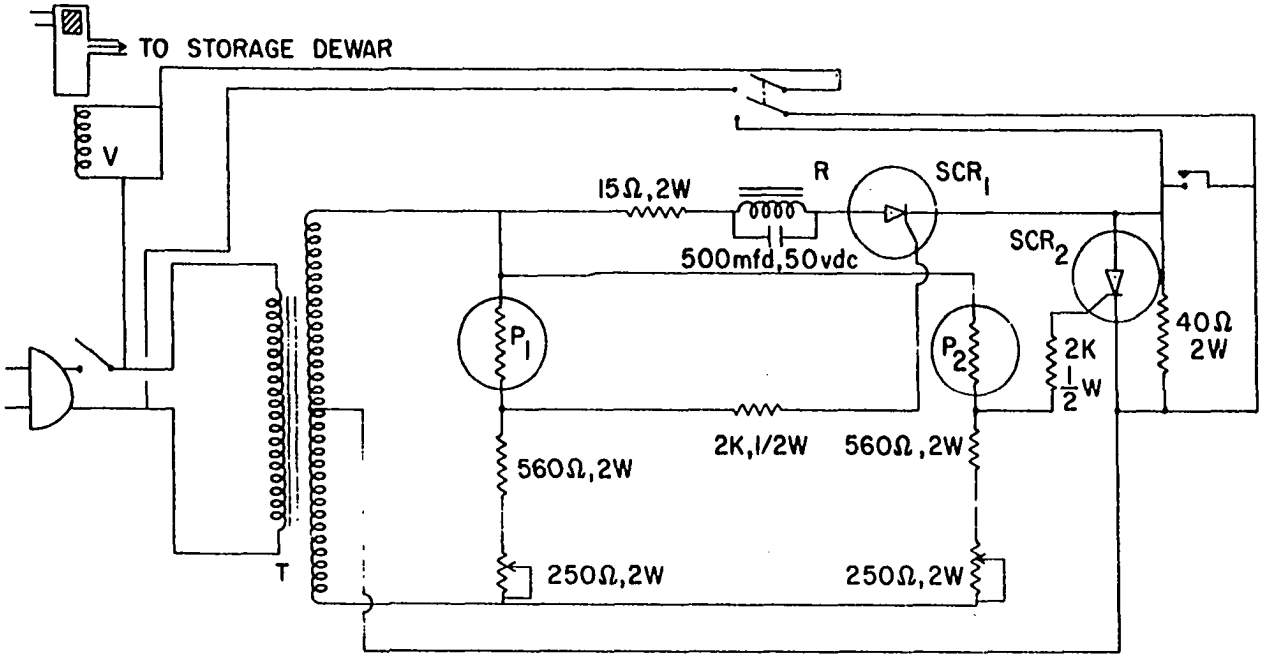

T - 25.2V c.t., 2A FILAMENT TRANSFORMER
R - DPDT RELAY
V - 3 WAY SOLENOID VALVE
P_1 - UPPER PROBE (470Ω 1/2W)
P_2 - LOWER PROBE (470Ω 1/2W)

Figure 5. The circuit of the nitrogen transfer system

the brass plate. A type 505 thermocouple pressure gauge was inserted in this line to monitor the vacuum jacket pressure. Also a 14 pin feed-through was mounted in this same line. It provided an outlet for the current and heater leads, which passed down the pumping line. The pumping line was continued below the brass plate with a thin-wall stainless steel tube. The tube was 2.0 ft. long and was mounted at the other end to a special brass-copper couple that had the upper section of a Ultek vacuum flange attached to it. The stainless steel tube extended slightly beyond the special coupling, to provide a mount for the sample holder. The coupling and flange constituted the top of the vacuum jacket for the sample assembly (see Figure 6).

The feed-through for the voltage and thermocouple leads consisted of a (0.5 in.) copper tube soldered at one end to the top of the brass plate and the other mounted with a (0.25 in. to 0.50 in.) copper reducer. This reducer received a specially machined and drilled nylon plug. The various leads were passed through one of the openings in the plug and epoxied in place with stycast. This allowed these leads to be continuous and still retain a closed system. The feed-through was continued beneath the plate with a stainless steel tube mounted to the plate at one end while the other end was left free. This tube contained the voltage and thermocouple leads and ran to within approximately three

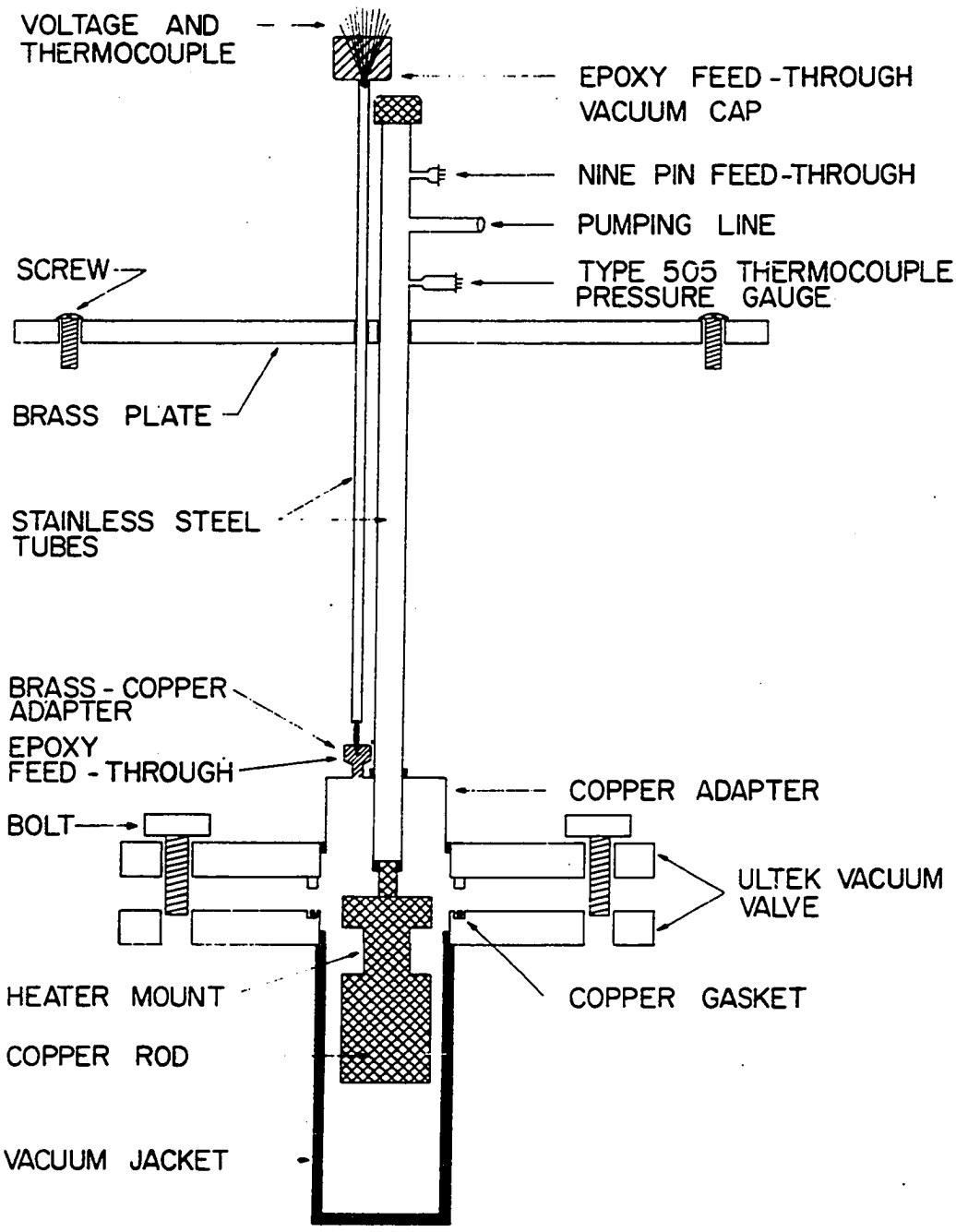

Figure 6. The sample holder assembly showing the sample holder and vacuum jacket

inches of the vacuum jacket top. The main purpose of this tube was to provide protection for the leads. Just beneath the tube, a special brass-stainless fitting was mounted in the top of the vacuum jacket and served as a feed-through for the leads. The fitting consisted of a (0.25 in.) drilled brass rod soldered into a (0.25 in.) hole in the top of the vacuum jacket. The other end of the rod had been drilled out as large as possible to receive a nylon plug. The plug had been drilled with several holes to allow the leads to pass through. Once the plug and leads were in place, epoxy was used to seal the system. This allowed the voltage and thermocouple leads to be exposed directly to the bath, thus eliminating any heat conduction from outside the system.

The bottom section of the vacuum jacket consisted of the matching section of the Ultek vacuum flange helium-arc welded to a (1.5 in. diameter) thin-wall stainless tube. The other end of the tube was plugged with a special brass cap that was also helium-arc welded in place. A special copper gasket was used to seal the jacket by bolting it between the two flanges. The samples were mounted on a specially-machined piece of (0.50 in.) copper round. The round was machined to provide four (0.25 in.) perpendicular flat sides (see Figure 7). These sides were 0.25 in. wide. A section at the top and in the middle was allowed to remain round. A portion of the upper section was machined and threaded to fit a (0.25

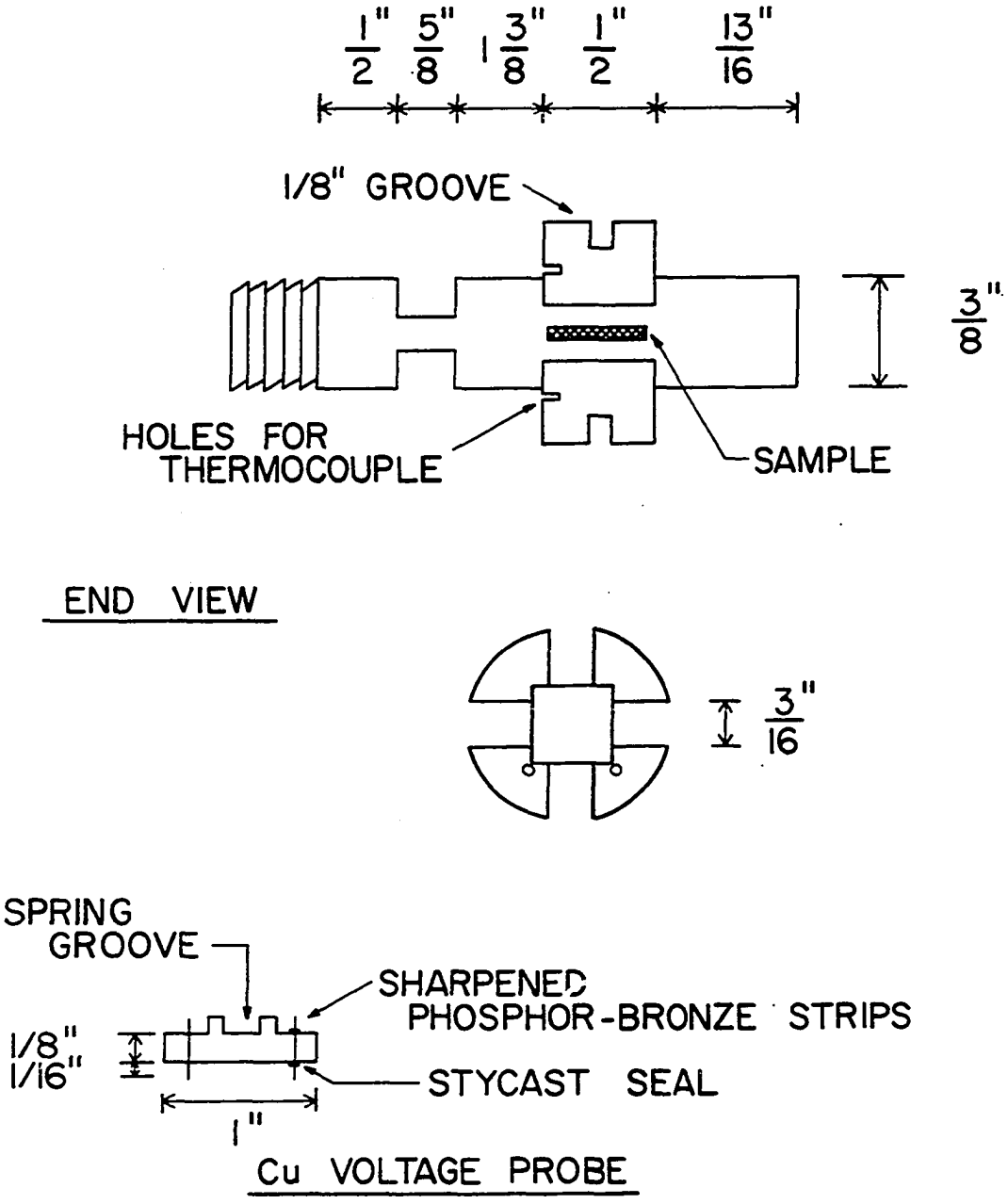

Figure 7. The sample holder with heater mounts

in.) bolt opening. The middle section had a 0.125 in. groove cut into it perpendicular to the length of the round. This would be used later to retain a tantalum spring. Four somewhat narrower (0.125 in.) parallel flat surfaces, each rotated 90° from the other, were machined through the round section in the middle. These four surfaces served as a base for mounting the samples, and the upper walls served as a support for the voltage lead mounts. To provide electrical insulation for the samples, the mounting base was later covered with marlair tape. Four copper bars (1.0 in. X 0.25 in. X 0.25 in.) were mounted with copper-bronze knive edges. This was done by cutting slits into the copper bars and epoxying the blades in place. The voltage mounts were provided with a 0.125 in. grove to match those in the copper round. To complete the sample holder, two indentations were made in the round near the sample mounts. These would be used to receive the two thermocouples used in determining sample temperatures. By placing the voltage mounts into the opening in the sample holder and aligning the groves, the tantalum spring could be fitted into the grove and around the sample holder. This provided the necessary means of holding the voltage leads in contact with the samples.

A second (0.50 in.) piece of copper round was used to provide the heater block for the sample holder. The round was machined to provide a 0.125 in. indentation. This served

to receive heater windings. The windings were wrapped around the heater block and GE #7031 varnish was used to glue the heater in place. A small indentation was made near the windings to receive a third thermocouple. The upper end of the heater block was machined to have a quarter-inch base. The base was used to attach the heater block to the stainless steel pumping tube that extended just inside the vacuum jacket. The lower end of the heater block was tapped to receive the sample holder. This provided good thermal contact between the heater block and the sample holder, while providing a certain amount of ease in the removal of the sample holder. At the upper base of the heater block, two thermal anchors were provided for the incoming voltage leads. They consisted of two pieces of (0.125 in. diameter) copper rod screwed in the heater block. The leads were wrapped around these anchors to ensure that they were at the same temperature as the sample holder.

The preliminary sample assembly used in this experiment differed slightly from that described above (49). The major differences were the lack of a separate tube for the voltage leads and a different sample holder. The previous sample holder used a specially machined synthane rod mounted with a copper plate. One end of the plate contained heater windings while the other end was used to mount the samples. Thermocouples were mounted in holes drilled in the copper plate.

Sample Preparation

Samples were prepared from 99.99 Johnson-Matthey electrolytic flakes of alpha-manganese. Other elements used in this experiment came from a variety of sources. Their purity and sources are summarized in Table V and Table VI.

Table V. 3-d impurity elements.

Elements	Purity	Major Impurity (in PPm)	Source
Cr	99.95	C < 20	Ames Labs
Co	99.95	C,Fe < 320	Ames Labs
Fe	99.95	O,H < 500	Ames Labs
Ni	99.99	-	-
Ti	99.80	Fe,W < 2000	Ames Labs

The Mn flakes as received were etched in a dilute nitric solution (200 parts water: 20 parts nitric) to remove

Table VI. 4 and 5-d impurity elements.

Elements	Purity	Major Impurity (in PPm)	Source
Ir	99.9	-	Martin Metals
Rh	99.90	-	Ames Labs
Re	99.98	O <150	Ames Labs
Os	99.999	-	United Minerals
Mo	99.95	C, Al < 100	Ames Labs

oxides that coated the flakes. The appropriate compositions of Mn and impurity elements were measured to provide the necessary alloys. The metals were arc-melted into buttons approximately 3 cm. in. diameter and 5 to 6 mm thick. Spark erosion was used to cut samples into appropriate sizes. The buttons were first sliced parallel to their face to remove a section approximately 2 mm thick from the center of the buttons. From these sections, parallelepipeds of approximately (2 mm. X 2 mm. X 6 mm.) were cut. It was often difficult to prepare samples of the appropriate size because of

the brittleness of the material. The brittleness of the samples appeared to be a fuction of not only the quantity of impurity present, but also the quality of the impurity present in the sample.

Once samples of an approximate size were obtained, they were annealed under continuous vacuum for 6 hours at 620°C. This procedure was used to ensure that the samples were in the alpha-phase and to remove any hydrogen that might be present (50). The annealing temperature is just below the alpha-beta transition. For pure Mn, this temperature is 727°C. Since hydrogen has the effect of washing out any structure that might be present in the resistivity (51,46), it was important to maintain a high vacuum during the annealing process.

In crder to remove any surface damage and other possible surface contaminations, the samples were electropolished. The electropolished mixture used was dilute perchloric acid (12 parts perchloric:200 parts methanol). The electropclishing gave the samples a shiny metallic finish. This ensured good electrical contact for voltage and current leads. Since the samples oxidized very readily, it was necessary to maintain them under vacuum, if the samples were to be retained any length of time without oxides forming on the surface.

To ensure that the samples were in the alpha-phase, several were submitted for X-ray analyses. An X-ray diffraction method was used to scan these annealed samples for the major alpha and beta Mn peaks. To check if samples were single phase, high-power microscopic studies were made of the samples. These studies would reveal if the impurities were in solid solution. Also chemical analyses were run on each sample to determine the amount of solute present. The results from these studies will be discussed in a later section.

Once samples had been electropolished and were ready to be studied, current leads were attached by soldering on #34 or #36 copper wire with the aid of a ultra-sonic solder gun. Pure indium was used as the solder. It was necessary to make use of the special solder gun because of the difficulty in attaching leads due to the quick oxidation of the sample surface. Since copper-bronze blade edges were used for the voltage contact, it was not necessary to solder on the voltage leads. The only exception was with the first sample holder, which used the copper plate for mounting samples.

The samples were placed under the blade edges with the aid of a pair of tweezers. A tantalum spring held the voltage-blade edges snugly against the sample and the sample snugly against the copper mounting thus providing both good electrical and thermal contact.

Once samples were mounted the sample holder was sealed and allowed to pump down to less than 20 microns. While the sample holder was being evaluated, voltage and thermocouple leads were attached to the instruments and anchored in an ice bath.

Once the system had reached the above pressure, liquid nitrogen was transferred to the outer dewar. After the samples had reached nitrogen temperature, liquid helium was transferred to the inner dewar. This provided a temperature near 4.2 K.

A current of 100 ma was passed through each sample and the potential drop across the sample was monitored. The current was passed first in the forward direction and then in the reverse direction with corresponding voltages observed. This was done to eliminate any possible effects due to thermal emfs, by later averaging the two voltages. The temperature and current were also determined. Once the first sample readings were completed, the rotary selector switch was used to select another sample and the procedure was repeated.

Once measurements were completed at one temperature, a new temperature was set on the temperature controller. This automatically reset the temperature and additional readings were taken. Readings were taken in 2 K intervals over critical region with somewhat wider intervals in less critical

regions.

Once data was completed on a series of samples, the resistivity was calculated. The calculation was done as fcllows: the voltages across the sample were averaged and divided by the current and multiplied by the respective A/l ratio for each sample. A traveling microscope was used to determine the cross-section area A, and the distance l, between the voltage contacts. It was not always possible to determine the A/l ratio to any great accuracy due to large uncertainties in the l value and also due to the brittleness of the samples. This was particular the case when the voltage leads were soldered to the samples. Thus the absolute resistivity has uncertainties that may vary from 10% to 20%.

RESULTS AND DISCUSSION

The results of this electrical resistivity study have given valuable information on the variation of the Neel temperature of alpha-manganese. This information allows for quantitative discussion of the nature of the antiferromagnetism which characterizes Mn.

As pointed out in the introduction, this experiment was undertaken, in part, to provide some qualitative results on the shift in the Neel temperature of Mn as a function of the shift in Fermi level. To this end, a systematic approach has been taken to provide Mn alloys of several neighboring elements. The impurity elements used in the Mn-rich alloys are summarized in Figure 8. Those elements with shading in the upper right hand corner indicate that the result for those Mn-rich alloys were reported earlier by Williams and Stanford (2) and are included in this study for completeness. Those elements with shading in the upper left hand corner are those Mn-rich alloys that were studied in this work.

As can be seem from Figure 8, efforts were made to provide results on the variation of the Neel temperature as one alloys across periods, where physical and chemical properties of the elements are changing rather rapidly. Also the variation of the Neel temperature down several columns, where these properties should not be changing so drastically, is

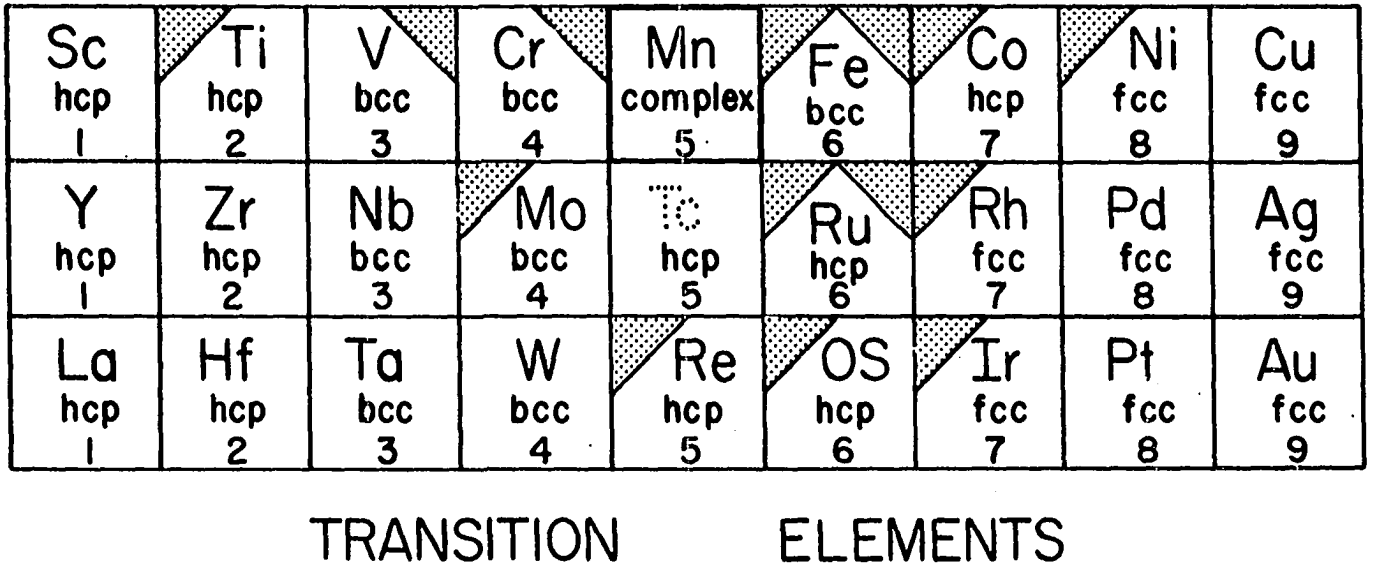

Figure 8. Alloy systems investigated. Shading in the upper right-hand corner indicates those alloys reported by Williams and Stanford; in the left, this study. The crystal structures for each element are indicated

considered.

Several series of binary alloys, and later, ternary alloys were studied. The binary Mn-rich alloys are shown in Table VII.

TABLE VII. Chemical analysis of solute present.

Alloys	Series (at.%)				
	I	II	III	IV	V
Co	-	1.10	-	1.70	3.30
Ni	-	0.90	-	1.90	-
Ti	-	0.70	-	1.80	2.90
Rh	0.84	1.50	2.14	-	-
Os	0.32	0.74	-	0.82	-
Ir	0.75	-	1.49	1.15	-
Fe*					

*The Fe concentration were 5.1 and 9.6 at.%.

The results for the ternary alloys will be discussed later.

Since Mn has several crystal structures, it is desirable to ensure that the samples used in this study were in the alpha-phase. This was checked by X-ray analyses. The Mn-Co, Mn-Ni and Mn-Ti alloys were scanned by a X-ray diffractometer. Cu radiation (λ = 1.54178 A°) was used to check for major peaks of alpha and beta-Mn. Although the study was not very detailed, the major peaks could be attributed to the alpha-Mn structure. A few of the higher concentration samples showed what might be weak beta peaks. These peaks may have resulted from a slight freezing in of the beta phase upon cooling after arc-melting. If this is the case, the slow annealing process that samples were submitted to would remove any remnant that remained. It was thus concluded that these samples were in the alpha-Mn structure.

The alloys of Mn-rich Ir, Rh, and Os were studied with a Debye-Scherrer camera. The samples were submitted to Cr-radiation for approximately two hours. Since the samples were not in powdered form, most of the lines were in the back reflection region. However, all observed lines could be identified as belonging to the alpha-Mn structure.

The X-ray studies also provide some information on the effect of alloying on the lattice constant of Mn. As pointed out above, the X-ray studies were not detailed enough to provide values of the absolute change in the lattice constant of

Mn. However, it did indicate that the lattice constant for Mn-rich Ir, Rh and Os alloys was increased above that for pure Mn. A somewhat more detailed X-ray study by Kohara and Asayama (22), has been conducted (see Figure 9). In this figure, the percentage change in the lattice constant is shown as a function of concentration of solute for several Mn alloys. With the exception of Fe, all impurities to the right of Mn increase the lattice constant, while those impurities on the left decrease the lattice constant. Thus, our result would appear to be consistent with their findings. The lattice constant dependence of the various Mn-alloys may prove to be significant in explaining the shift in the Neel temperature observed in these alloys.

A second concern was the question whether the solute entered into solid solution. This, of course, would be indicated in part by the X-ray studies. However, to ensure that the solute was in solid solution, high power microscopic studies were conducted on several of the alloys studied. Magnification of 250X was used. Although these studies were not conclusive, the results suggested that the solute did enter into solid solution.

The selection of the Neel temperature, in such work as this, has been customarily chosen at the point of a maximum or minimum in the measured transport property. In particular, for electrical resistivity data, the minimum in the

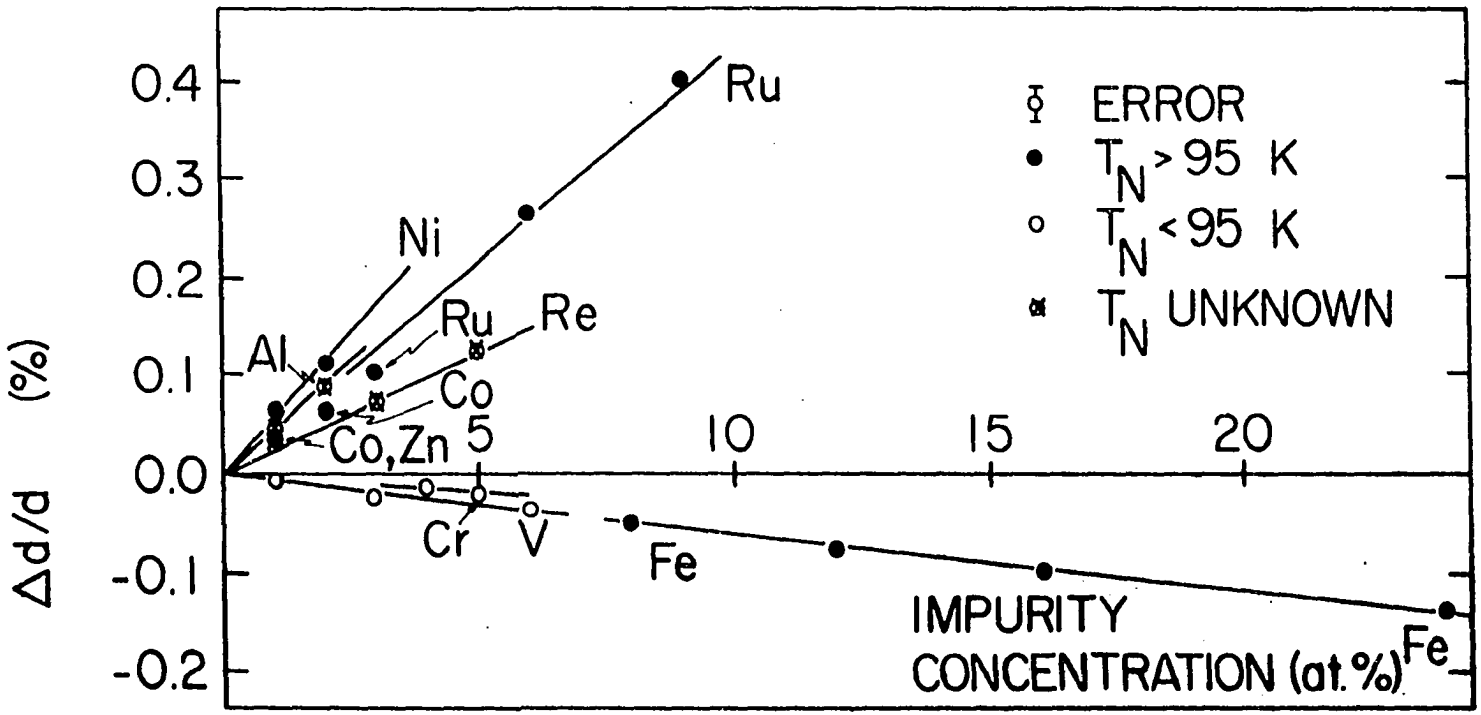

Figure 9. The variation of the lattice constant for several Mn-rich alloys as a function of solute concentration [from the data of Kohara and Asayama (22)]

resistivity versus temperature curve has been selected. Recently, Arajs, et al. (52) have applied a new criterion for the selection of T_N from electrical resistivity data for the Cr system. T_N is selected at the temperature at which the temperature derivative $d\rho/dT$, is a minimum. They point out a 1.5 K over-estimation of T_N by the resistivity minimum technique for pure Cr.

Efforts to apply the $d\rho/dT$ technique to the Mn-rich alloys did not provide much in the way of an improvement in the selection of T_N. This was probably due in part to slight scatter in the data, which made numerical differentiation difficult and partly because of the lack of a sharp transition at the Neel temperature in many cases. For a comparison see Figure 10.

Since in this case, the $d\rho/dT$ criterion provided little or no improvement over the resistivity minimum technique, we have therefore selected T_N based on the appearance of a mimimum in the resistivity versus temperature curve. In several cases where there is no apparent minimum, the point of inflection was taken as indicating the Neel temperature. The resistivity minimum method provides values of T_N believed to be correct to within ± 2 K in most cases. These values should be sufficiently accurate to provide the means of comparing any future theoretical prediction with experimental results.

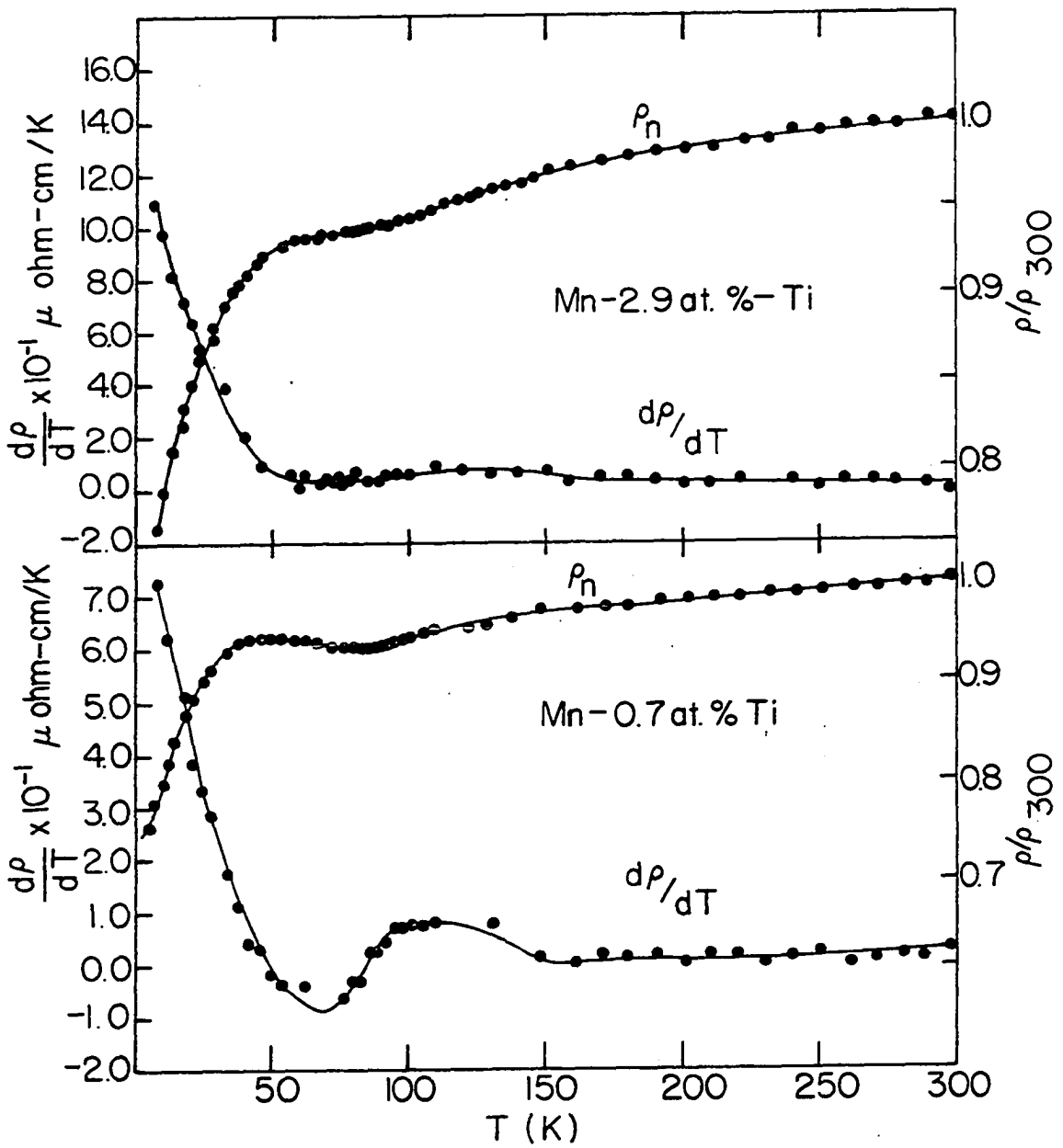

Figure 10. A comparison of the dρ/dt criterion with the resistivity minimum technique for Mn-Ti data

A remark is perhaps in crder regarding the absolute resistivity values. The resistivity data in this work is reported as normalized resistivity, ρ_N ($=\rho/\rho_{300}$) in most cases. This has been done because of uncertainties in the absolute value of the resistivity for some samples. These uncertainties may be as high as 20% or more in some samples. In order not to provide misleading information, ρ_N data is reported. However, to provide some idea of the magnitude of the absolute resistivity, the absolute resistivity for several selected samples at two selected temperatures is reported in Table VIII.

The remainder of this section will be devoted to the discussion of the data and pcssible explanation of the antiferromagnetic behavior of Mn. The discussion will be divided into two major parts. The first will be concerned with the treatment of the binary alloys, while the second section will look at the results cf ternary studies.

Binary Alloys

We will be concerned here with dilute Mn-rich alloys in which the host and sclute are in a homogeneous random solid sclution. Random here refers to the occupancy of various available positions of any given site, since there appears to be preferential selection amcng the four possible inequivalent crystal sites in Mn by solute atoms. The above require-

Table VIII. Several electrical resistivity values.

Mn Alloys	ρ_{295}	ρ_0**	$\rho_{0/295}$	ρ_a/ρ_p*	
				295 K	0 K
Mn-5.1%-Fe	307	245	0.79	2.13	49
Mn-0.89-Ru	218	155	0.71	1.51	31
Mn-1.90%-Cr	422	374	0.88	2.93	79
Mn-1.82%-Ti	151	110	0.72	1.04	22
Mn-1.69%-Co	157	167	1.06	1.09	33

* ρ_p and ρ_a represents the resistivity of pure Mn and Mn-rich alloys respectively.

** ρ_0 represents the estimated resistivity at 0 K.

The value of ρ is 144 μ ohm-cm and 5 μ ohm-cm at room temperature and 0 K respectively.

ment is very important if the alloys are to reflect the nature of the host modified by the addition of small percentages of impurities. Without a solid solution, the resistivity would reflect the sum total of the two constituents acting alone.

We undertook a study of more than a half-dozen binary alloys of Mn. These alloys provided a positive, as well as a negative shift of the Fermi level of the host metal, Mn. Since the alloys were dilute, they provided shifts in the level that ranged from 1.0% up to about 10.0%.

Based on the idea of the rigid-band approximation, such alloying should provide information on how the shifted Fermi level affects transport and magnetic properties. The alloys would provide direct information on the electrical resistivity and Neel temperature, while perhaps providing indirect information on the type of magnetic coupling, the density of states and the nature of the Fermi surface in pure Mn.

The discussion of the binary alloys will be divided into three sections based on the three transitional periods. We will discuss in turn, Mn-rich alloys of the first, second and third periods.

3-d transitional impurities

Mn-rich Fe alloys Fe is the only transitional metal that readily alloys with Mn in any sizable amount. Over 30% of Fe can be alloyed into the alpha-phase of Mn (53). Some data on Mn-Fe have been reported (1,26,46,2), nevertheless, it is worth reporting some details of those studies. Also, this work extends the observation of the Neel temperature to

an alloy of higher concentration (10% Fe) than previously reported. The normalized electrical resistivity results from Williams and Stanford (2) for two Mn-Fe alloys are shown in Figure 11. The results of a resistivity study for a 5% and 10% Mn-Fe sample is shown in Figure 12. The high-temperature end of the resistivity shows a rather large and nearly constant value for ρ. As in the case of pure alpha-Mn, this large value for ρ is probably accounted for in terms of additional scattering caused by the presence of magnetic moments on the various Mn atoms. It is believed that moments exist in the pure metal, well above T_N (16).

Work by several researchers (1,32,31) have shown fairly conclusively that the Fe atoms preferentially select the two smaller sites (sites III and IV) in the Mn-crystal. Kasper (32) reports that the Fe atoms go into sites III and IV in a 1:2 ratio respectively. Mossbauer studies (31), over the concentration range from 5% to 30% Fe in Mn, showed nearly constant values for the quadrupole splitting ΔE, the isomer shift ε, and line-width Γ, (full width at half maximum). Since ΔE, ε and Γ are not concentration dependent, it appears that at a Fe nucleus the neighboring Fe atoms produce the same electronic effect as a neighboring Mn atom. That is to say, on the average, as one increases the Fe/Mn ratio, each Fe nucleus sees an increasing number of Fe near-neighbors. If the Fe near-neighbors behave much differently from the Mn

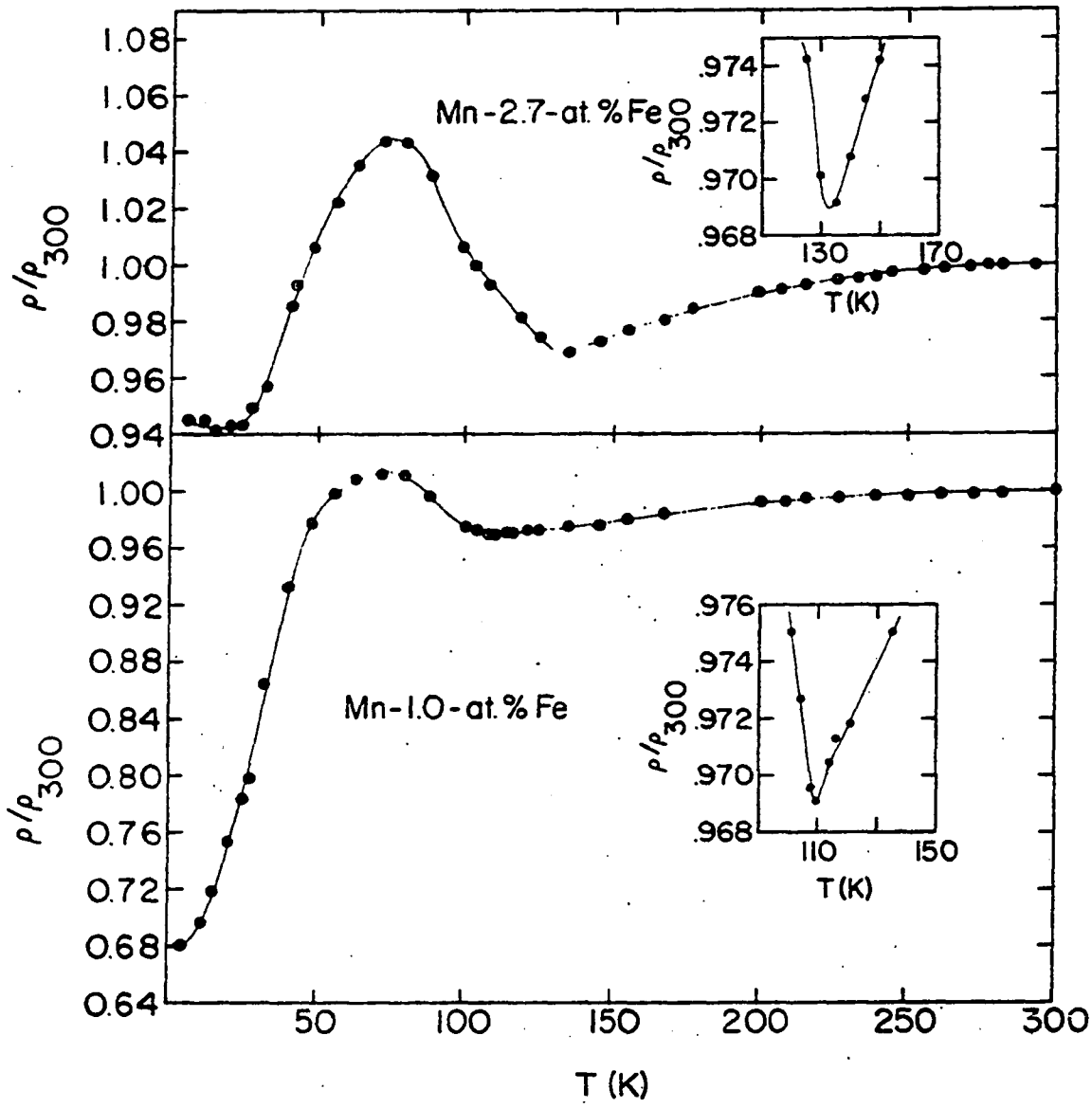

Figure 11. The normalized electrical resistivity for a 1.0% and 2.7% Mn-Fe alloy

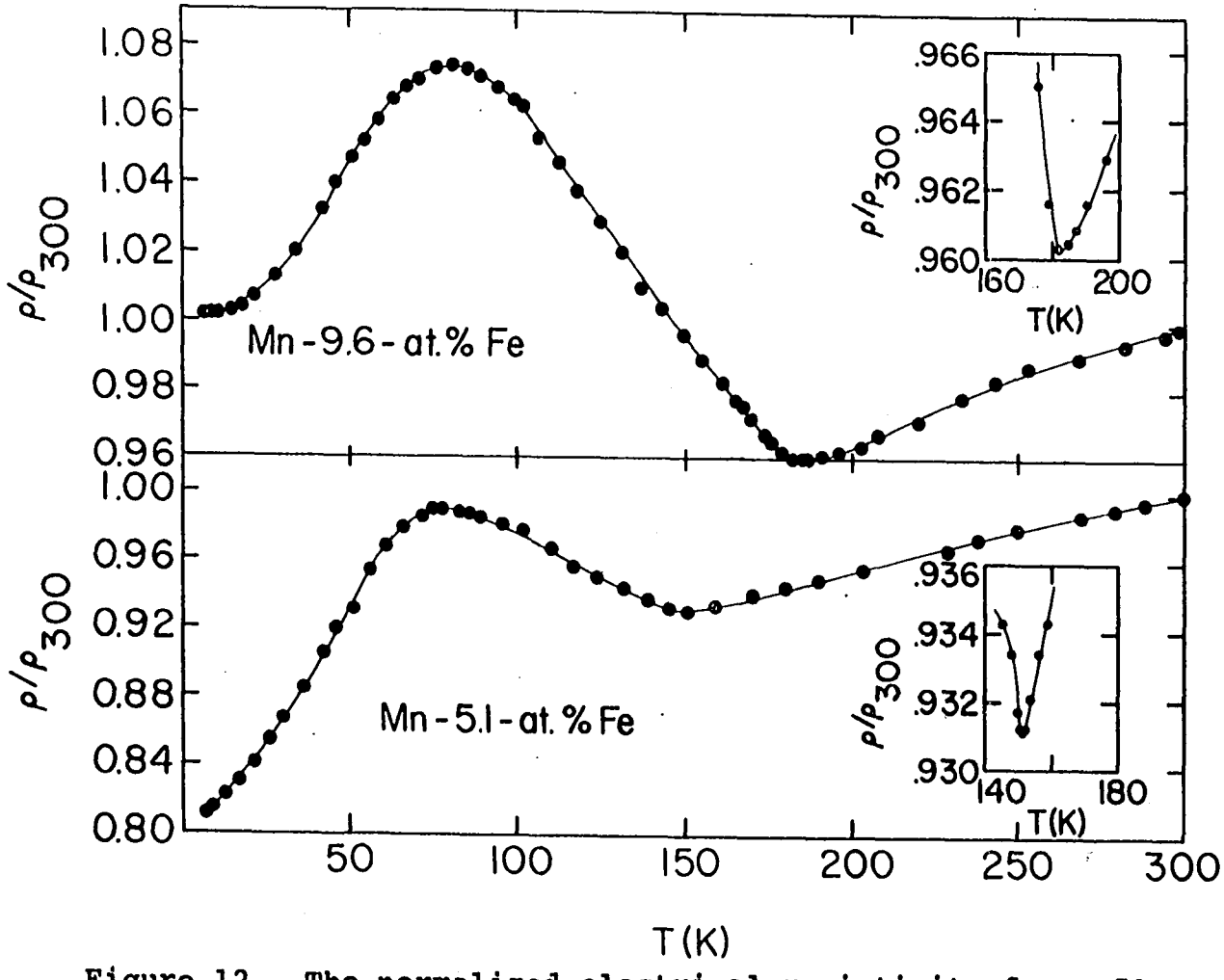

Figure 12. The normalized electrical resistivity for a 5% and 10% Mn-Fe alloy

near-neighbors, a concentrational dependence should be seen in either $\Delta E, \varepsilon$ or Γ. The associated hyperfine fields were reported to vary from H_{III} = 5 kOe and H_{IV} = 16 kOe to H_{III} = 7 kOe and H_{IV} = 16 kOe for the 5% and 30% alloys the respectively. This constitutes a very small change over this concentration. Thus, these small values for the hyperfine field would suggest that the Fe atoms have little or no aligned 3-d moments, which is consistent with that reported for those sites in pure Mn (13,54,14). Recent NMR (22) studies have ccnfirmed in part the Mossbauer studies. They report slight increases in the internal field at sites I, II and III. As a result of the increased internal field, an increase in the magnetic moment μ_B, of 0.02 μ_B/at.% Fe, 0.07 μ_B/at. % Fe and 0.04 μ_B/at. % Fe are reported for sites I, II and III respectively.

The resistivity study shows a concentration dependence for the shift in the Neel temperature. The initial rate is about 14 K/at. % Fe for the first few atomic percentages of Fe (see Figure 13). Above this, T_N appears to begin to change at a slower rate. Below the Neel temperature, as in pure Mn, there is an increase in the resistivity. Moreover, this increase has become quite pronounced in the alloys. It maybe possible tc attribute this increase, as is suggested for pure Mn, to new gaps in the allowed energy bands caused by the introduction of an additional periodicity due to the

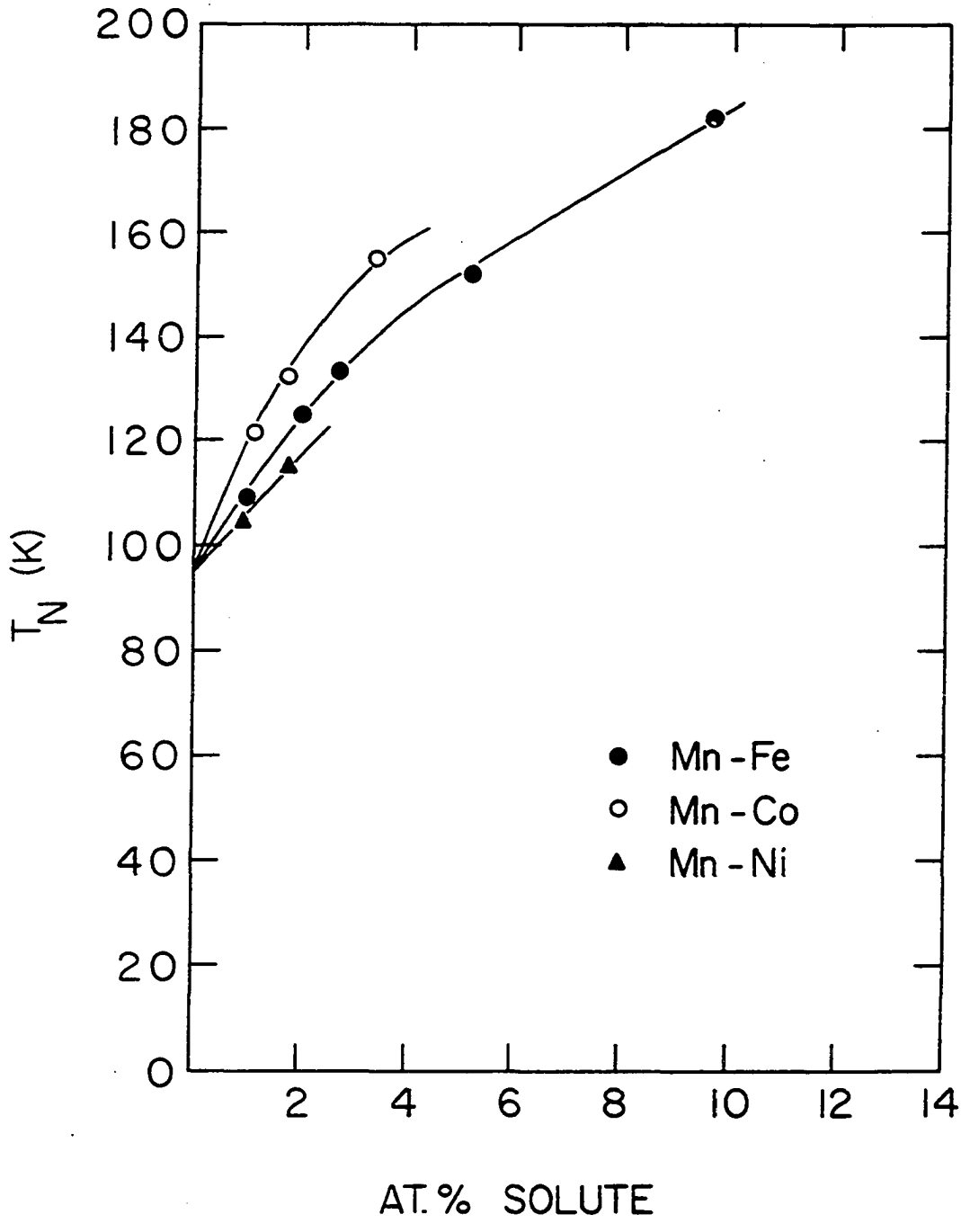

Figure 13. The variation of T_N as a function of atomic percent solute for Mn-Fe, Mn-Co and Mn-Ni alloys

antiferromagnetic ordering. This new periodicity is incommensurate with the lattice. The gap should reduce the effective number of carriers in the conduction band. As suggested above, the extra electrons on the Fe atom may be given up to the conduction band or to other Mn atoms rather than remaining localized about the Fe atoms. Then, by direct or indirect interaction with the 3-d electrons, the additional electron can cause an increased coupling between the conduction band electrons and the localized d-electrons. If it is a direct interaction, one can imagine the excess electron on the Fe atom becoming localized about one of inner sites in the Mn crystal. (Inner sites will be used to refer to sites I and II in the Mn crystal). This could easily result in an increased magnetic moment at the inner sites. Alternately, we could imagine an indirect interaction where the excess electron enters into the conduction band. Thus, the Mn atoms could interact via the conduction electrons. This too would lead to an increased magnetic coupling between atoms.

The available experimental results lend support to the former idea. One observes an increase in the magnetic moment on the inner sites in the Mn crystal when Fe is alloyed into Mn. Now the energy gap should be proportional to the magnetic moments, which in term may be proportional to the solute concentration. Thus, an increasing amount of solute may cause an increase in the gap, which may be reflected in an

increasing enhancement of the electrical resistivity below the Neel temperature.

Another important mechanism that affects the resistivity below the Neel temperature is spin disorder due to thermal excitation. A part of the observed resistivity could very easily stem from this source. One could imagine the moments being, on the average, ordered, but because of thermal fluctuations, the conduction electrons may see a rather disordered array of moments. Remembering, of course, that the ordering has introduced severe restrictions on the conduction electrons, the slightest amount of disorder may increase the electrical resistivity.

Whether it is the presence of an energy gap or the spin disorder that is responsible for the increased resistivity, it varies with concentration. We will define a so-called enhancement factor, F [$=(\rho_{max} - \rho_{min})/\rho_{min}$], where ρ_{max} and ρ_{min} are the values of the resistivity at the maximum and minimum in the resistivity versus temperature curve respectively. A plot of F as a function of the e/a ratio is shown in Figure 14. It is interesting to note a rather sharp increase in the enhancement factor for the first few percent Fe, with a much slower increase at higher percentages. This is reminiscent of the variation of T_N with concentration. Certainly, the significance of such a graph is open to question, particularly in light of the lack of theoretical or additional experi-

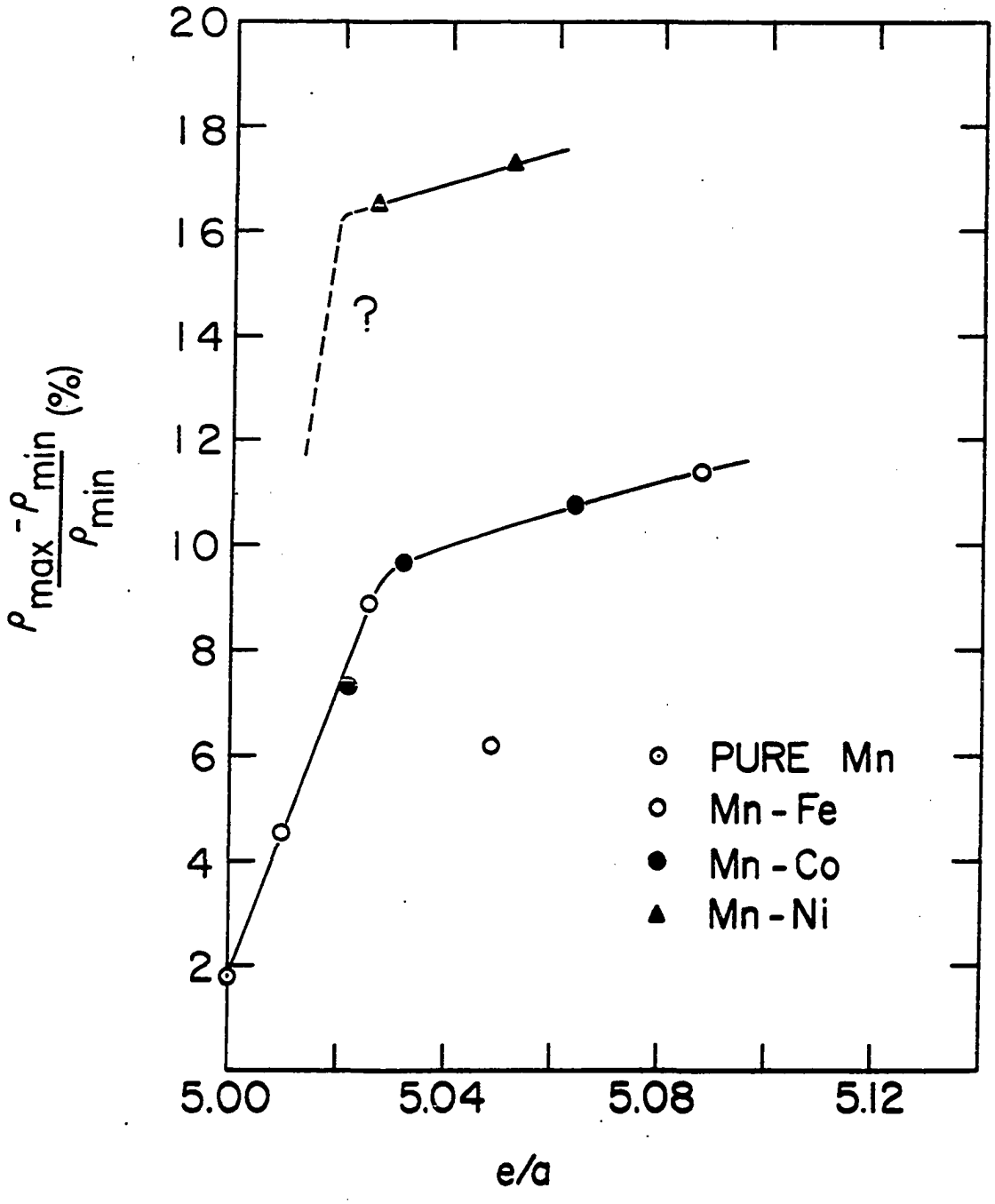

Figure 14. The variation of the enhancement factor, F, as a function of e/a for Mn-Fe, Mn-Co and Mn-Ni alloys (for the Mn-Ni alloys, this is not a true maximum but the value at 4.2 K)

mental results to support it. It should be noted that Overhauser used a similar approach in getting an estimate of the size of the gap in Cr (55).

The remainder of the low temperature end of the resistivity shows little or no anomalous effect. It falls off rather rapidly, as does that for pure Mn. A few of the higher concentration alloys show a weak minimum at temperatures on the order of 10 K. This may be the result of some type of impurity-impurity interaction. The shape of the resistivity resembles that of the Kondo-systems. However, there is no definite evidence to support this case. The accuracy of the data did not allow a check for Kondo behavior.

We may summarize the behavior of the Mn-Fe alloys as follows:

(a) Reduced lattice constant: Since the reduced lattice constant is accompanied by an increase in the Neel temperature, a direct coupling, rather than an indirect coupling between Mn atoms may be suggested. However, Williams and Stanford (2) pointed out that there should be little overlap of d-wave function from atom to atom in pure Mn. Although Fe does decrease the lattice constant, the change is probably too small to cause a substantial increase in the overlap of the d-wave functions.

(b) Increase in T_N: In light of the reduced lattice constant for the Mn-Fe alloys, the increase in T_N might lend credence to the idea of a direct type of interaction. However, in light of the Mossbauer study, which suggests that Fe atoms behave electronically like other Mn atoms, a more indirect coupling via the conduction electrons is suggested. The implications are that the excess Fe electrons become a part of the conduction band or become localized at other sites in the Mn structure.

(c) Increased enhancement factor: Whether the enhancement factor represents the effect of the energy gap and/or the strength of the magnetic moments or some other mechanism, it clearly suggests a strong dependence of the scattering mechanism on the e/a ratio. As the NMR studies suggest, an increasing magnetic moment with Fe concentration could be occurring. This could create a large spin disorder and energy gap, which results in an increased enhancement factor.

(d) Linear dependence of T_N: This seems to suggest that the Fe atoms do not disturb the energy band of the pure metal very greatly. In fact, it suggests that the Fermi energy is only shifted and the rigid band approximation holds. This is reminiscent of the suggested two-band model for Cr.

Mn-rich Co alloys In the case of Co, solubility in Mn is limited to only a few percent. This limits the range of study and makes a determination of the concentrational de-

pendence of quantities like the hyperfine field, electrical field gradient or charge density at the Co sites difficult. However, some efforts have been made along this line by Kohara and Asayama (22) in their NMR study. Although no quantitative numbers are avialable, qualitative results suggest that the Co atoms behave like the Fe atoms, preferentially selecting the smaller sites (sites III and IV). Also a slight increase in the internal field at sites I, II and III are observed. Thus, the Co atoms also tend to increase the magnetic moments on the inner sites.

The normalized electrical resistivity results for the three Mn-Co samples studied in this work is shown in Figure 15. One observes a large and slow varying high temperature dependence for the resistivity. Again, this is probably due to scattering from disordered magnetic moments. The data shows characteristic resistivity minimum, after which we see an enchancement in the resistivity.

As with the Fe alloys, there is a concentrational dependence for the shift in T_N. The dependence is no longer linear and tends toward a lesser power for its variation. The rate of change is only slightly slower than that observed for Fe (see Figure 13). If one looks at the enhancement factor F, for the various Mn-Co samples, it falls on the previous curve for Mn-Fe (see Figure 14). Without attempting to say what this graph may represent, one fact is very clear:

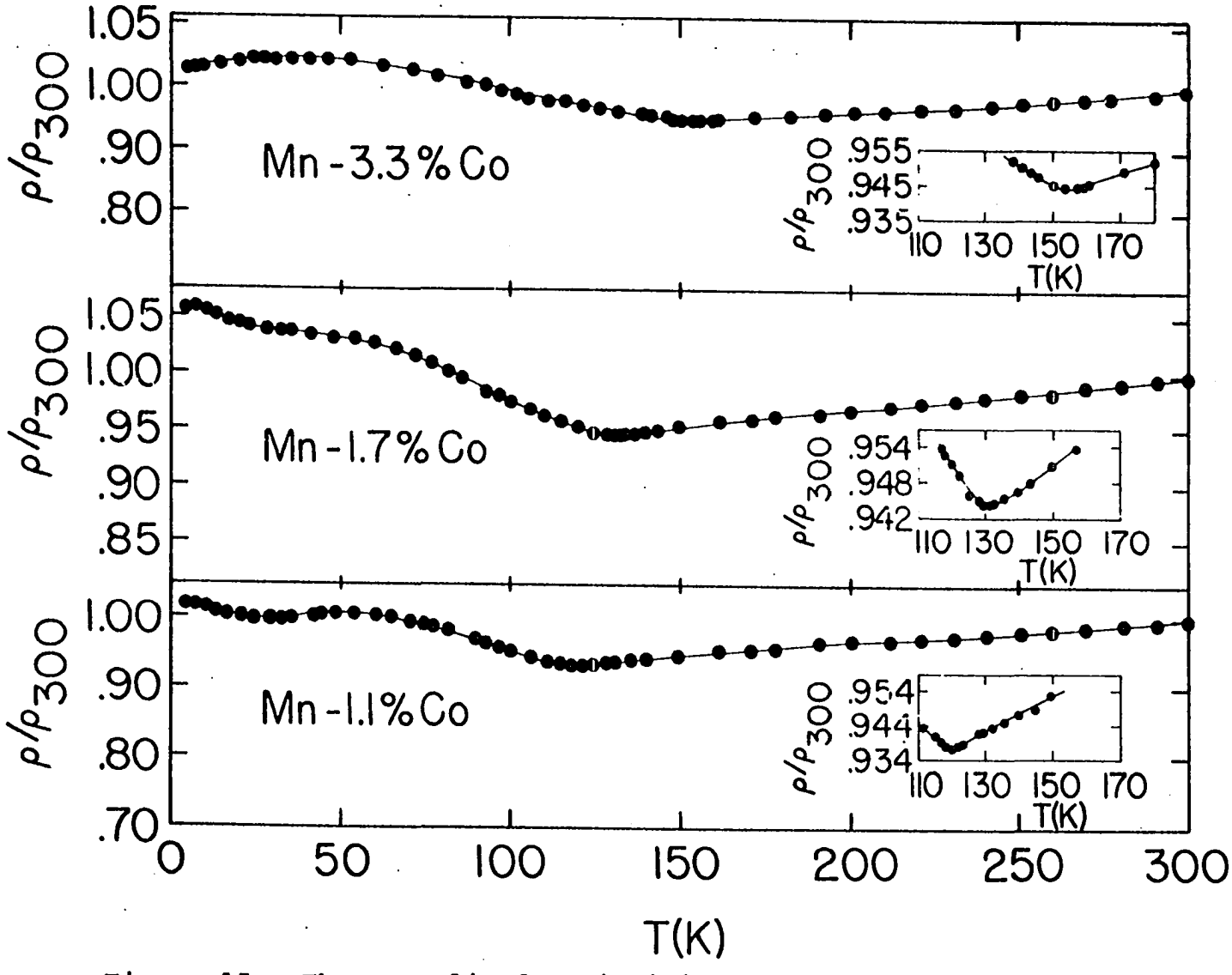

Figure 15. The normalized resistivity for several Mn-Co samples

whatever the mechanism that is responsible for the enhancement, it shows a marked dependence on the e/a ratio.

If, as was suggested for the Fe impurities, the two excess electrons on the Co atoms entered either into the conduction band or became localized about one of the Mn sites, we should see a change in the Neel temperature that is just twice that for Fe impurities. However, this is not quite the case as can be seen from Figure 13. The change in T_N for 1% Co is about 26 K, which is not quite twice the change for Fe (14 K/at.%). Also, the dependence of T_N on concentration is no longer linear.

This behavior would suggest that the shift in the Neel temperature depends indirectly or perhaps directly on some other factor other than the number of extra d-electrons introduced in the Mn lattice. Co, unlike Fe, increases the lattice constant and perhaps provides for a bit less direct exchange between the atoms. Such a contribution to the shift in the Neel temperature is in the right direction to account for the observed behavior. However, as will be pointed out shortly in the case of Mn-Ni alloys, where the increase in the lattice constant is even greater, we observed a unproportionately smaller shift in T_N. That is to say, the relative change in the lattice constant on going from pure Mn to Mn-Co is approximately 1/2 the change observed in going from pure Mn to Mn-Ni alloys; yet the observed change in T

for the Ni alloys is over 30 K smaller than what might be expected.

It would seem plausible that the Co atoms do not give up both excess d-electrons, but rather retain some small fraction of these electrons, localized about its nucleus. This would result in a slight reduction in the available d-electrons that might go into increasing T_N. This would probably result in a potential at the Co atom which is slightly different from that at the other Mn atoms. This, of course, would disturb the electronic structure of Mn and we might see a slow distortion of the rigid band approximation. Unlike the Mn-Fe samples, the low temperature end of the resistivity shows little or no tendency toward decreasing with decreasing temperature. It is interesting to note the vestige of a resistivity maximum that was so characteristic of the Mn-Fe alloys. This behavior would tend to suggest a large temperature-dependent spin disorder resistivity at low temperature. It is possible that the effect of alloying in Co has increased the moments to such an extent that the initial mode of AFM ordering is somehow becoming unstable. No doubt the exact situation will be revealed only through very accurate resistivity measurements and neutron diffraction studies.

We may summarize the results for the Mn-Co alloys as follows:

(a) Increased lattice constant: The increase in the lattice constant is opposite that observed for Fe, yet we observed an increase in T_N for one atomic percent that is only a few degrees from being twice that observed for Fe. This would seem to argue against the importance of direct coupling in causing the AFM ordering in Mn.

(b) Increase in T_N: This increase in the Neel temperature points up the importance of the e/a ratio in determining the onset of AFM in Mn. Although we do not see a perfect one-to-one correspondence between the number of excess d-electrons and the shift in the Neel temperature, there is clearly an over-riding and marked dependence on the number of d-electrons.

(c) Increased enhancement factor: This is in keeping with the effect observed in the Mn-Fe samples. An increased moment is observed at the inner sites in Mn by NMR studies. So if the enhancement results from the variation of the magnetic moment, this then is in keeping with of the magnetic moment, then this is in keeping with observed studies.

(d) Non-linear dependence of T_N: The failure of the Neel temperature to follow a linear dependence on concentration for the Mn-Co alloys, may suggest the failure of the rigid band approximation to hold for Co.

Mn-rich Ni alloys Ni, like Co, is soluble only up to a few atomic percent. Although the solubility is limited,

Kohara and Asayama (22) have suggested from their NMR studies very similar behavior for Mn-Ni alloys as that seen in the Mn-Fe and Mn-Co alloys. It would appear that the Ni atoms occupy the smaller sites (sites III and IV) in the Mn structure. They report a slight increase in the internal field at the inner sites (sites I and II). This would lead to an increased moment on these sites.

The results from the electrical resistivity measurements are shown in Figure 16. Like the previous samples, we see a rather large high-temperature resistivity. The mechanism responsible for the high temperature scattering is little affected by the alloying of elements with excess d-electrons. This might be expected if the mechanism is disorder-moment scattering above T_N. The resistivity very gradually decreases into the characteristic resistivity minimum, as the temperature is lowered. Below the resistivity minimum we see an enhancement in the resistivity which no longer has any vestige of a resistivity maximum. In Figure 14, we have plotted the enhancement factor selected at helium temperature (4.2 K) for lack of a better choice.

It is interesting to note a progressive disappearance of the resistivity maximum as we alloyed from Fe to Ni. The mechanism responsible for the enhancement must depend not only on the e/a ratio, but very markedly on the type of the impurity introduced. As can be see from the Fe alloys, which

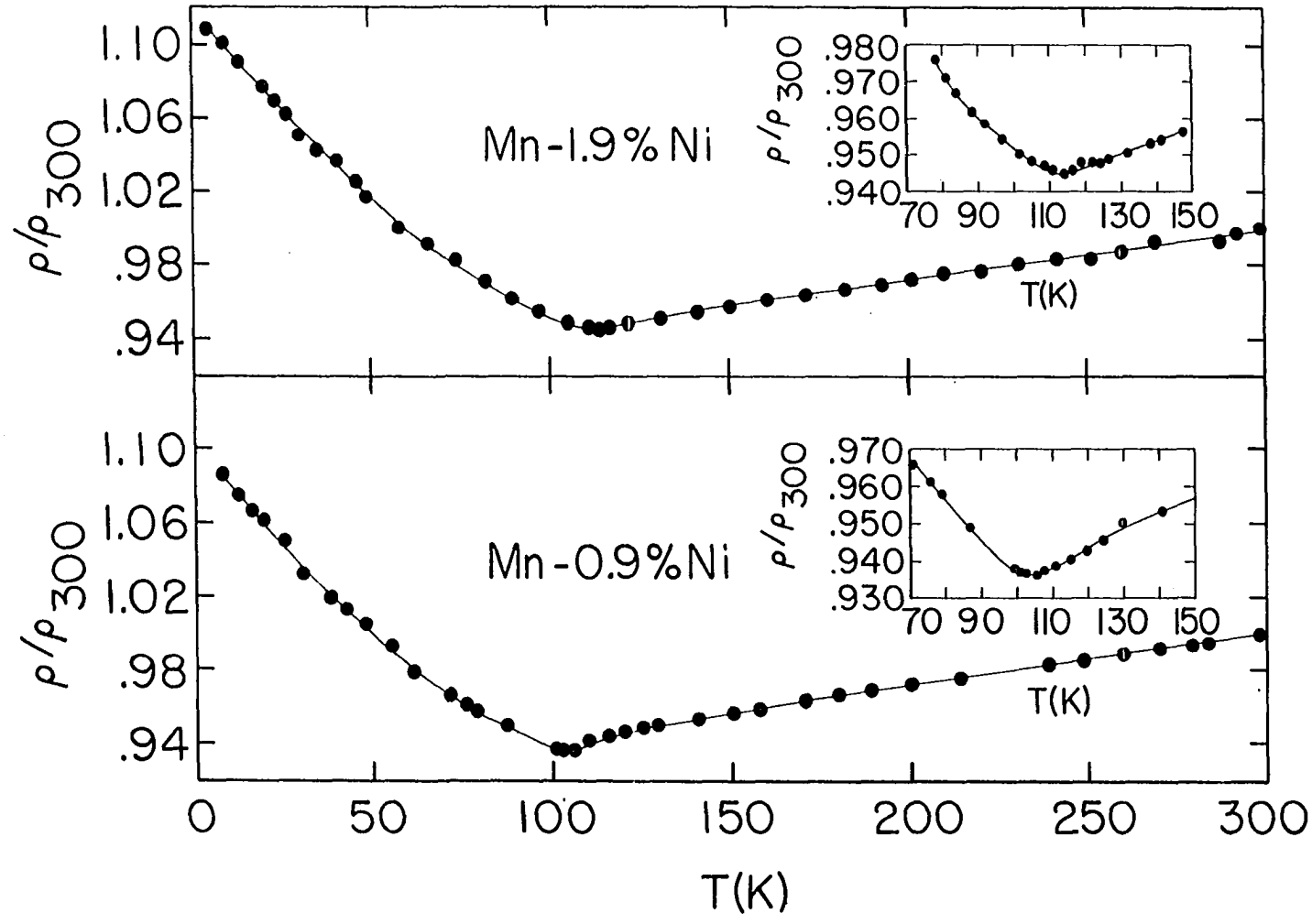

Figure 16. The normalized resistivity for several Mn-Ni samples

far exceed the e/a ratio of any of the Co or Ni alloys, there is a very pronounced maximum in all such alloys. This is difficult to reconcile with either of our previous models for the resistivity enhancement. In either mechanism, the spin disorder or energy gap should respond in a similar way for a given e/a ratio.

Alternately, one could propose an additional mechanism for the scattering below 45 K or 50 K. This could account for the slight secondary minimum in the Fe alloys, as well as the tendency toward an increased resistivity in the Co and Ni alloys. This mechanism could be sensitive to the particular electronic structure that each impurity brings to the Mn crystal. If one attempts to retain the rigid band approximation, which is not unreasonable in light of the systematicness of the data. The choice of such a mechanism is not obvious.

As alluded to above, the lack of a definite resistivity maximum is not the only anomalous characteristic of the Mn-Ni alloys. Instead of an increased Neel temperature with respect to the Co alloys, we find a marked decrease in the shift in the Neel temperature as a function of concentration. We find a change of about 10 K/at.% Ni. Also, the variation in the Neel temperature is now linear again. This is very difficult to reconcile on any of our previous models because of two observations. First, the Mn-Ni alloys increase the

the lattice constant an amount which is approximately twice the amount the Mn-Co alloys increased the lattice constant and almost three times that of Fe. Thus, we should see a much smaller decrease in the Neel temperature. Secondly, Ni contributes three extra d-electrons per Ni atom to the Mn lattice. So we should see an effect three times as strong if only the number of excess d-electrons are important. It is almost as if the Ni atoms contributed less than one electron per Ni atom to the mechanism that is responsible for the shift in the Neel temperature, if the simple model of a stronger AFM ordering accompanies the addition of extra electrons to the Mn lattice.

It would appear that we may take one of two approaches to the problem of the Ni alloys. One is to assume that Ni does not behave any differently from the Fe or Co impurities. The second is to assume a breakdown in the rigid band approximation. Let us consider for a moment the former. If Ni is in fact causing the same kind of change in T_N as the other impurities, we must assume that there is an underlying pattern of behavior that is common to all three sets of alloys. We had formerly suggested that it was the mere presence of additional d-electrons that was the all important factor. Certainly, they must have a lot to do with the AFM ordering but perhaps not in and of themselves. Suppose that an oscillating electron density is set-up surrounding the Ni

impurity. This type of idea has been suggested by Blandin (56), Daniel (57), and Blandin and Daniel (58). They have shown that the screening of an impurity by the conduction electrons is not necessarily concentrated in the immediate neighborhood of the impurity. There maybe a residual effect of longer range that falls off only as the square of the distance from the impurity atom. If this oscillating electron density had a minimum in the vicinity of site I, or II, a reduced electron density might be expected (see Figure 25). If we further assume that the tendency toward an oscillating electron density is small or non-existence for the Fe and Co impurities, a consistent model begins to appear. As the alloying process began with Fe, little or no distortion is caused in the lattice potential. This also could be largely true for Co. Thus, a large share of the excess electrons go into the conduction band or become localized about inner sites in the Mn crystal. By the time Ni is reached, a large share of the excess electrons may remain localized about the Ni nucleus. This would cause a reduced amount of participation by excess Ni electrons. If we then ascribe an oscillating electron density to the Ni impurity, we could see a reduced electron density at the inner sites in the crystal.

It is interesting to recall the Fedders and Martin (59) two-band model for the variation of the Neel temperature of antiferromagnets. According to them, T_N should be given by

the equation

$$T_N = B \exp(-1/\alpha) \qquad (3)$$

where α is sensitive and proportional to $A\gamma^2$ among other factors. γ^2 is the main overlap matrix element for an electron in the same band and A is the interaction area. In the case of Fe, Co and Ni impurities, all three impurities increase A, the interaction area, but both Fe and Co seem to increase the electron density (see Figure 25). Now, since γ should be directly related to the electron density and enters equation 1 as γ^2, γ should be the controlling factor in determining the Neel temperature. Thus, we may see a decrease in T_N for Ni as a result of a decrease in γ, although A is increased by Ni additions. This however, is probably only coincidental.

Let us now return to the latter suggestion of a breakdown in the rigid band model. This is certainly possible and was suggested by Shimizu (60). However, the breakdown of the rigid band appears difficult to reconcile on the basis of the symmetry of the shift in the Neel temperature. Intuitively, the experimental result would point to some other fundamental mechanism at work.

We may summarize the results for the Mn-Ni alloys as follows:

(a) Increased lattice constant: The increased lattice constant and reduced Neel temperature would suggest a direct type of coupling between the Mn atoms. However, there is no evidence of consistency between the changes in the lattice constant and the Neel temperature. Kasper and Roberts (5) have suggested that there are ranges of interatomic spacing, where the type of exchange between the respective Mn atoms differ. This would allow us to presuppose that the pure metal is near one of these change-over points, and the introduction of Ni carries the structure into a different type of exchange. This seems unlikely based on the results that will be reported below.

(b) Increase in T_N: Although we see an increase in T_N, it is disproportionately smaller for the number of excess d-electrons that the Ni atom has. However, it is not evident that all the Ni excess d-electrons participate in the ordering process. The NMR study would suggest that there is a lower electron density at the inner sites in the Mn crystal, when Ni is introduced, than when Fe or Co are introduced.

(c) Increased enhancement factor: The Ni alloys show a much larger enhancement factor than the Fe or Co samples. If this reflects the magnetic moment or energy gap as was suggested above, one might expect a reduction in the enhancement factor. This should occur if in fact there was a reduction in the magnetic moment as a result of a reduced electron den-

sity. Another possibility that exists, which we have not considered is an increasing moment below the Neel temperature. Oberteuffer et al. (13) have suggested a temperature dependence for the magnitude of the moments on sites I, II and III. Their study shows a slight increase all the way to helium temperatures. This is not inconsistent with measurements of the expansion coefficient of pure Mn (18,19). These measurements show a negative expansion below the Neel temperature. This probably has to be magnetic in origin and attributable (18) to spin waves, but certainly at least the results of a varying magnetic component. If there is a progressively greater temperature dependence on the moments as one alloys from Fe to Ni, the observed effect might be expected.

(d) Linear dependence of T_N: Because T_N varies linearly with concentration, one is forced to believe that the rigid band approximation is still in force. The dependence of T_N parallels that for Fe, where Ni appears to contribute effectively one excess d-electron to the ordering process.

Mn-rich Cr alloys Now we turn our attention to those impurity elements to the left of Mn in the periodic table. Cr has one less d-electron than does Mn. NMR studies have suggested that Cr atoms preferentially select the inner-most site (site I) in the Mn structure. More important perhaps is the observation that the moments on site I and site II are

greatly reduced and become comparable to those on sites III and IV.

The normalized electrical resistivity for two Mn-Cr alloys is reproduced from Williams and Stanford (2) and is shown in Figure 17. One notes a somewhat large drop in the high temperature resistivity. This is in keeping with the idea that the scattering is due largerly to the presence of magnetic moments above the Neel temperature, which are now reduced by the presence of the Cr atoms.

The change in the Neel temperature is about -14 K/at.% Cr. This is shown in Figure 18. This change is complementary to that observed for the Mn-Fe alloys. This strong dependence on the e/a ratio reemphasizes the importance of the d-electrons in determining the ordering in the Mn alloys with near-neighbor impurities. It is interesting to note that slightly over 3 atomic percent Cr will replace all of the type 1 atoms (at site I) in the Mn crystal. The relative percentage composition of the Mn atoms at each of the different crystal sites is shown in Table IX. Studies on a 5 at. % Cr sample (5,24) have shown that the onset of antiferromagnetic ordering does not occur in this alloy. This would tend to support the idea that the Cr atoms occupy site I with a marked decrease in the magnetic moments associated with that site.

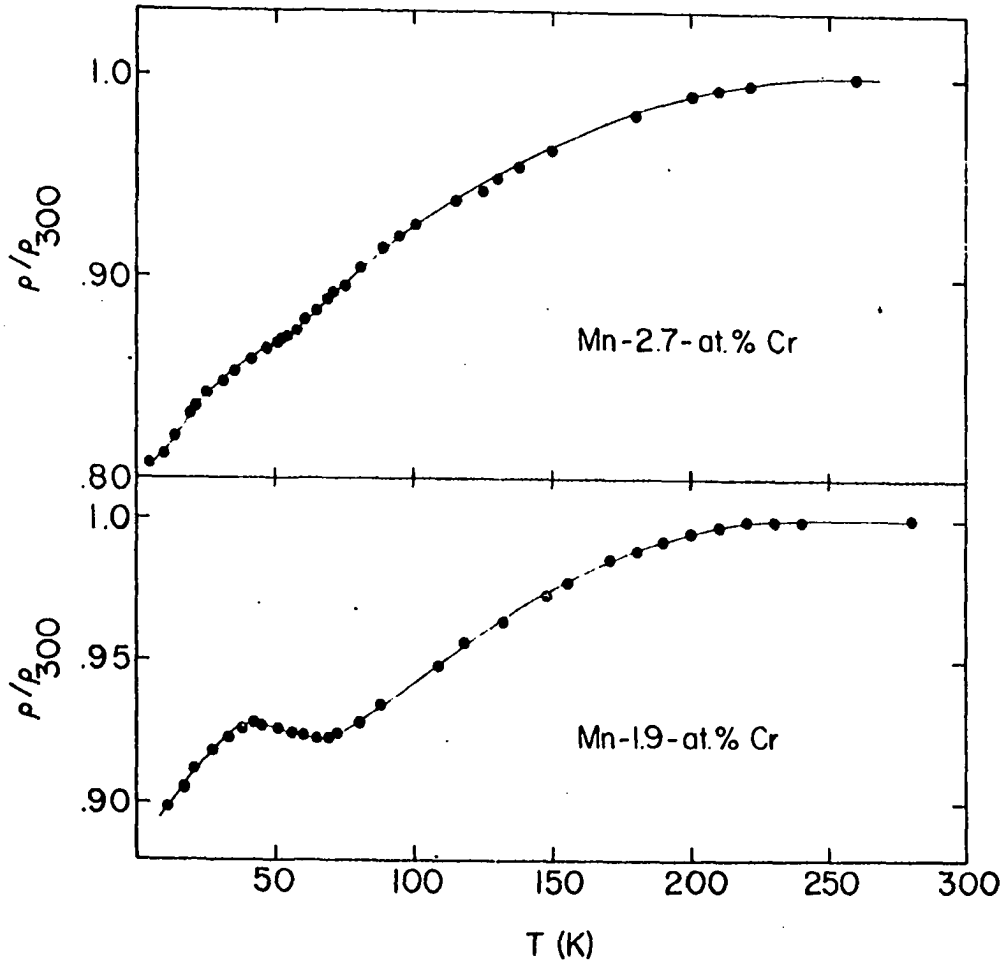

Figure 17. The normalized resistivity for several Mn-Cr samples

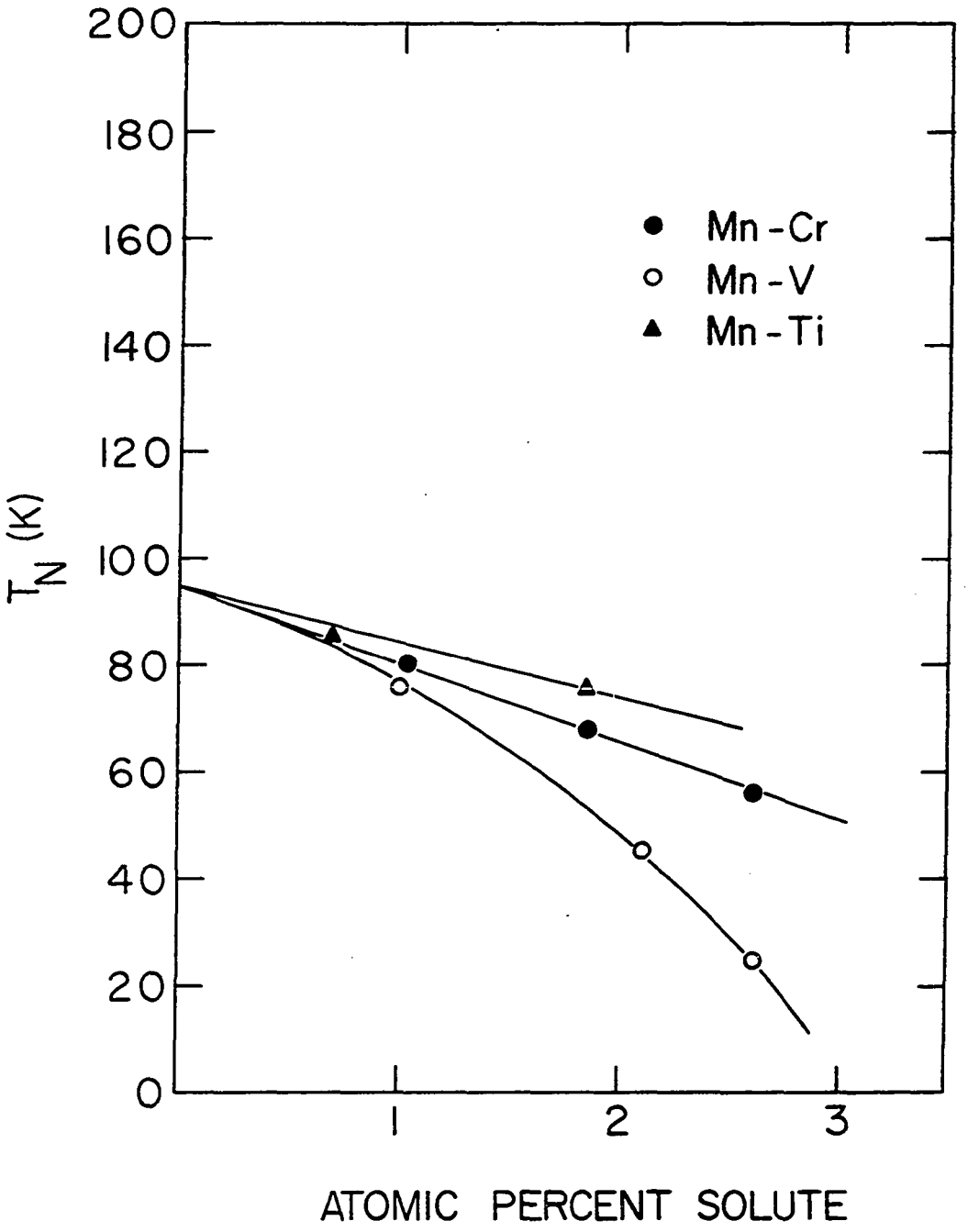

Figure 18. The variation of T_N as a function of atomic percent solute for Cr, V and Ti alloys

Table IX. Percentage of atoms in each Mn site.

Site	no. of atoms	at. %	CN*
I	2	3.45	16
II	8	13.79	16
III	24	41.38	13
IV	24	41.38	12

*CN refers to the coordination number for a site.

As can be seen from the resistivity data, a Mn-2.7 % Cr sample shows very little of the anomalous maximum and minimum observed in previous samples. This is consistent with the idea of a decreased magnetic moment resulting in a reduced coupling between respective atoms. It is interesting to note that the enhancement factor for these alloys has dropped below the value for pure Mn (see Figure 19). This is in accordance with what would be expected with a decreasing magnetic moment and energy gap. Yet, it would equally represent a decrease in the spin disorder or a marked decrease in the temperature dependence of the moment's magnitude below the Neel temperature. Of course those effects are not indepen-

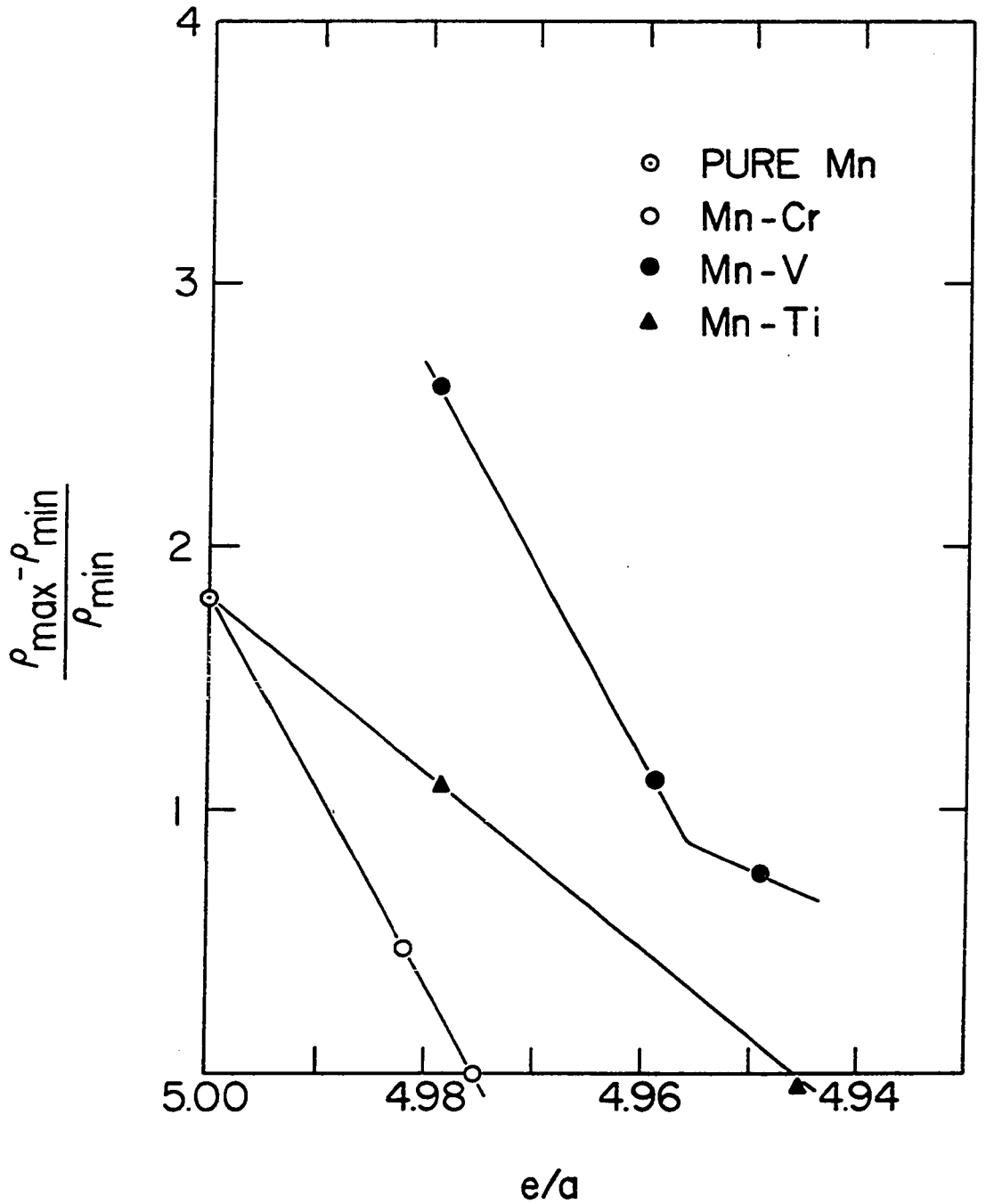

Figure 19. The variation of the enhancement factor, F, as a function of e/a for Cr, V and Ti alloys

dent of each other and the observed decrease in the enchancement factor is probably the result of a combination of them.

It would seem plausible to expect that the addition of Cr to Mn will not modify the electron structure of pure Mn to any great extent. Some limited experimental results are available from a NMR study (24) to support this assertion. The nuclear spin-spin relaxation time, T_2, was observed for several Mn-Cr alloys and it was found that T_2 showed the same behavior in the alloys as in the pure metal. It would appear that the important factor may be the relative shift in the positicn of the Fermi energy level.

It may be tenable to suggest for Mn, as was the case for Cr, two nearly symmetrical and equal Fermi surfaces. One such surface would be associated with electrons, while the cther with holes. Under the assumption of the rigid band approximation, the effect of alloying Cr into Mn is to reduce the size of the electron Fermi surface. Now T_N should be determined in part by the interaction between the two surfaces across an area A. Thus, as the electron surface is reduced, the interactien area is correspondingly reduced, and we see a drop in T_N. In a similar fashion, the introduction of Fe into the Mn lattice would be expected to increase T_N, since A has been increased by the addition of extra electrons to the electron surface. This kind of idea fits well with the

results for nearest and next-nearest neighbor impurities, but seems to breakdown for alloys beyond this.

This seemingly quick disappearance of AFM with Cr additions to Mn might be understood on the above model by assuming that the separation between the two surfaces in the pure metal is such that it is very near the minimum interaction area. The further decrease of the interaction area very quickly makes it impossible for the AFM state to exist. Contrasted with the addition of Fe, no such upper limit exists until the shifted electron surface begins to penetrate the hole surface. This may not occur until the e/a ratio has been changed by 15 or 20 %.

We may summarize the Mn-Cr results as follows:

(a) Decreased lattice constant: Now a decreased lattice constant should show an increased exchange coupling if the major mechanism was one of direct coupling. We do not see an increase in T_N, but rather a decrease. Moveover, we observed a decrease in the lattice constant for Fe but an increase in T_N. This behavior would suggest that although direct coupling may play a role in the AFM ordering, it is not a major factor.

(b) Decrease in Neel temperature: This again suggests that the mechanism responsible for AFM ordering is strongly coupled to the e/a ratio. This is further emphasized by the complementary nature of the Fe and Cr results.

(c) Decreased enhancement factor: This is in harmony with the observed disappearance of AFM ordering and the decrease in magnetic moments on the inner sites in Mn. Since a decreasing magnetic moment implies a decreasing energy gap, the effects on the transport properties below the Neel temperature should not be as drastically affected as in the previous alloys. This is reflected in the resistivity data, by a decrease and finally disappearance of a resistivity maximum. In the discussion of the previous samples, we alluded to a possible spin-disorder resistance below the Neel temperature. Such a resistance would be equally affected by a reduction in the strength of the magnetic moments. Thus, we can not resolve which is the more important mechanism.

(d) Linear dependence of T_N: The almost linear dependence of T_N on the amount of solute present would suggest an almost direct addition or substraction of a constant shift in T_N depending on the sign of the net change in d-electrons. That is to say, the exchange interaction is made stronger or weaker by the excess or deficiency of d-electrons in the Mn structure. This is comparable to a situation where only the relative position of the Fermi level is important. Thus, little or no distortion of the rigid band approximation is caused by the alloying of the two nearest-neighbor impurities Cr and Fe, into Mn.

Mn-rich V alloys The introduction of V into Mn further reduces the Neel temperature. At first sight, this would be expected since V has two less d-electrons than does Mn. The decrease is no longer quite linear as it was for Cr. The variation of the Neel temperature is reminiscent of the Mn-Co results (see Figure 15). The NMR study of Kohara and Asayama (22) has shown that the V atoms, like the Cr atoms, prefer the inner sites (sites I and II) in the Mn crystal. Moreover, their introduction in Mn shows a reduction in the moments on the surrounding sites.

Although the Mn-V alloys were not studied in this present work, it is worth noting some of the findings of Williams and Stanford (2). To this end, the electrical resistivity from their study is reproduced in Figure 20. There appears to be a reduction in the high temperature resistivity in accordance with a reduced moment on the Mn atoms. Unlike any of the other alloys, the resistivity reduces into a rather broad minimum. After the minimum, the resistivity shows a tendency toward a resistivity maximum. The maximum is not sharp and varies from one concentration to the next. This would suggest the presence of an increased amount of the mechanism responsible for the resistivity increase below the Neel temperature in the Mn-V samples. If the V atoms not only entered site I, but also entered site II as well, this low temperature behavior might follow. To ef-

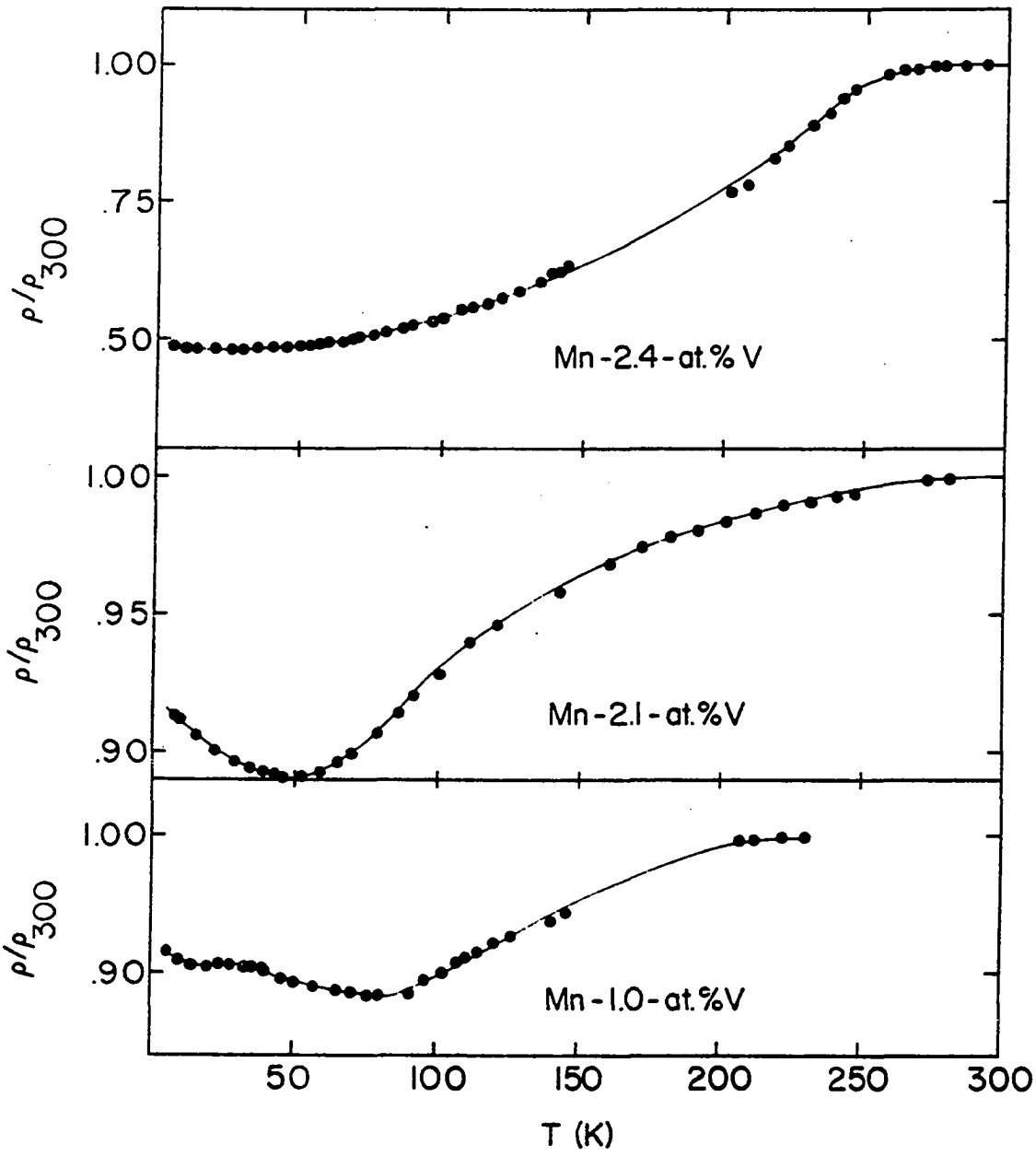

Figure 20. The normalized resistivity for several V alloys

fectively reduce the scattering mechanism may require a much larger percentage of V atoms.

Recalling the enhancement factor, we see a gradual reduction with increasing solute concentration. However, the factor appears tc be correspcnding higher than that observed for the Mn-Cr alloys (see Figure 19). This would be consistent with the idea of the V atoms selecting site II more often than site I. With a larger number of site II positions taken by the V atom than were taken by the Cr atoms, we might expect a slightly increased moment and energy gap, as well as perhaps a larger tendency toward spin-disorder. Furthermore, if our interpretation of the position of the Cr atoms in the Mn structure is correct, we might expect to see the AFM order disappear in the Mn-V samples by the time we have reached a 2.0 % V concentration, if the effect was an indirect one. This does not appear to happen, which lends support to a direct effect or possibly the occupancy of some of the site II positions by V atcms, if it is indirect.

The variation of the Neel temperature with concentration is shown in Figure 18. Although the change in T_N is not linear, it is comparable to what might be expected for the first few percent on our model of simply substracting electrons from the electron piece of Fermi surface. By so doing the interaction area is reduced and the Neel temperature is correspondingly reduced. We may attribute slight deviations

to other factors such as the amount of overlap of d-wave functions and distortion of the rigid band approximation. However, the plausibility of this will have to be seriously question as we move to a later discussion of the Mn-Ti results.

We may summarize the results for the Mn-V alloys as follows:

(a) Decrease in lattice constant: The change in lattice constant for V is comparable to the change observed for Fe. Yet, we see a positive shift for the Mn-Fe alloys and a negative one for the Mn-V alloys. Thus, if the direct coupling between atoms plays any role in the AFM ordering, it is far out weighed by other mechanisms.

(b) Decrease in the Neel temperature: The decrease in the Neel temperature is in accordance with the idea of a reduced interaction. Since we observed a decrease in the lattice constant, favoring an increased direct interaction, we must attribute much of the change in the Neel temperature, to an indirect interaction.

(c) Decrease in enhancement factor: This is expected as a result of a decreased moment on the Mn atoms. The scattering mechanism below the Neel temperature appears to be linked to the moments that exist in the Mn structure. Whether it is the result of spin-disorder or temperature varying moments on the atoms, a reduction in these effects would be expected with a decreasing magnetic moment.

(d) Non-linear dependence of T_N: The appearance of a non-linear dependence in T_N in the next-nearest neighbor impurities gives support to the idea of an optimum e/a ratio for Mn. Whether this is a manifestation of the breakdown in the rigid band model or represents a change in the exchange interaction is not obvious at this point.

Mn-rich Ti alloys We now turn our attention to the last of the 3-d transitional impurities. Ti has three less d-electrons than Mn. We do not have available any information on the effect Ti has on the crystal structure of Mn. In β-Mn the introduction of Ti leaves the lattice constant unchanged. Of course, there are grave differences between the α and β structure of Mn. We will assume that Ti probably enters the inner sites (sites I or II) where it decreases or at least leaves the lattice constant unchanged. This assumption is supported in part by the systematic trend observed in the previous alloys and also by the observed shift in the Neel temperature for Mn-Ti alloys. We further assume that there is a reduction in the moment on the Mn atoms. This is in keeping with the observed trend.

The normalized electrical resistivity for several Mn-Ti alloys is shown in Figure 21. The data shows a somewhat smaller rate of decrease in the high-temperature resistivity when compared to Cr or V alloys. This may be an indication of slightly larger moments remaining on the Mn atoms than

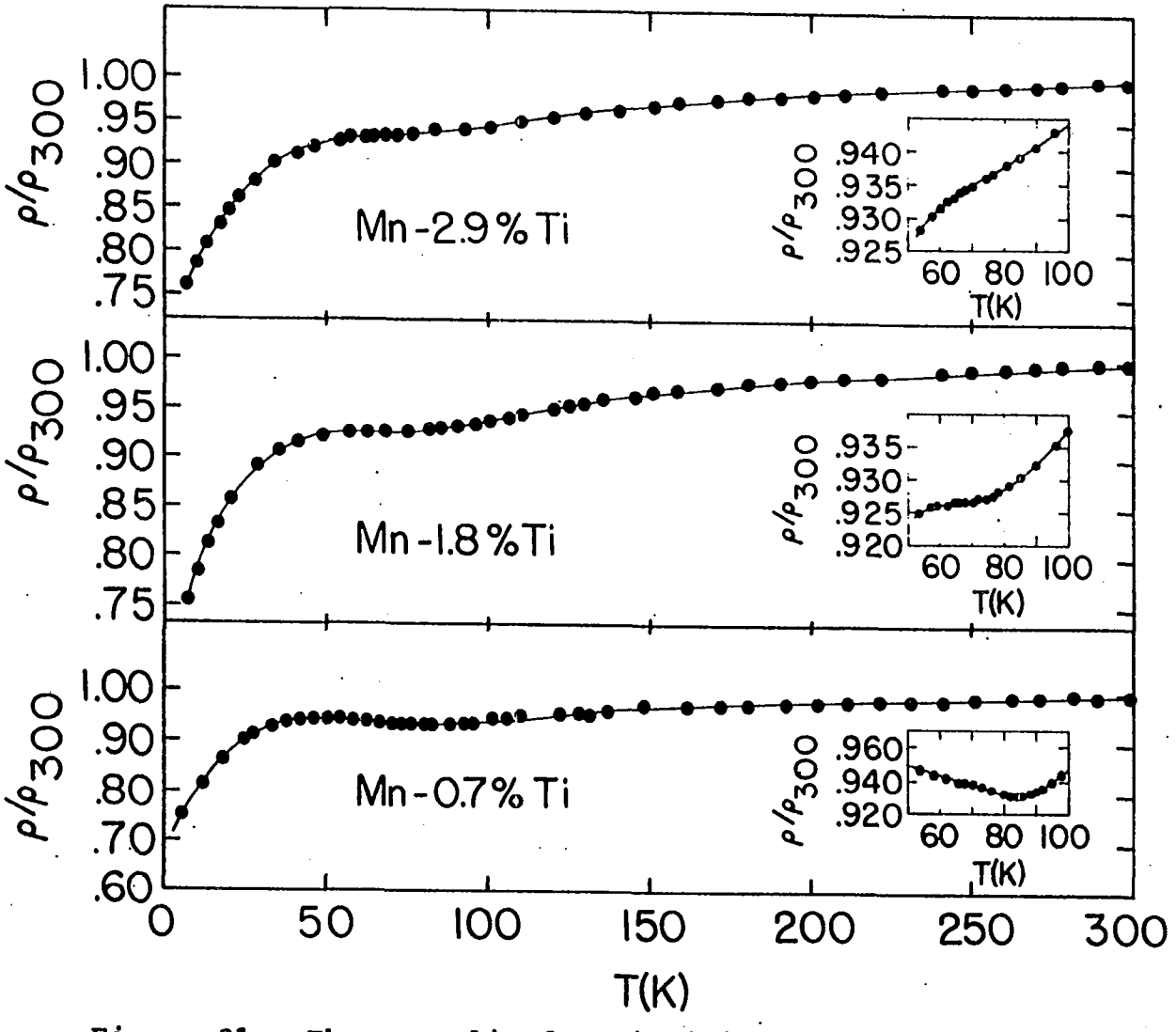

Figure 21. The normalized resistivity for several Ti alloys

was the case for Cr or V. This could be the result of Ti atcms entering site II as opposed to site I. The resistivity shows the characteristic minimum and surprisingly a very definite remnant of the resistivity maximum in the 1% sample. This low temperature behavior lends credence to the idea of a slightly larger moment existing in the Mn-Ti alloys than existed in either the Mn-Cr or Mn-V alloys.

The change in the Neel temperature with concentration of Ti is about 10 K/at. % Ti. The variation is again linear (see Figure 18). It is interesting to recall that the Ni results for the variation of the Neel temperature was also linear. Moreover, the Ti results complement the Mn-Ni findings. It is difficult to reconcile first a linear, than a non-linear and finally a linear dependence in T_N for nearest, next-nearest and next-next-nearest neighbor impurity respectively. If it was a simple breakdown in the rigid band approximation, one would not expect to see such a symmetrical variation in T_N among neighbor impurities. One is forced to look for some fundamental underlying mechanism.

One simple approach to the problem would be to attribute variation in the Neel temperature to a direct variation in the magnetic moment on the inner Mn sites. The excess electrons from the Fe and Co atoms could become localized in part about the inner sites causing an increased moment. By the time we reach Ni the moment has begun to decrease. It is at

this point that we need to provide a mechanism to account for a reduced moment. Similarly, we may argue that the addition of Cr and V reduces the moment by a reduction in the number of 3-d electrons available to contribute to the moment. However, once we get to Ti, we are again faced with the problem of providing a mechanism responsible for increasing the moment. The anomalous behavior of the next-next-nearest neighbor alloys does not, at first sight, lend itself to an immediate explanation. We will return to this point in the closing paragraphs of the discussion sections on Mn-alloys of the first transitional period.

Let us return for a moment to the low temperature behavior of the resistivity. We observe for the Mn-Ti alloys a progressive disappearance of both the resistivity minimum and maximum. The 3% Ti sample shows little or no minimum in its resistivity curve. This may be an indication of the disappearance of AFM ordering. Although there may be a slight inflection point near 85 K, it is much too faint to be conclusive. Whether the disappearance of AFM ordering occurs at exactly this concentration is not critical. The important observation is that it does seem to disappear within a few percent of this concentration. This would not be inconsistent with the Ti atoms selecting site II over site I. We may summarize the result for the Mn-Ti alloys as follows:

(a) Variation of the lattice constant: The variation of lattice constant is not experimentally known, but may decrease as indicated by the shift in the Neel temperature.

(b) Decrease in Neel temperature: This has been reflected in all samples that are to the left of Mn. However, the variation would suggest not only a dependence on the e/a ratic but some other mechanism. This is made clear by the anomalous behavior of the Mn-Ti alloys.

(c) Decrease in the enhancement factor: This is in agreement with a decreasing moment on the Mn atoms. Unfortunately, the experimental dependence of the magnetic mcment for the Mn-Ti system is not known.

(d) Linear dependence of the Neel temperature: This behavior reflects the idea of a simple reduction of the Neel temperature by a decrease in the number of d-electrons. However, there is no one-to-one correspondence observed.

Can the behavior of all the 3-d Mn-alloys be explained cn the bases of one model? The answer is probably no. If we consider the two nearest-neighbor impurities Fe and Cr, their linear tendency in shifting the Neel temperature would imply a simple addition or subtraction of d-electrons from a band structure that approximates that of pure Mn. As such, we may postulate a model along the lines of the two band model for Cr, where there are two nearly equal pieces of Fermi surfaces in close proximity of each other. One is an electron Fermi

surface, the other a hole surface. These two surfaces interact over an area A, which determines in part where the Neel temperature will occur. The introduction of Fe enlarges the electron surface, while contracting the hole surface. Thus, the effect of the introduction of Fe atoms is to increase the interaction area A, and we see a corresponding increase in T_N. On the other hand, the introduction of Cr impurities shrinks the electron surface, while enlarging the hole surface. By so doing, the effective interaction area is reduced and we see a corresponding decrease in the Neel temperature.

Here we assume the d-wave functions for Fe and Cr are not very different from that for pure Mn, so the all important factor becomes the relative shift in the Fermi surface. This type of behavior is clearly suggested by the variation of the Neel temperature with solute (see Figure 22). The figure reflects a near perfect inversion about the Neel temperature for pure Mn up to two or three atomic percent solute. This is particularly true for nearest and next-next-nearest neighbor impurities.

From consideration of the implications of Figure 22, one is led logically to plot the Neel temperature as a function of the e/a ratio. If the important factor is the relative position of the Fermi surface, an e/a graph of the Neel temperature should reveal this. The Neel temperature as a func-

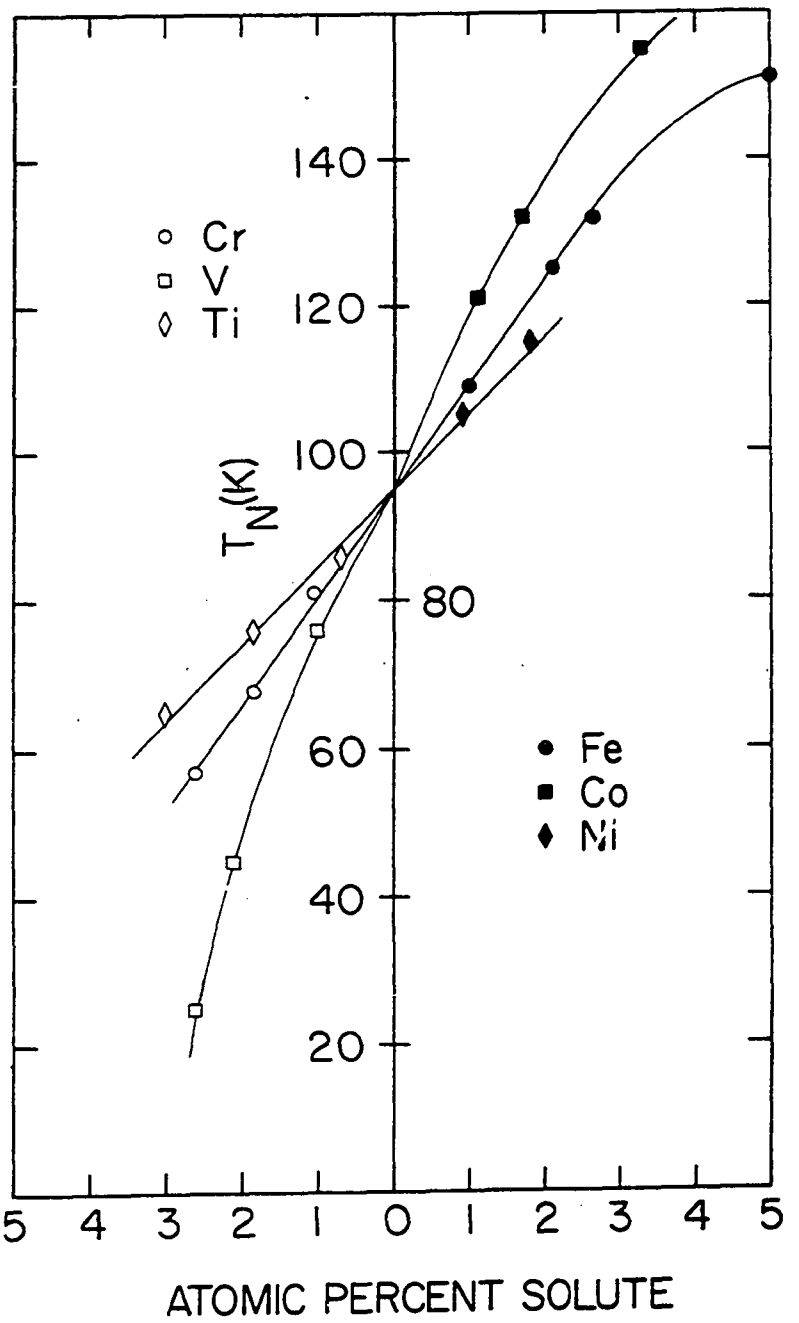

Figure 22. The variation of the Neel temperature as a function of atomic solute for alloys of the first transitional period

tion of the e/a ratio is shown in Figure 23. Although one line has been fitted to the data for the nearest, and next-nearest neighbor impurities, two separate lines could be drawn for each of the impurities without much overlap. However, we feel one line best represents the data when one allows for small departures from the rigid band model for higher alloys concentrations. Yet, it is probably beyond question to attempt to account for the clearly different line for next-next-nearest neighbor impurities. This marked departure makes it evident that the previous model is much too simple to account for the observed variation in the Neel temperature.

According to our simple model, as we move further away in our choice of impurities, we should see a change in the Neel temperature equalling factors of two and three for the next-nearest and next-next-nearest neighbor impurities, if the model is correct. However, we do not see this behavior. For the next-nearest neighbor we find a discrepancy of 3% to 5% below what would be predicted by the above model. The discrepancy for-next-nearest neighbor is as much as 20%.

This may be attributed to one of two considerations. The first is a breakdown in the rigid band approximation. We may be able no longer to approximate the energy bands of the alloys with that of pure Mn. This is certainly not implausible in light of the delicate balance that must exist

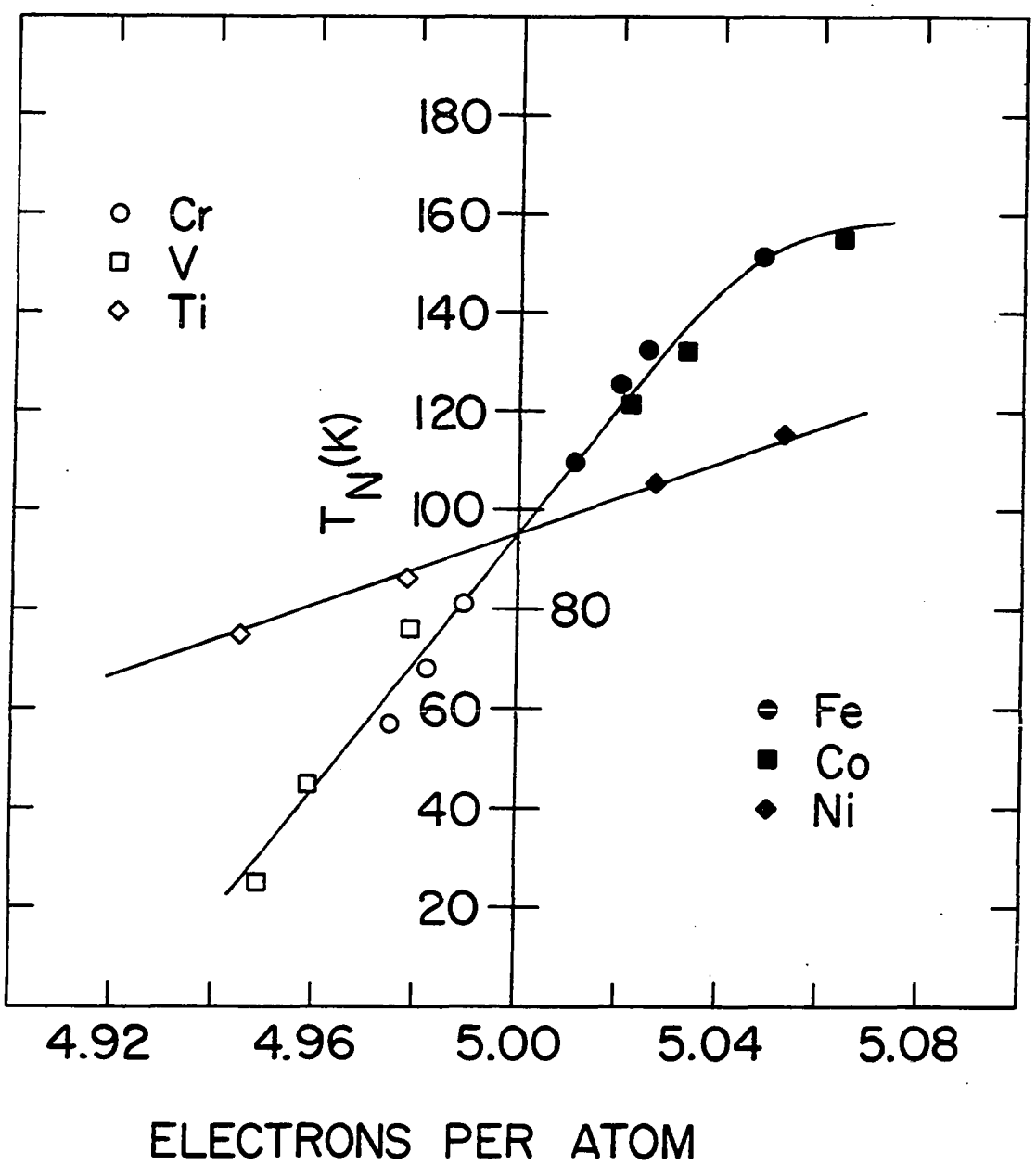

Figure 23. The variation of the Neel temperature as a function of the e/a ratio for the alloys of the first transitional period

in the pure metal. Yet, it does seem untenable in light of the symmetry of the data. One is hard pressed to accord a symmetrical breakdown in the rigid band model (see Figure 24). Certainly there should be an upper limit to which impurities can be added to Mn before affecting the energy band significantly, as well as some limit on the type of impurity. The occurrence of the former may be ruled out on the basis of the behavior of the higher percentages of Fe solute. However, the latter cannot be so easily ruled out.

One must grant that there may well be a limit on the type of impurity that the Mn structure will accept before becoming markedly changed. The intra-atomic Coulomb potential could become very different as one alloys across transitional periods. Yet, the interesting point is the need to account for a near one-to-one change in the Coulomb potential of the impurity solute on the right and left of Mn, coupled with the relatively different sites of occupancy. Of course, we can not completely rule this possibility out on the basis of this observation, but surely it is not the most probable cause.

The other alternative is to introduce one or more additional mechanisms that contribute to the actual determination of the Neel temperature. One such mechanism would be the variation in the amount of localization of the d-wave functions as one moves across the transitional period. It is ex-

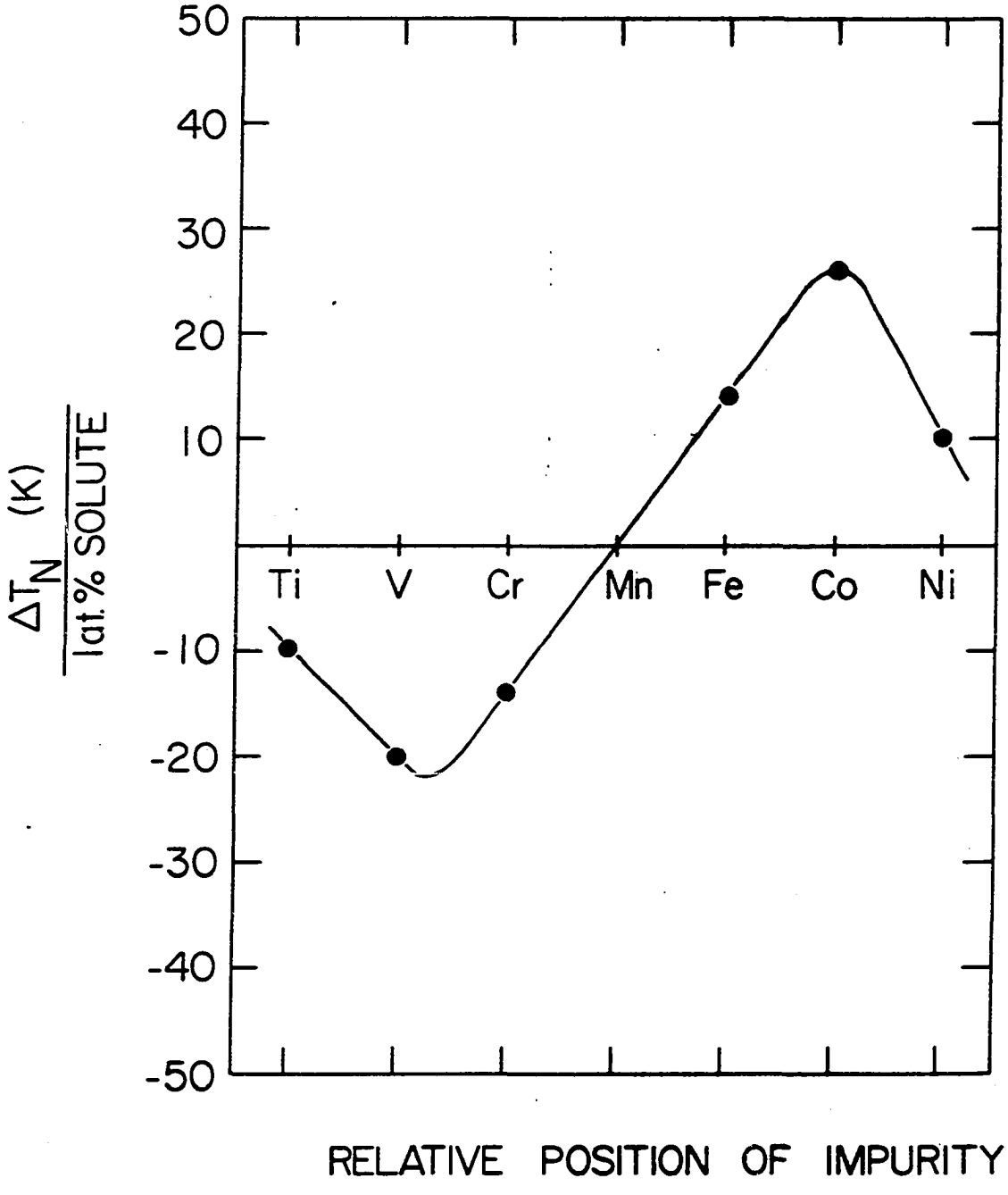

Figure 24. The variation of the Neel temperature per one atomic percent solute as a function of the position of the 3-d impurities

pected that the d-wave functions become more localized as the period moves from Ti to Ni. This is in the right direction if a direct coupling between atoms existed, since this would tend to reduce the exchange. For an indirect exchange mediated by conductiсn electrons, this is in the wrong direction, since a more localized wave function would tend to polarize the conduction electron even more and presumably result in an increased Neel temperature.

Even if we could associate a negative contribution to the Neel temperature as a result of more localization of the d-wave functions, it would seem unreasonable to expect to account for such large discrepancies in the Neel temperature of the next-next-nearest neighbcr impurity alloys. We observed over a 20% discrepancy in the Neel temperature of these alloys, when ccmpared to the expected Neel temperature based on the simple model of direct dependence of T_N on the number of excess d-electrons.

Another possibility which was mentioned earlier is a varying electron density. If the electron density, say at site I, depended on the type of impurity that was introduced into Mn, we might well see a similar dependence in the Neel temperature. In Figure 25, we have plotted the shift in resonance frequency per 1 at. % solute for the alloys studied in the first transitional period by Kohara and Asayama (22) using the NMR technique. Now this shift is related to the

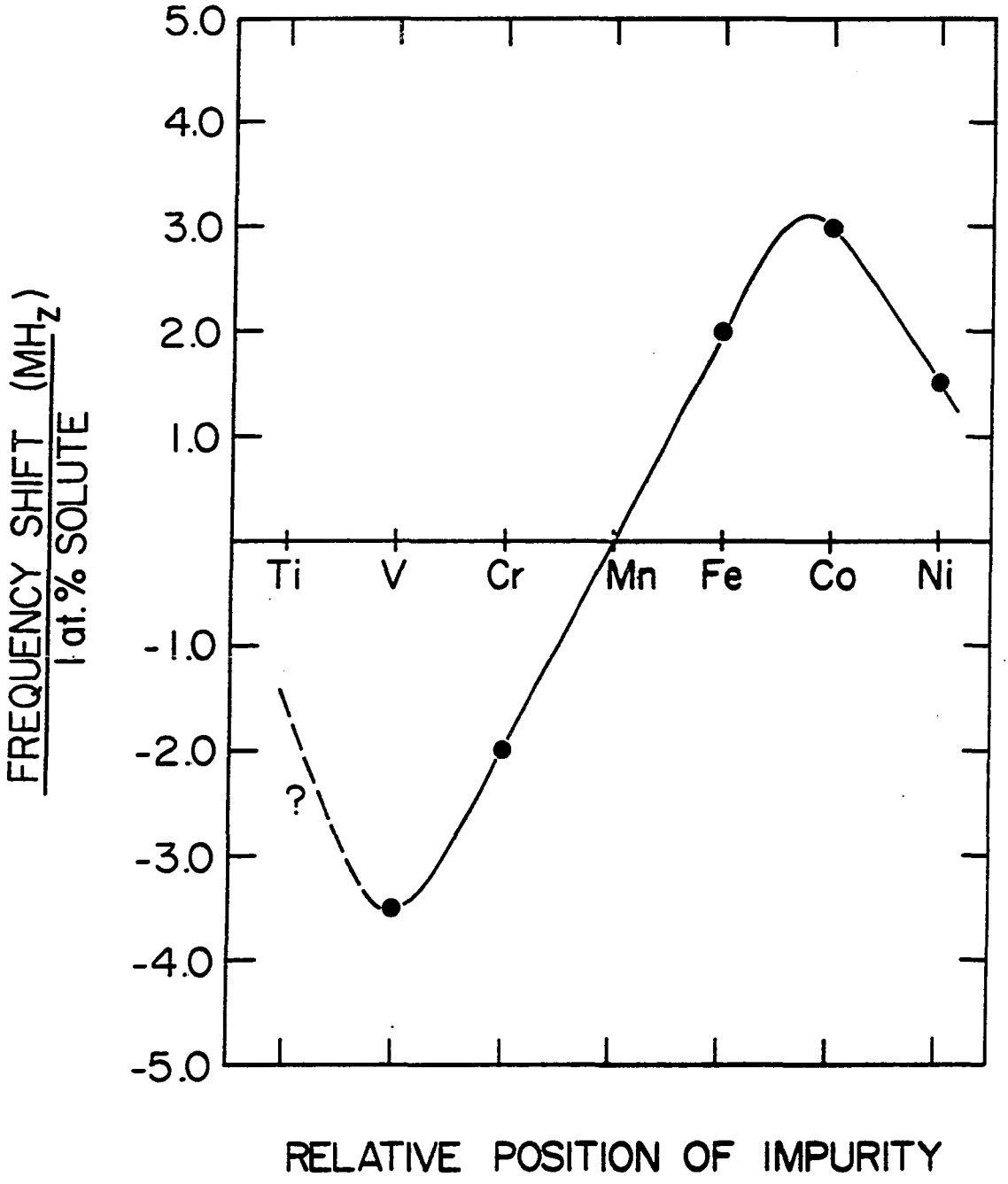

Figure 25. The variation of the frequency shift per one atomic percent solute as a function of the relative position of 3-d impurities [from the data of Kohara and Asayama (22)]

electron density and to a first approximation represents the variation in the electron density. As can be seen by comparing Figure 25 with Figure 24, there is a very similar pattern of behavior. Figure 25 shows the shift for site I in the Mn crystal, where the largest moment resides. Clearly this site will determine in a larger part where the Neel temperature occurs. The fact that the variation of the resonance frequency at site I follows closely the variation in the Neel temperature gives support to this idea. If we assume that the nearest and next-nearest neighbor impurities contribute to the electron density at the inner sites proportionately to the sign and magnitude of the change in the e/a ratio, the Neel temperature would increase or decrease accordingly. If by the time the next-next-nearest neighbor impurities are reached the electron density at the inner sites is no longer proportional to the e/a ratio, anomalous effects may appear in the variation of the Neel temperature. That is to say, the electron density may become proportional to some fraction of the e/a ratio perhaps due to shielding or some other similar mechanism.

4-d transitional impurities

We now turn to 4-d impurities, where the d-wave functions have become less localized. At the beginning of the period, for ground state configuration, there are two elec-

trons in the 5-s level. By the time niobium is reached, there is only one electron in the 5-s level, which continues to be true for the rest of the period. This implies that when compared to the 3-d and 4-s levels of the first period, the 4-d levels in the second period are relatively lower than the 5-s level.

Mn-rich Ru alloys Ru has one more additional 4-d electrons than the 3-d electrons of Mn. It is in the same column with Fe. X-ray work by Kohara and Asayama (22) indicates that the lattice constant of Mn is increased upon the introduction of Ru into the crystal. In the same work the authors report the probable occupation of the smaller sites (sites III and IV) by the Ru atoms. Ru atoms tend to increase the internal field on the crystal, particular at the inner sites (sites I and II). The increase is slightly larger than that observed for Fe. This is worth noting when the variation of T_N for the Mn-Ru alloys is compared to that for the Mn-Fe alloys (See Figure 26).

The initial report on the variation in the Neel temperature for Mn-Ru alloys was reported by Williams and Stanford (2). We have reproduced, in part, the electrical resistivity from their study (see Figure 27). The resistivity shows a rather large high-temperature value, with little temperature dependence. This is in agreement with the observation of the 3-d impurities to the right of Mn in the periodical table.

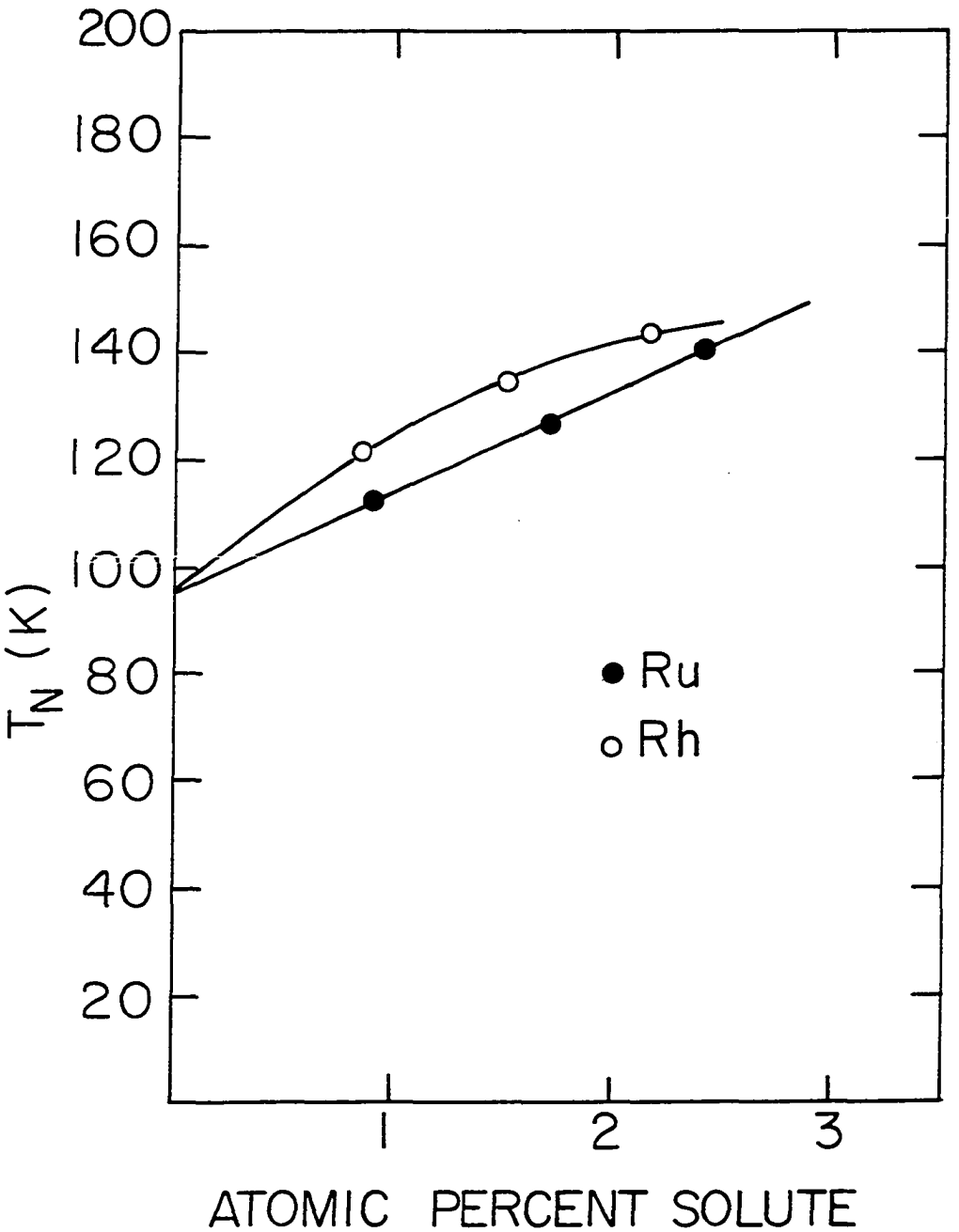

Figure 26. The variation of T_N as a function of atomic percent solute for Mn-Ru and Mn-Rh alloys

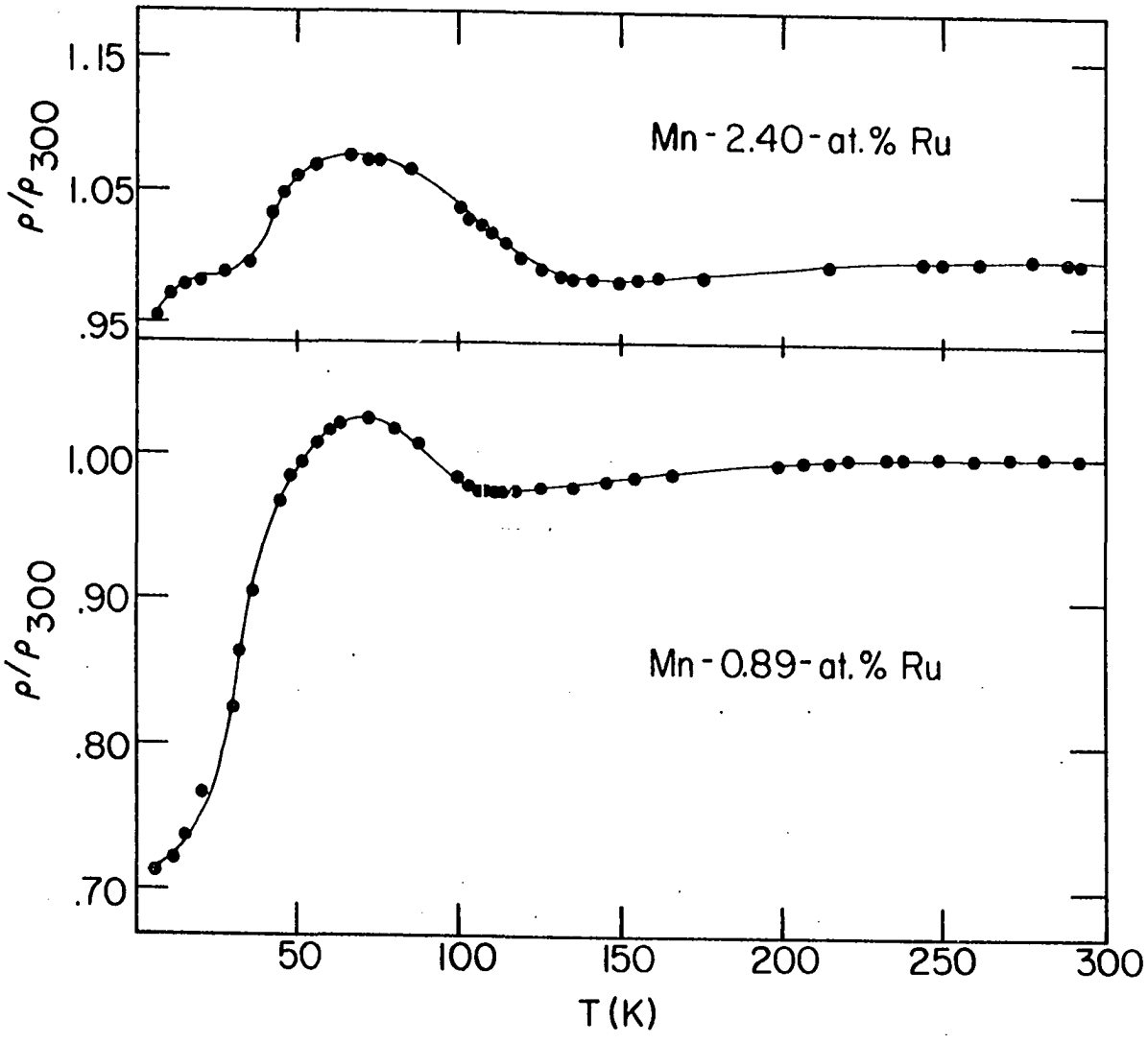

Figure 27. The normalized resistivity for several Mn-Ru alloys

As pointed cut before, this is probably the result of scattering due to disordered moments. The resistivity shows a characteristic minimum and maximum. The parallel between the Ru and Fe data is unmistakable. Based on the structure of the resistivity, it would appear that there is little difference between the effect of Ru and that of Fe on the AFM ordering in Mn. This provides a strong argument against direct coupling since Ru increases, while Fe decreases the lattice constant, but yet the shift in T_N is comparable. Also the importance cf localization of the d-wave function is eliminated as a serious mechanism since, there is a marked difference in localization in going from 3-d to 4-d elements.

We observed a large enhancement in the resistivity below the Neel temperature. The enhancement factor is shown in Figure 28. The enhancement factor must represent some fundamental property of the AFM ordering. Furthermore, this must be closely linked to the size and perhaps the variation of the magnetic moments. We have observed an increasing enhancement factor with increasing moment and likewise a decreasing enhancement with decreasing moment. As can be seen by comparing Figure 29 with Figure 28, the variation of the enhancement factor looks very much like the variation of the internal field and thus the magnetic moment. The conclusion is tempting.

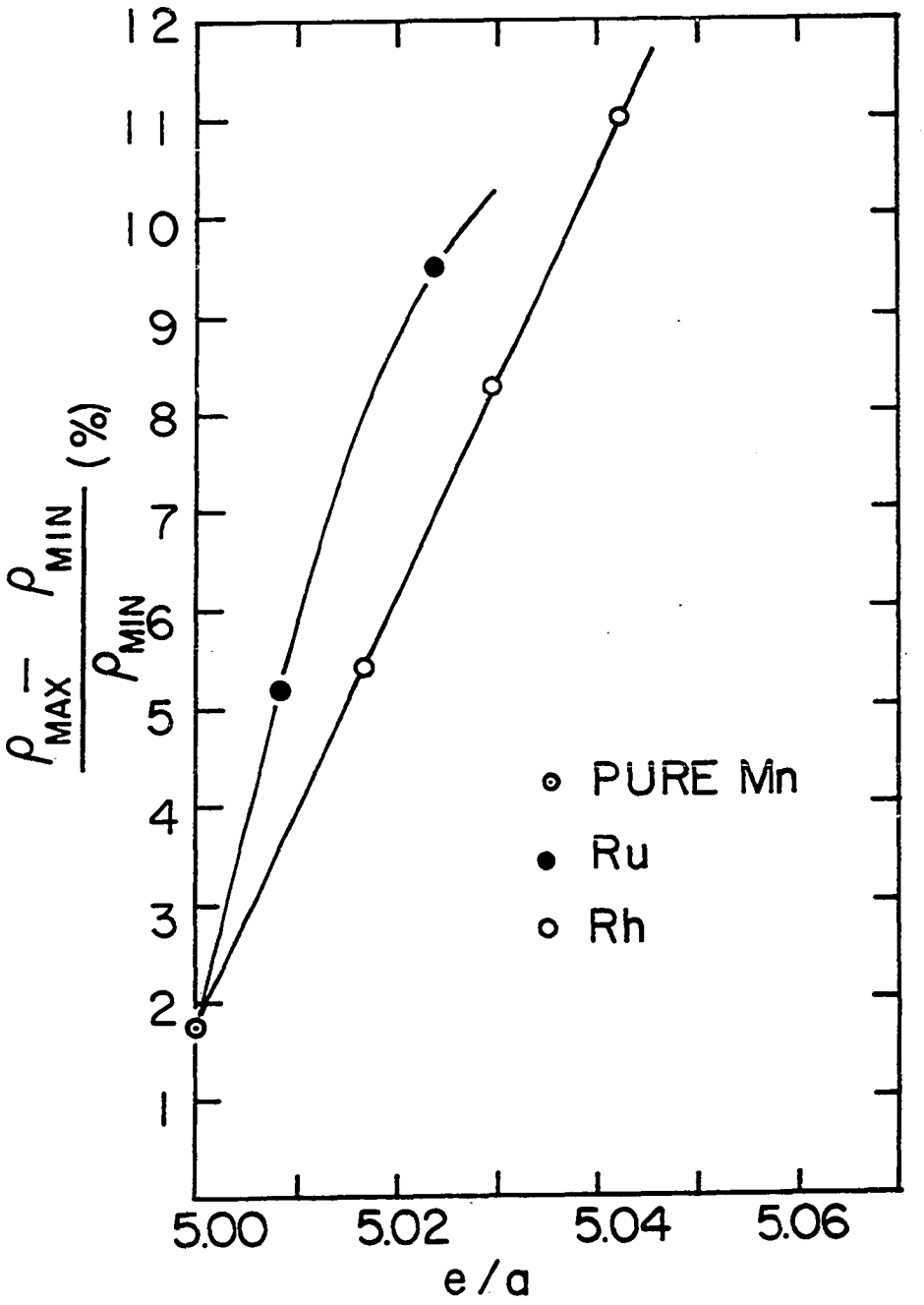

Figure 28.. The variation of the enhancement factor, F, as a function of e/a for Ru and Rh alloys

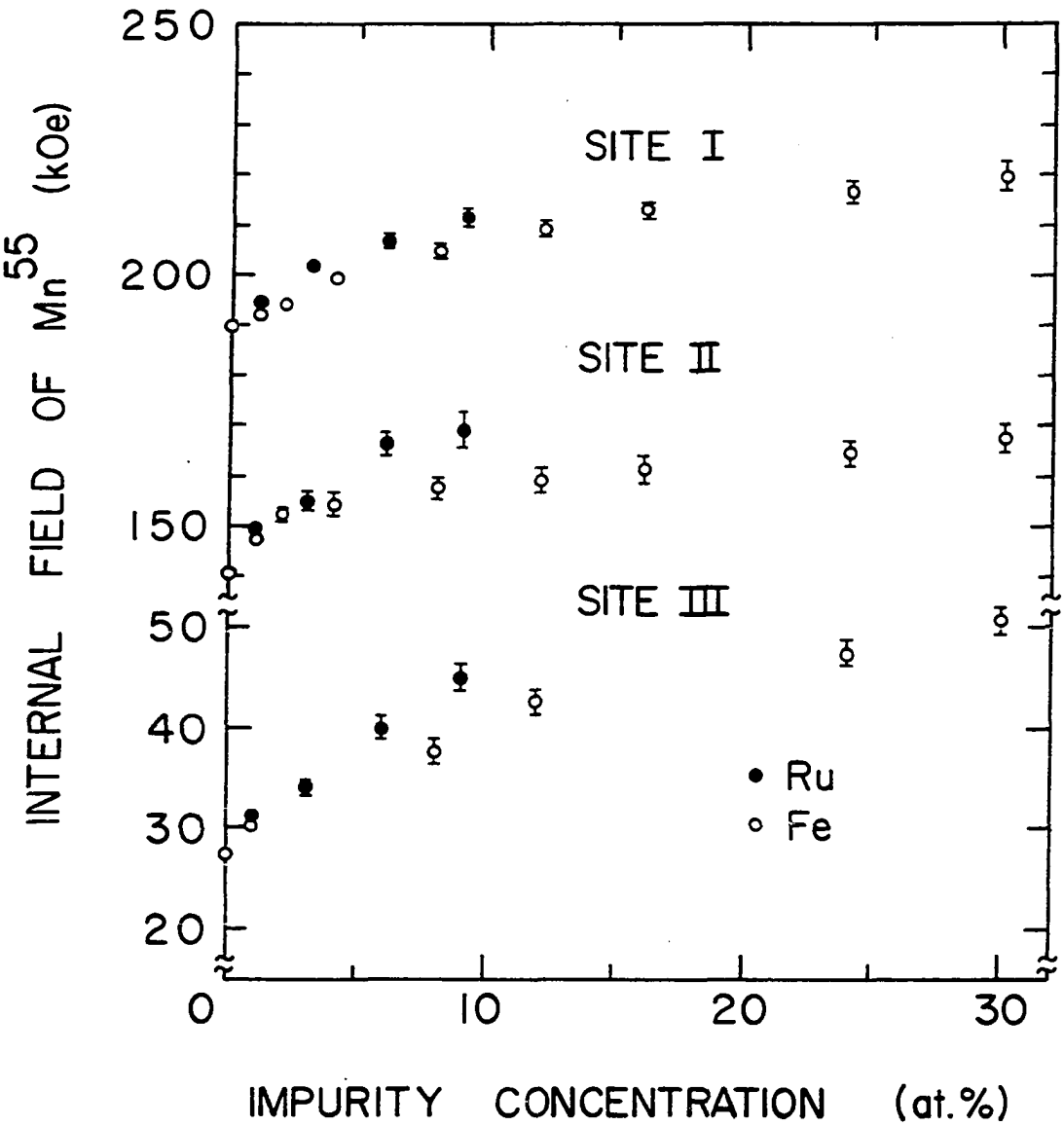

Figure 29. The variation of the internal field at several of the Mn sites [taken from the data of Kohara and Asayama (22)]

The concentration dependence of the Neel temperature is shown in Figure 26. The initial change in T_N is about 17 K/at. % Ru. This is slightly larger than what was observed in the Mn-Fe samples. It is worth recalling that the internal field in the Mn-Ru alloys is slightly larger than in the Mn-Fe alloys. This points up the importance of the strength of the magnetic moment in determining the AFM ordering. We must look for a indirect exchange coupling, perhaps mediated by the conduction electrons. Suppose that the moments are completely localized on the Mn lattice, and there is little or no direct exchange between atoms. This idea of a localized moment is supported by the work of Yamada et al. (14). Futhermore, let the major mechanism for providing ordering be the conduction electrons that are polarized as they move about the lattice. If the effect of alloying is to increase or decrease the magnetic moment and perhaps contribute to or deplete the conduction band, we could account for the variation of T_N with solute for nearest and next-nearest neighbors impurity alloys. Each impurity would either increase or decrease the existing magnetic moment while perhaps changing the number of carriers in the conduction band. Let us suppose that the dominant mechanism is the change in the magnetic moment. This need not be the case, since a reduced or increased number of carriers will have the same effect on this simple model. Thus, the Neel temperature would be ex-

pected to follow the moment variation. This we have seen in the data.

Now to account for the variation of the Neel temperature for next-next-nearest neighbor, we need to introduce a sharply varying density of states at the Fermi level of the pure metal. There are indications from susceptibility measurements (35,36) that this is the case. With increasing e/a the density of states drops. Now, if the density of states is decreasing and we further allow for a reduced number of available carriers because of the greater need to shield the Ni nucleus, the increase in the magnetic moment might be outweighed. Thus, we might see a smaller change in T_N. On the other hand, the decrease in the magnetic moment for Ti impurities may be counterbalanced by an increase in the density of states and therefore, a smaller decrease in T_N for the Mn-Ti alloys. Thus, on this model, we would expect the Mn-Ru alloys to behave much like the Mn-Fe alloys.

However, it is interesting to recall that a Mn-5% Fe alloy, which is comparable to a Mn-2% Ni alloy, shows a much larger Neel temperature (151 K). The Mn-2% Ni sample has a Neel temperature of approximately 115 K. Based on the above model, the Mn-Fe sample would require a factor of almost three times more available conduction electrons than the Mn-Ni sample with all other factors being equal. This appears to be rather large. Based on this comparison, the model does

not satisfactorily explain the observed behavior. A reduction or increase in the next-next-nearest neighbor impurity alloys would bring the model more in line. However, at the moment, there is no provision for such a mechanism. We will return to this point.

The low-temperature behavior of the Mn-Ru data shows no anomalous effects. It decreases with temperature as might be expected from observation of pure Mn and Mn-Fe samples. The mechanism responsible for the enhancement in the resistivity is once again arrested as the temperature decreases.

We may summarize the results for the Mn-Ru alloys as follows:

(a) Increased lattice constant: The observed increase in the lattice constant is comparable to that observed in the Mn-Co samples. When this is coupled with very parallel behavior in both the Mn-Fe and Mn-Ru data, the importance of direct coupling become even less important as a major mechanism for AFM ordering in Mn.

(b) Increased Neel temperature: This would suggest the importance of the excess d-electrons whether they are 3-d or 4-d in nature. The importance of localization does not seem to be critical since 4-d wave functions tend to be less localized than 3-d wave functions.

(c) Increased enchancement factor: The enhancement factor must be closely linked to the increase in the magnetic

moment. In all instances where the moments have increased, we have seen an increase in the enhancement factor. This observed connection will prove useful for inference about several other alloys.

(d) Linear dependence of the Neel temperature: This emphasizes once again the great similarity between the Mn-Fe and Mn-Ru samples. It also suggests that the rigid band approximation is still enforced for 4-d impurities.

Mn-rich Rh alloys The solubility of Rh in the Mn is very limited. We report here the only known result on the variation of the Neel temperature in these alloys. Very rough X-ray work shows an apparent increase in the lattice constant for the Mn-Rh alloys. We do not know if the magnetic moment is increased. However, the enhancement factor and the shift in the Neel temperature may shed some light on this.

The normalized electrical resistivity for several Mn-Rh alloys are shown in Figure 30. There is once again a large and slowly varying very high temperature resistivity. As the temperature is lowered, the resistivity falls off into a minimum and thereafter increases into a slight maximum. This is again typical of those alloys that contain impurities to the right of Mn in the periodical table. It is worth noting the tendency toward little or no decline in the resistivity at low temperatures. The same type of trend was observed in the

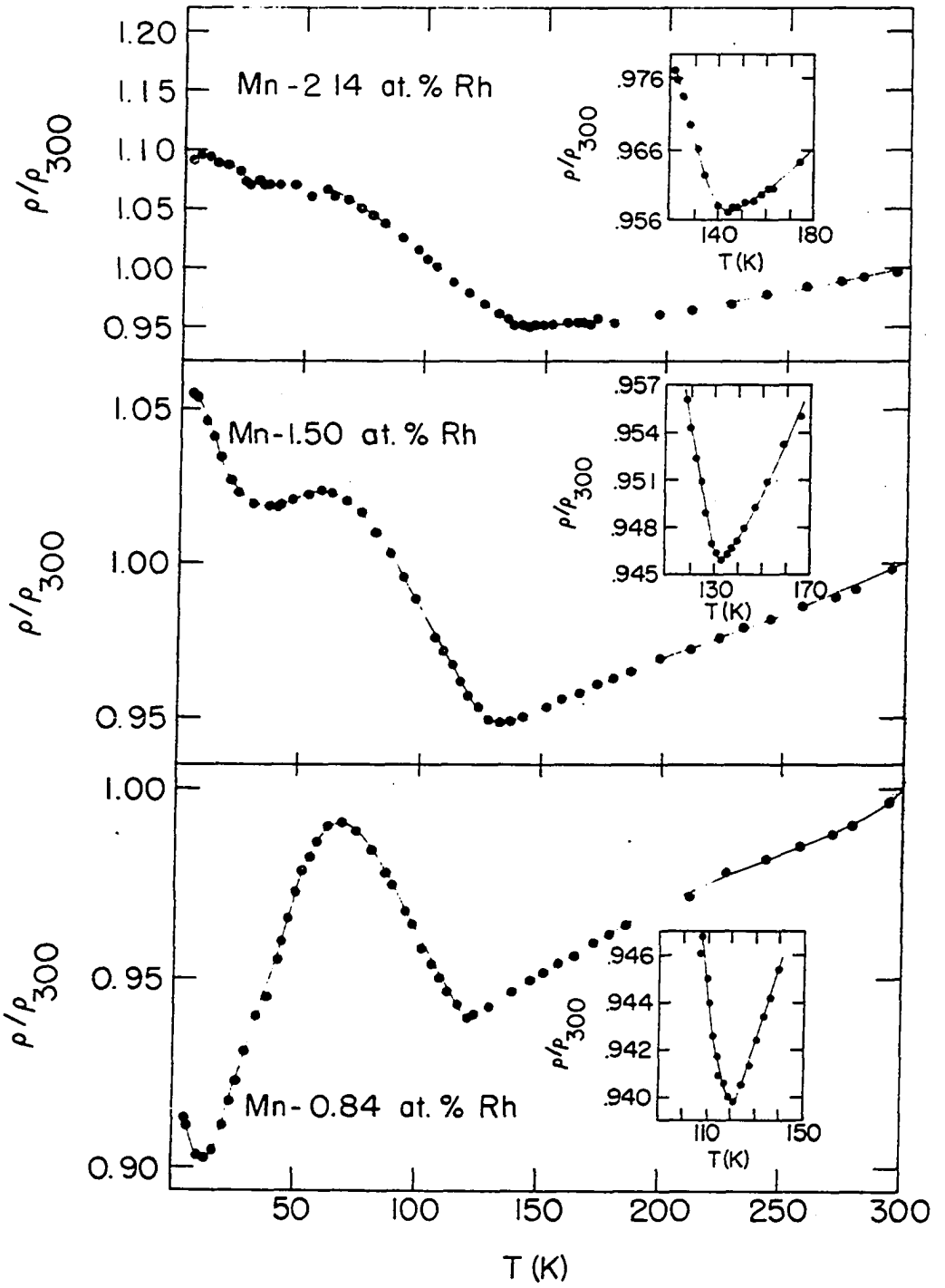

Figure 30. The normalized resistivity for several Rh alloys

first period as we alloyed across it.

As alluded to above, the enhancement factor may give some indication of the type of moments in this alloy system. The enhancement factor is shown in Figure 28. If we may take the trend in the enhancement factor as representing in at least a general way, the strength of the magnetic moments, then clearly the moments have increased as a result of the alloying of Rh into Mn. Also the increase in the Neel temperature would further indicate this since in all cases an increased moment has been associated with an increasing Neel temperature. The change in enhancement factor for the Mn-Rh alloys is comparable to that observed for the Mn-Ru alloys. This to is in agreement with what was observed in the first transitional period.

The variation of the Neel temperature with solute concentration is shown in Figure 26. The dependence is no longer linear. This is what was observed in the Mn-Co alloys. This lends support to the idea that the non-linearity that occurs in the next-nearest neighbor column to Mn has a physical significance in terms of the effect on the AFM ordering. The one clearly common connection is the two excess d-electrons per atom that such alloys contribute to the Mn crystal beyond the 5-d electrons per atom that the crystal already has. It is almost as if there is an upper and lower limit to the number of d-electrons that the Mn system likes

to have introduced with an impurity. Above this limit, the effectiveness of additional d-electrons on an impurity is greatly reduced. Physically, what this means is not immediately clear.

It is interesting to note that for small percentages of Rh, the resistivity shows a clear maximum. This is reminiscent of the near-neighbor impurities. This may indicate that for small enough percentages, the same concentraticnal dependence seen for the nearest-neighbor impurities may occur for next-nearest neighbor impurities. Also, the progressive disappearance of the resistivity maximum with concentration suggests a dependence on at least two additional mechanisms for the scattering below the Neel temperature. Cne could be just the effect of magnetic ordering, which results in the enhancement of the resistivity, while the other mechanism may be an increasing spin-disorder.

We may summarize the results for the Mn-Rh alloys as follows:

(a) Probable increase in lattice constant: Very limited informaticn from an X-ray study would support the idea of an increased lattice constant. Also this would be in keeping with the observation of other impurity elements located to the right of Mn in the periodical table.

(b) Increase in Neel temperature: We observed an increase in the Neel temperature associated with these alloys.

The shift parallel that observed in the first period for nearest and next-nearest neighbor impurities. However, the shift is more than 1.5 times greater for the 4-d impurities. This brings back the theme of a dependence on the number of d-electrons that seems to have characterized all the observations.

(c) Increase in the enhancement factor: This becomes a common observation with increasing Neel temperature. Previously, we observed an increased moment associated with an increased enhancement factor. It would appear that the moment is strongly related to this factor, as well as the shift in the Neel temperature. It does not seem unreasonable to accept the enhancement factor as an indication of at least the variation of the magnetic moments in the Mn-alloy.

(d) Non-linear dependence of the Neel temperature: The symmetry of the Mn system seems almost perfect. We observed non-linearity in next-nearest-neighbor impurities in the first period. One cannot help wondering if there is something magical about a two d-electron difference from that of pure Mn being associated with an impurity introduced into Mn.

Mn-rich Mo alloys For completeness, we report here briefly the results from an attempt to produce Mn-Mo alloys. Owing to the very limited solubility of Mo in Mn, the alloys produced were considered to be not of uniform concentration

and very probably not completely in solid solution.

With the abcve considerations in mind, however, we observed a tendency toward a reduced high temperature resistance. If the resistivity minimum still reflects the Neel temperature, we observed a decrease in all cases. Probably these observations can be viewed only lightly. Yet, the trend of the observations are interesting. It was unfortunate that the time factor for this work did not permit the study of additional 4-d impurities. It would be worth noting the behavior of Mn-Nb alloys, where the solubility of Nb is slightly greater than that of Mo. Also, Pd and Zr would have perhaps provided scme interesting results.

We have observed for the 4-d impurities, in part, a very similar behavior to these impurities of the 3-d period. One noted difference is a tendency toward a larger change in the Neel temperature for the 4-d impurities per atomic percent sclute. This may be the result of a less localized d-wave function for these particular impurities. This we will be able to check when we move tc 5-d impurities, since the d-functions tend to be even less localized.

We are once again faced with the question of what is important for AFM ordering in the Mn crystal and alloys. One factor would appear to be the magnetic moment. The size or strength of moments seems to follow the Neel temperature. Also, we have seen a close link between the number of d-

electrons that the crystal may have as a result of alloying and the change in the Neel temperature. Also, we have observed an increase or decrease in the lattice constant that is followed by a increase or decrease in the Neel temperature respectively. The exception occurred for Mn-Fe alloys, where the lattice constant decreased but the Neel temperature increased.

Let us assume for the moment that Fe in some way is an exception to the usual behavior. Now let us suggest that that there is a direct variation between the observed magnitude of the magnetic moment and the change in the lattice constant. This idea has been suggested by several other investigators (21,20,59). In particular, a calculation for ferromagnetic Fe has shown an asymptotic variation of the moment with increasing lattice constant. Based on the above idea, the magnitude of the moments in the Mn crystal may be dependent largely on the change in the lattice constant. An increasing lattice constant giving rise to an increase moment, while a decreasing lattice constant gives rise to a decreasing moment up to some limit. Thus, we might expect a curve for the variation of magnetic moment with lattice spacing to be at the very least asymptotic in nature or perhaps even having a peak. This is not unreasonable in light of Figure 26. Since the variation of the lattice constant tends to be a linear function of the concentration, Figure 26

represents equally well the variation of the internal field with changes in the lattice constant. If we then tie the variation of the Neel temperature directly to the shift in the moment size while having the conduction electrons carry the ordering information, there is fair agreement with observed variation of the Neel temperature for most alloys except Mn-Fe. We have also assumed that the number of conduction electrons depend on the density of states curve, which may be decreasing for increasing Fermi level and also on the nature of the impurity that is introduced. On the basis of this model, it would be expected that 4-d impurities would increase the lattice slightly more for a given concentration than 3-d impurities. As a result, we may expect for 4-d impurities a slightly stronger moment and an increase in the Neel temperature that is also larger than that observed for 3-d impurities. This is reflected in both Figure 26 and Figure 29 and perhaps in Figure 28, if we take the enhancement factor as an indication.

Based on this data, a plot of the e/a ratio, which is shown in Figure 31 for the 4-d impurities alloys, would not need to give the same change in the Neel temperature for the two different alloy systems. As the figure indicates, there is a very definite difference between the two systems. It is interesting to pose the question of whether a Mn-Pd alloy would give an additional line as did the Mn-Ni alloys.

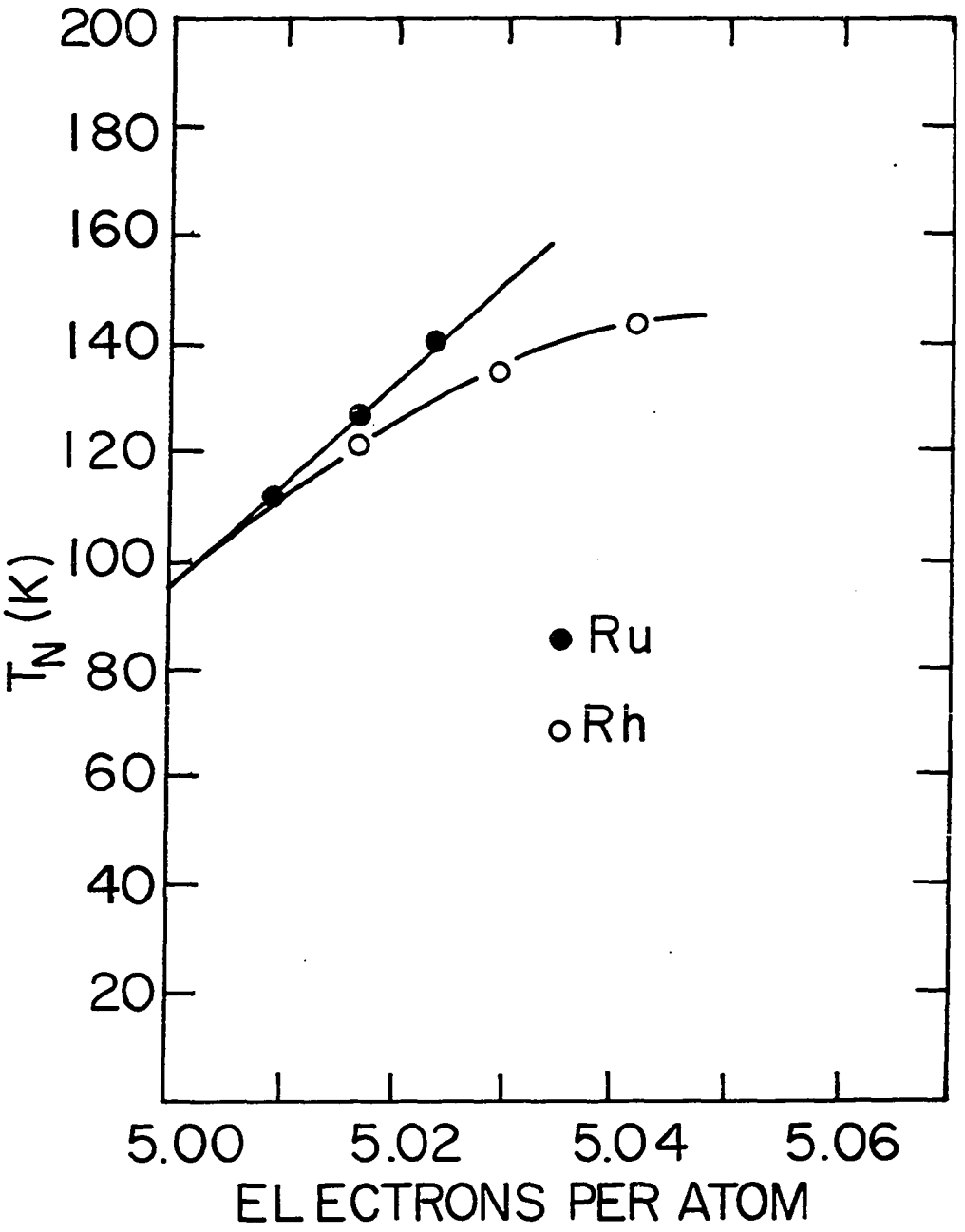

Figure 31. The variation of the Neel temperature as a function of the e/a ratio for the alloys of the second transitional period

Figure 32 shows the variation of the Neel temperature for 1 at. % solute as a function of the relative position of the impurity. A certain amount of suggestive additions are added for other 4-d impurities. It would be very interesting to investigate these other alloy systems. One point is clear, the 4-d impurities appear to have a stronger effect on T_N than do 3-d impurities.

5-d transitional impurities

By the time we have reached the third long transitional period, 5 additional subshells have been filled. The third period is much more like the first in that the 6-s level contain two electrons. This would suggest that the 6-s levels are slightly lower relative to the 5-d levels. The 5-d wave function should be very much less localized when compared to the 3-d wave function.

Mn-rich Os alloys Os is located in the same column as Fe and Ru. If the pattern continues, the Neel temperature should be increased. This is the case as can be seen from Figure 33, which shows the variation of the Neel temperature as a function of the atomic percentage of solute. The Neel temperature appears to be a linear function of the concentration. This is very parallel to the observation for the Mn-Fe and Mn-Ru alloys. The only commonly known factor between these impurities is their relative position to Mn and the

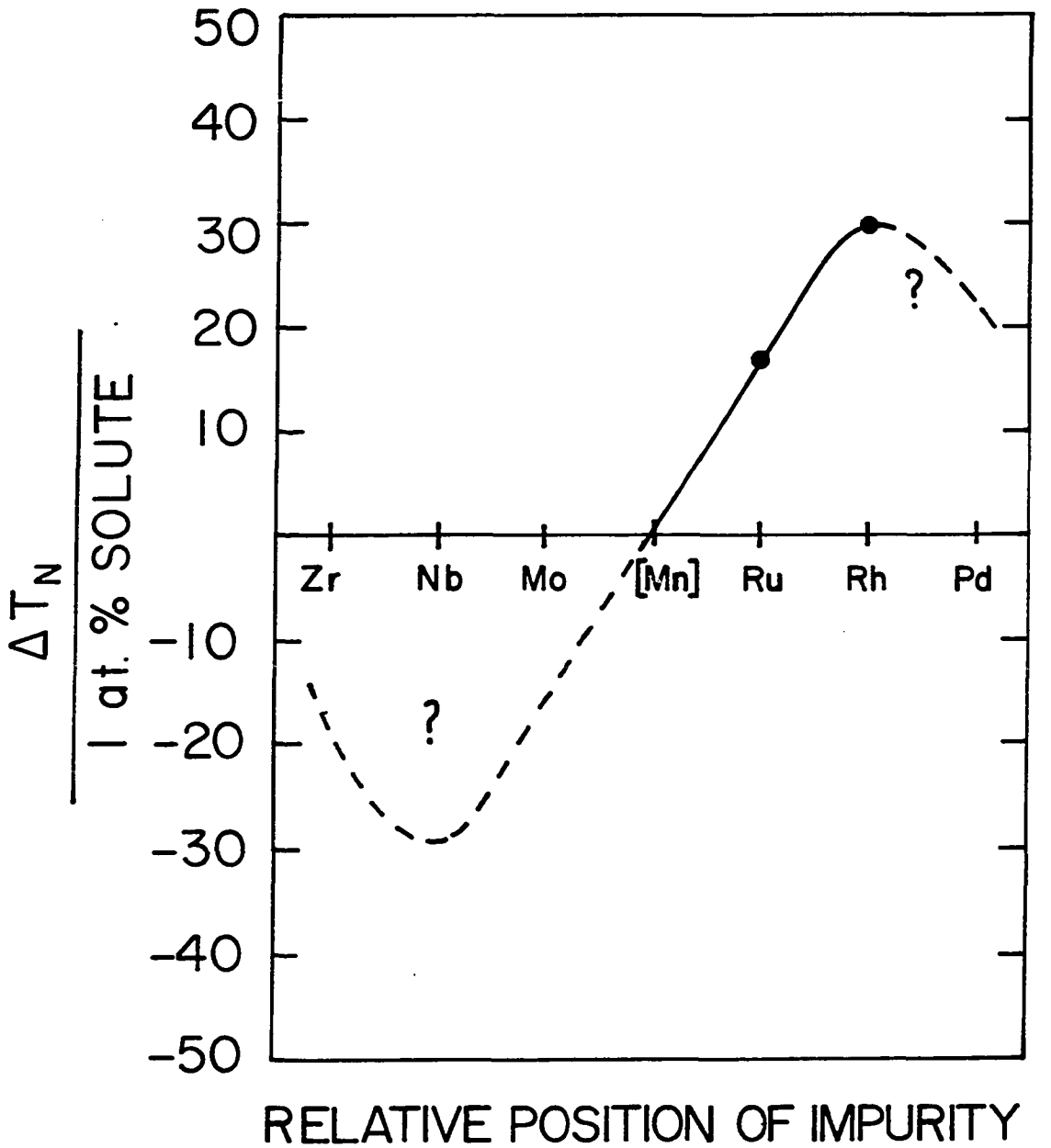

Figure 32. The variation of the Neel temperature per one atomic percent solute as a function of the position of the 4-d impurities

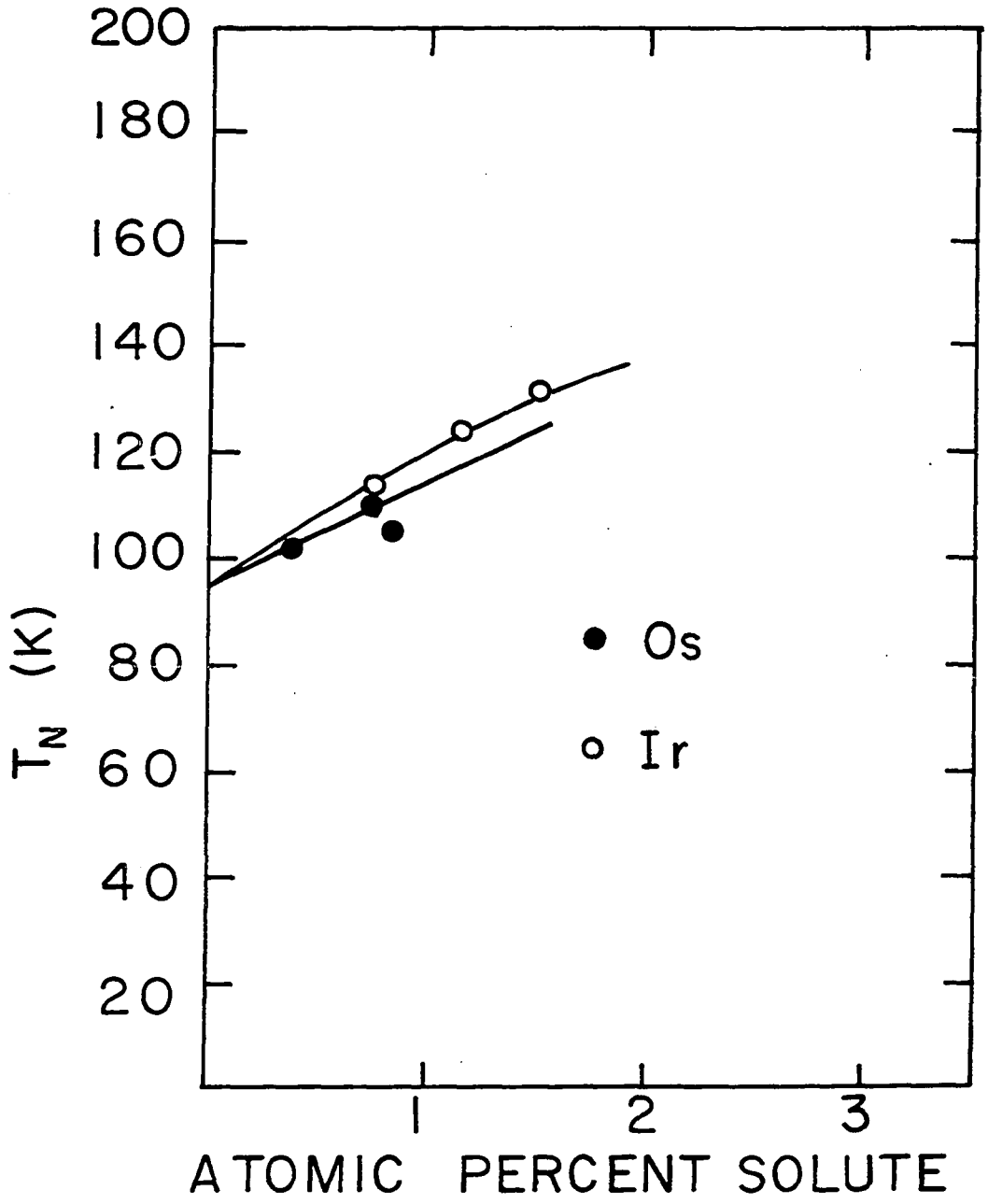

Figure 33. The variation of T_N as a function of atomic percent solute for Os and Ir alloys

fact that each has one excess d-electron more than Mn. It is interesting to ask whether this great similarity is the result of the one excess electron or the tendency of impurities in the nearest-neighbor column to cause a very similar physical change in the Mn crystal. We know that the d-wave function become less localized as we move from one period to the next. Also, there are indications that the lattice constant is increased by two of these impurities, with Fe being an exception. Probably the actual situation is a combination of the two effects, the excess d-electron and certain physical changes.

The normalized electrical resistivity is shown in Figure 34. The resistivity decreases almost linearly into a minimum, followed by a characteristic resistivity maximum. The resistivity maximum does not appear to be as pronounced as in the 3-d and 4-d impurities. This suggests that the mechanism responsible for the enhancement below the Neel temperature is somehow arrested by the 5-d impurities. If the enhancement is a reflection of moment magnitude or a measure of spin-disorder, it is not immediately clear why 5-d impurities should effect this mechanism differently from the 3 and 4-d impurities. As pointed out before, the shift in Neel temperature is comparable to the shift observed for Mn-Fe alloys. If the Neel temperature is closely linked with the magnitude of the moment (and this seem to be very likely in light of

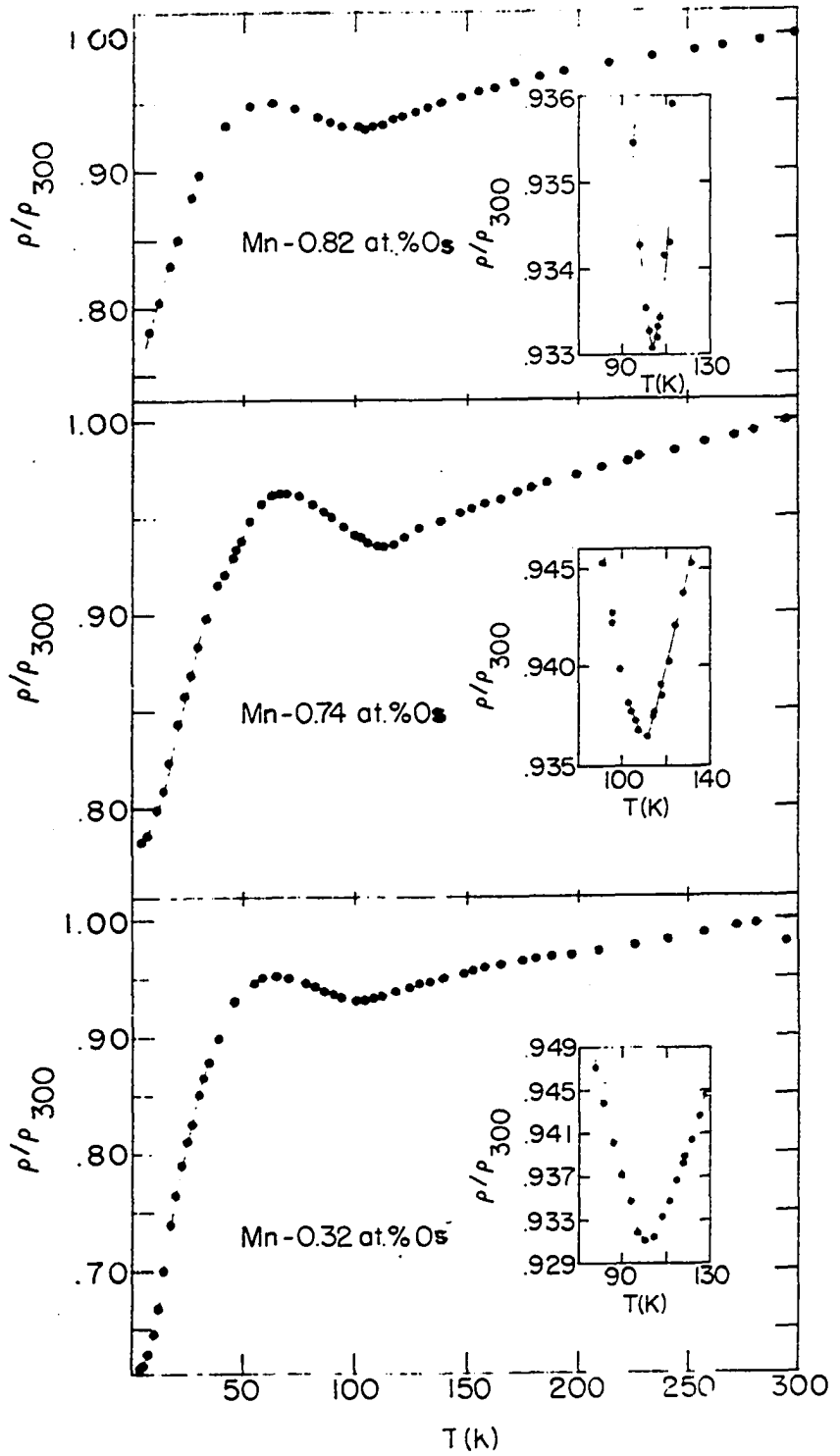

Figure 34. The normalized resistivity for several Os alloys

the trend we have observed sc far) the variation of the Neel temperature would suggest a moment comparable to that in the Mn-Fe alloys. Yet, the enhancement factor is proportionally smaller than observed in either Mn-Fe or Mn-Ru (see Figure 35). It would seem that either the enhancement factor or the Neel temperature does not fully represent the magnitude of the magnetic moment. Probably it is the enhancement factor, since there is more evidence to support a close tie between moment magnitude and the Neel temperature.

No cther known results have been published about this alloy system. Very rough X-ray measurements taken in the course of work suggest an increase in the lattice constant. This is consistent with observations on other such Mn-alloys. The location of the Os atoms in the Mn crystal is not known. It seems reasonable to assume that they would be found in smaller sites in Mn since we observed this to be the case for the 3-d impurities and one 4-d impurity that occurred to the right of Mn. We have no direct information on what happens to the magnetic moment. We may surmise from previous Mn-alloys that the moment probably increases.

The question of localization of the d-wave function seems to play very little role in determining the shift in the Neel temperature. The amount of localization in going frcm the first period to the third is greatly reduced, but we observe only a few degrees difference in the observed shift

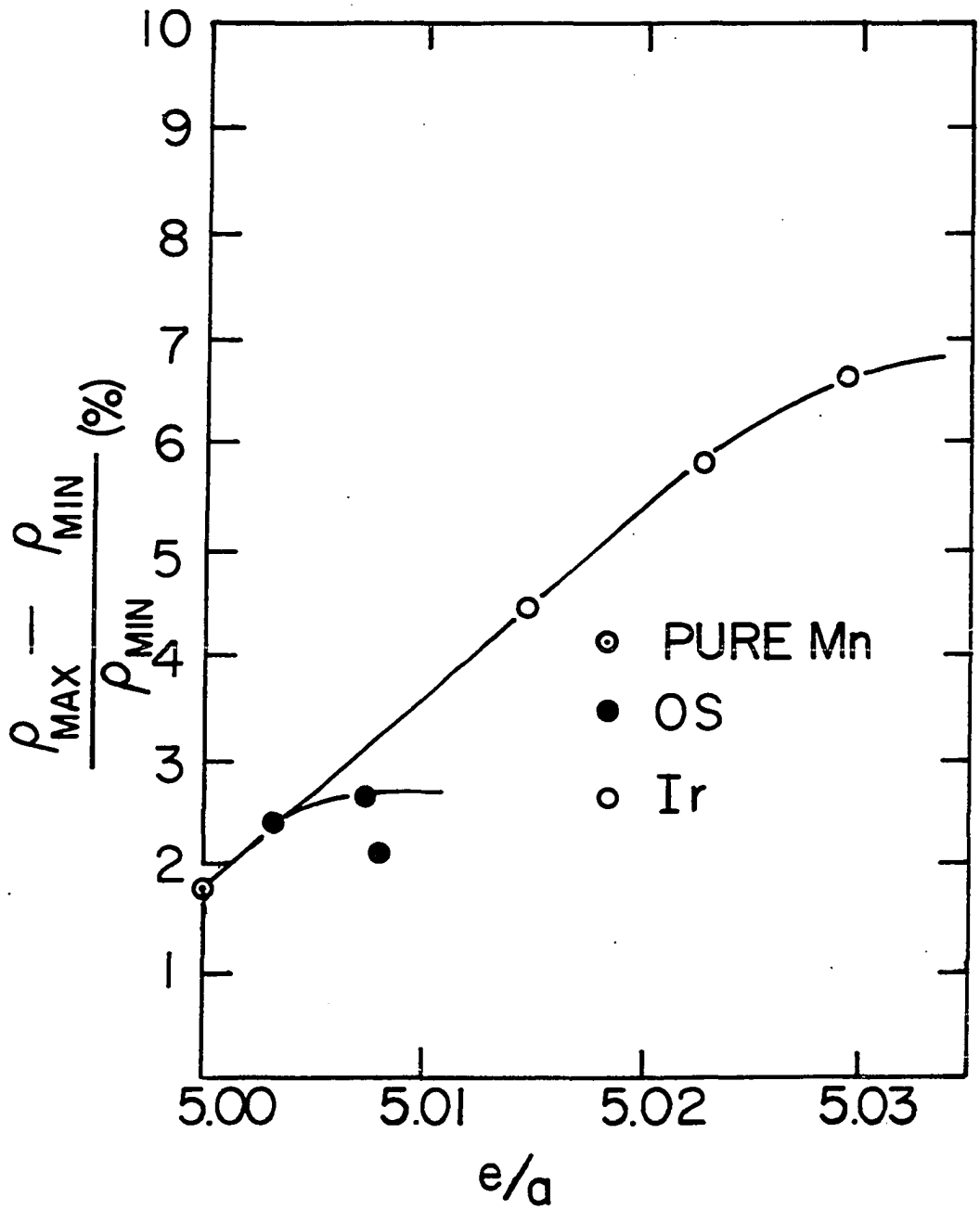

Figure 35. The variation of the enhancement factor, F, as a function of e/a for Os and Ir alloys

in the Neel temperature for the nearest neighbor impurities. This lack of dependence on localization of the d-wave function as we move from period to period should resolve the question of such dependence as we move across a particular period, since the variation in the localization of the d-wave function should be much less within any period than that observed on going from one period to the next period. It appears rather conclusive that this is not responsible for the anomalous effect observed in the first transitional period.

We may summarize the results for the Mn-Os alloys as follows:

(a) Apparent increase in the lattice constant: From a very rough X-ray study, we observed an increase in the lattice constant of the Mn-Os samples. Such an increase would be consistent with the observation for other Mn-alloys of this type, but not an essential consequence as can be observed from the Mn-Fe results.

(b) Increase in T_N: We observed an increase in the Neel temperature that is comparable to that observed for the Mn-Fe alloys. The increase could be expected based on the fact that so far all impurities with excess d-electrons have raised the Neel temperature. However, whether this increase in the Neel temperature is a direct result of the excess d-electrons or an increased magnetic moment resulting from

geometrical consideration is not clear. We have not been able to resolve this dependence. Yet, the greatest consistency is observed for the excess d-electrons, which have always raised the Neel temperature.

(c) Increased enhancement factor: If the idea of an increasing moment is always associated with an increase in the Neel temperature, the enhancement factor probably does not in a direct way represent the magnitude of the moments. This appears to be evident from the much smaller enhancement factor for the Mn-Os alloys, but a Neel temperature comparable to the Mn-Fe and Mn-Ru alloys.

(d) Linear dependence of the Neel temperature: The linear dependence of the Neel temperature lends support to the idea of a rigid band model. On this model, only the relative position of the Fermi level with respect to the energy bands is important. The major change in the Neel temperature would depend only on the e/a ratio with very small variations due to the physical difference each impurity brings to the Mn lattice.

Mn-rich Ir alloys Ir, like many of the other transition elements, has a very small solubility in Mn. We report here on alloys containing up to 2.0% Ir. Ir is located in the next-nearest-neighbor column to Mn, which is also shared by Co and Rh. We do not have available information on which particular sites the Ir atoms perfer. For the purpose of the

present discussion, we will assume that the smaller sites (sites III and IV) are the most probable. Also lacking is information on the change in the magnetic moment upon alloying Ir into Mn. Here again we will assume that such alloying increases the moment. The resulting effect on the lattice constant appears to be one of causing lattice constant to increase. This is indicated by a rough X-ray study.

The normalized electrical resistivity for the Mn-Ir alloys are shown in Figure 36 We note the characteristic resistivity minimum and maximum. The high temperature resistivity appears to be typical of those alloys that involve impurities to the right of Mn in the periodical table. It is slow-varing and rather large, suggesting the probable presence of disordered moments. The low temperature resistivity shows a marked break from other alloys that contain impurities from this column. There appears to be no tendency toward increasing resistivity with decreasing temperature, which was fairly pronounced in the Mn-Co and Rh alloys. This would suggest a strong suppression of the scattering mechanism that was at work in the other two Mn alloys of this transitional column. It is not immediately clear why this should happen.

The enhancement factor for the Mn-Ir alloys is shown in Figure 36. The factor increases as has been the case for other Mn alloys with impurities to the right of Mn in the

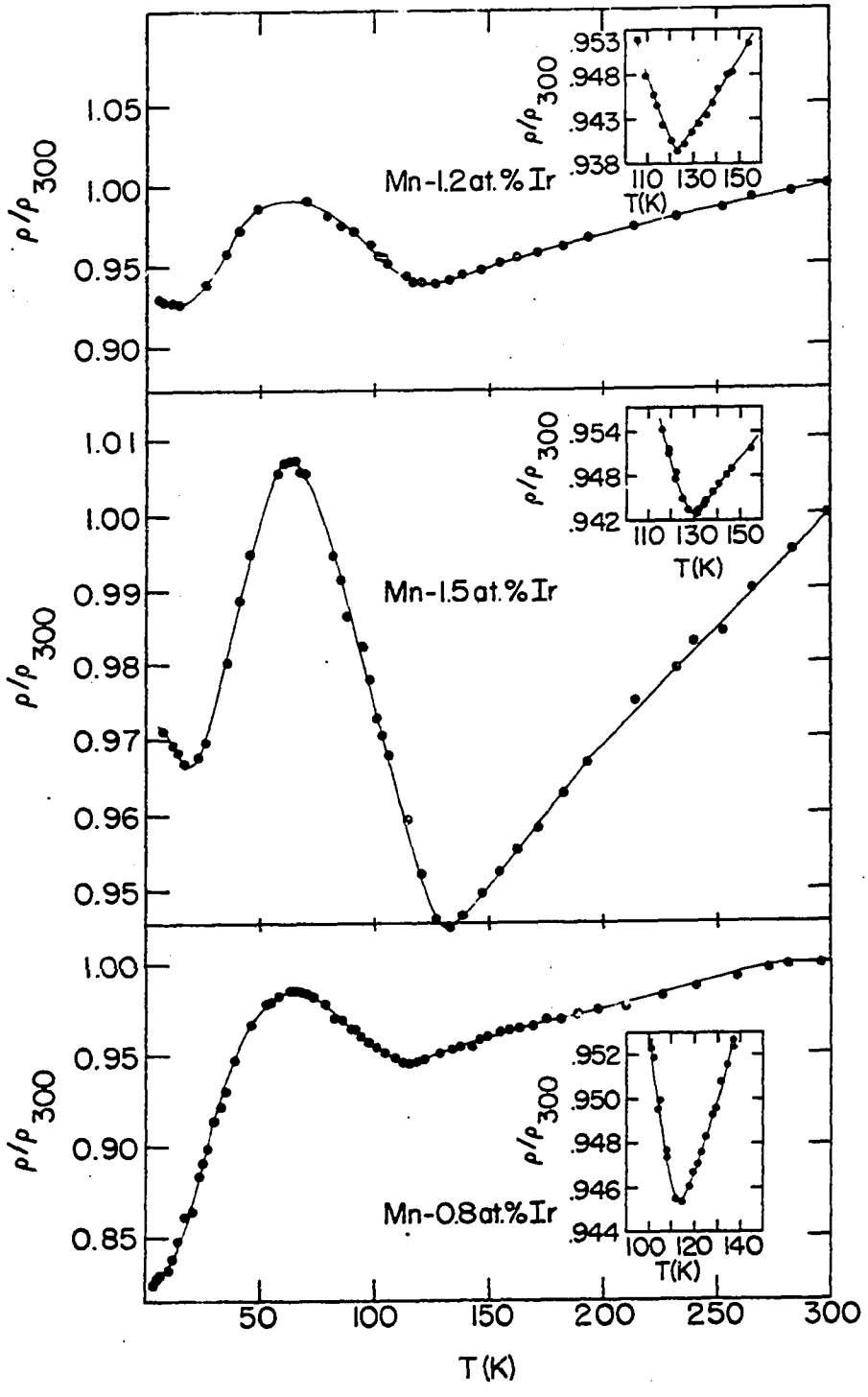

Figure 36. The normalized resistivity for several Ir alloys

periodic table. The enhancement factors dependence on the e/a ratio support in part the idea of an energy gap being responsible for the observed enhancement. According to Suezaki and Mori (61), the effective number of carriers is directly related to the energy gap. The energy gap has a direct effect on the observed resistivity. Suezaki and Mori's calculations show an increase in the resistivity just below the Neel temperature. If their argument applies to Mn, then the enhancement factor is an indirect measurement of the gap for these alloys. This is an interesting possibility.

The concentrational dependence of the Neel temperature is shown in Figure 32. We observed a non-linear dependence for T_N which follow the observed pattern for other alloys of this column. This constancy probably is the result of more than just mere coincidence. A very definite and probably different type of change in the geometrical consideration and perhaps in the type of ordering has occurred. By the time the alloys containing impurities from third nearest-neighbor column is reached, the changeover is completed. We know that for pure Mn the ordering is accompanied by a slight increase in the lattice constant (58, 19). This has been alluded to be the results of a spin wave (58). This is not the only suggestion that Mn may have a static spin density wave associated with its ordered phase. If there are spin waves involved, we know from studies of Cr that the presence of impu-

rities atoms in the lattice can effect the wave vector. Such effects will be reflected in the change in the Neel temperature.

We may summarize the results for the Mn-Ir alloys as follows:

(a) Increase in the Neel temperature: The Mn-Ir alloys shows a shift in the Neel temperature which is comparable to other impurities in the next-nearest-neighbor column. This increase has been observed for all Mn-alloys that increase the e/a ratio. Although the e/a ratio is not the critical factor, it is somehow very closely linked to the shift in the Neel temperature. It is clear that the sign of the relative e/a ratio for alloys relative to the ratio for pure Mn determines the sign of the relative shift in the Neel temperature for that alloy. That is, positive e/a ratios gives rise to a positive shift, and negative e/a to a negative shift in the Neel temperature.

(c) Increase in the enhancement factor: The enhancement factor has also followed the e/a ratio. Positive e/a have been accompanied by an increased factor, with negative e/a ratio being associated with a decrease in the factor. The enhancement factor appears to be sensitive to the number of excess d-electrons and the relative position of the impurity element with respect to Mn. The Mn-Ir alloys show a somewhat smaller increase in the enhancement factor than pre-

vious Mn alloys of this type.

(d) Non-linear dependence of the Neel temperature: We again observe this type of dependence for the next-nearest-neighbor impurities. This dependence seem to be linked closely to a ±2 d-electrons per atom difference from the number of d-electrons per atom associated with pure Mn. Why this particular number of d-electrons is critical is not clear.

Mn-rich Re alloys The Mn-Re alloys turn out not be in solid solution. However, there are several reasons why these alloys are worth mentioning in passing. First of all, any data on Mn-Re alloys should go along way in helping to explain the AFM ordering in Mn. Since Re is in the same column as Mn, it should not add or substract d-electrons. Thus, Mn-Re alloys would be expected to be more Mn-like than possibly any of the other alloys. Our results on the variation of the Neel temperature of the Mn-Re alloys are inconsistent owing to the metallurgical problem mentioned above. However, we observed a slight increase for low concentrations and a decrease for higher concentrations. We do not report this as being the pattern for such alloys, but results for those two-phase alloys studied. Oberteuffer et al. (13) have looked at a Mn 1% Re sample and reported an increase in the Neel temperature, if we accept their reported temperature minimum, T_{min}, as the Neel temperature.

Once again, we have observed very similar behavior as we alloy across a period. This pattern is intricately linked to the electronic nature of the impurity introduced into Mn. It is difficult to explain and yet impossible to avoid the continual correlation of the shift in Neel temperature and and the number of d-electrons associated with impurity atoms. Certainly, geometrical consideration of the impurities are of small importance, since in moving from the first period to the third period there are considerable changes in these factors.

It is interesting to ask if the first period pattern of shifts in the Neel temperature will be continued in the third period. The answer is probably yes and we show a rather suggestive graph in Figure 37. It would be most interesting tc verify this graph by studying Mn-Pt and several of the alloys to the left to Mn. If this graph is in fact representative of the third period Mn alloys, it would almost completely rule out dependence cf the Neel temperature on the size of the impurity atoms. It would also tie the variation of the Neel temperature to the number of ± d-electrons per impurity atcm relative to the number of d-electrons per atom in pure Mn, with an optimum number near ± 2 d-electrons.

In Figure 38 is shown the variation of the Neel temperature as a function of the e/a ratio. Again the results do not fall completely on one line. Such variation could be the

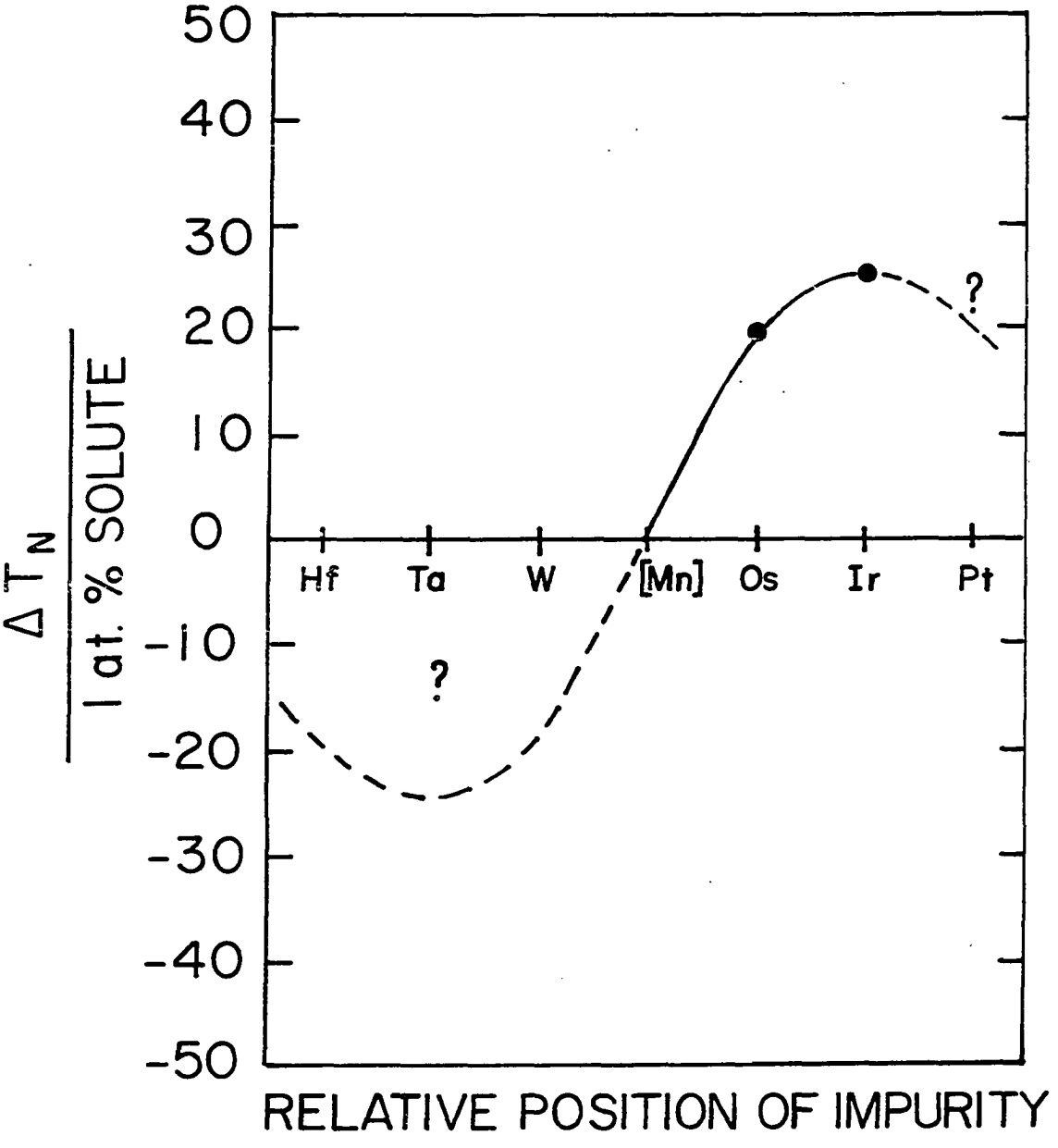

Figure 37. The variation of the Neel temperature per one atomic percent solute as a function of the position of the 5-d impurities

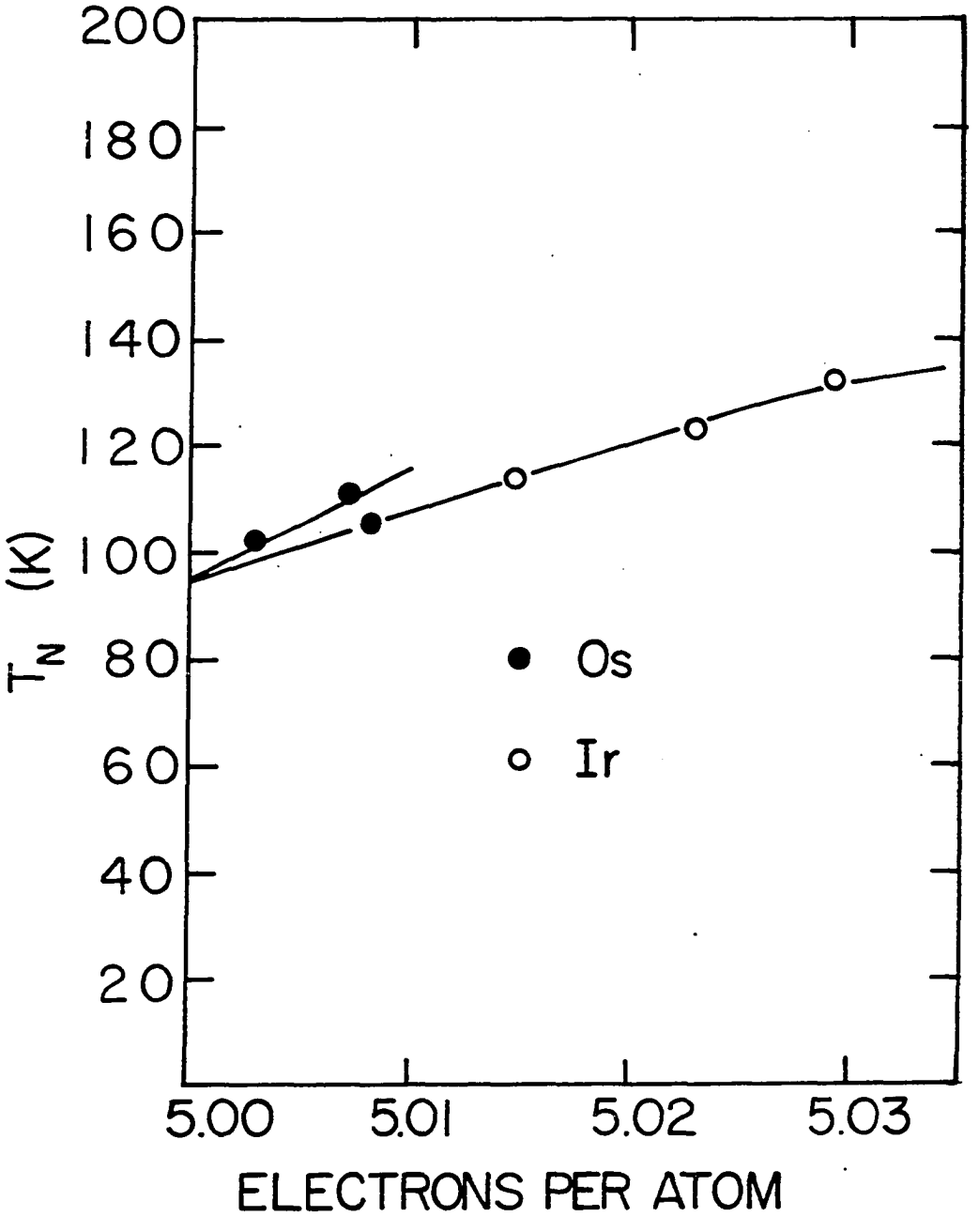

Figure 38. The variation of the Neel temperature as a function of the e/a ratio for the alloys of the third transitional period

results of differences that are intrinsic to each impurity. But, as may be recalled from the first transitional group, the real anomalous behavior did not begin until we reached the next-next-nearest columns. Only if the data from Mn-Pt alloys came near to fitting on the same line in Figure 38 would such an intrinsic property seem to be a plausible explanation. If Mn-Pt alloys show a completely different dependence, it is likely some other fundamental mechanism is responsible.

Finally, in this section, we would like to look at variations in the Neel temperature for alloys along a transitional column. We have two such columns completed. These are the nearest-neighbor and next-nearest-neighbor column. Two points are immediately clear (see Figure 39). First, in going from next-neighbor to next-nearest-neighbor column, the fluctuation in the Neel temperature increases. That is to say, one observes a maximum fluctuation of 25% between Neel temperature for 1 at. % solute for nearest neighbor impurities and a 34% fluctuation for the next-nearest-neighbor impurities (see Figure 40). This indicates that more than just the e/a ratio is important, since all impurities contribute the same e/a ratio. Secondly, we observed a peak in variation of the Neel temperature for second period impurities. This is interesting in that it follows the trend for variation along a period. However, it probably bears little rela-

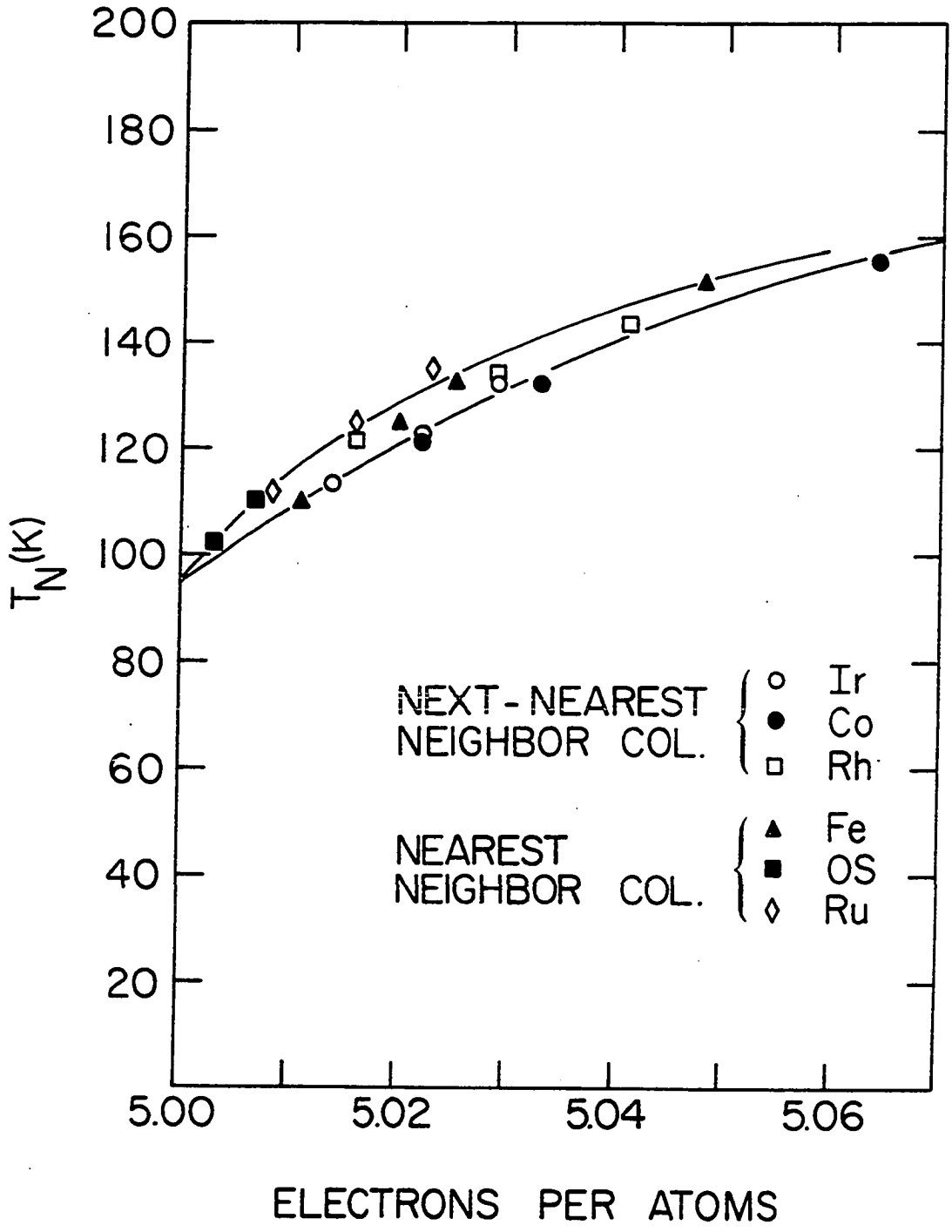

Figure 39. The variation of the Neel temperature as a function of the e/a ratio for the nearest, next-nearest and next-next-nearest column impurities

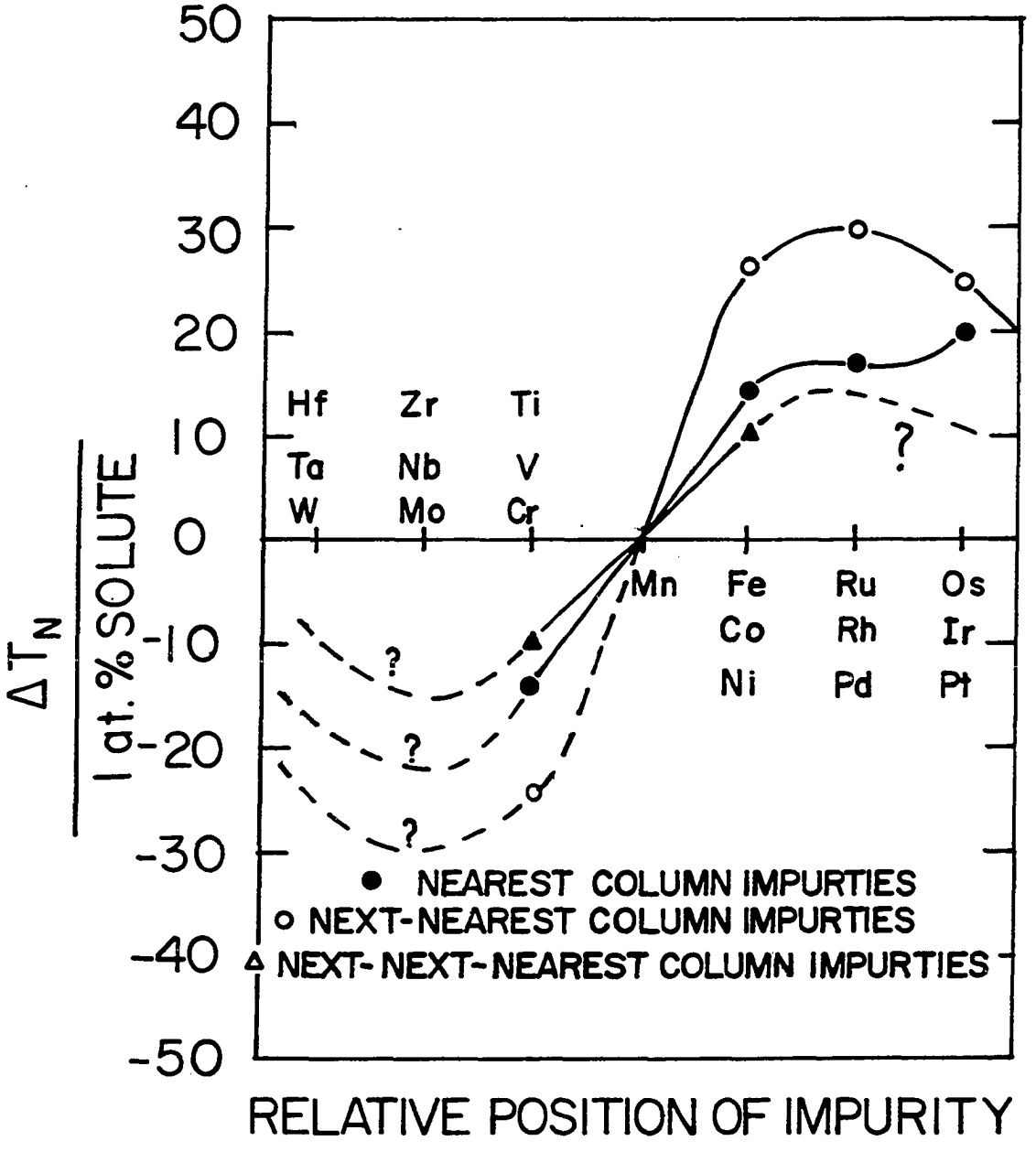

Figure 40. The change in the Neel temperature as a function of the relative position of the nearest, next-nearest and next-next-nearest column impurities

tion to the mechanism responsible for the variation along a period.

At this time it is not obvious why such a pattern should develop. The variation of size, localization of d-wave functions or nuclear charge do not provide any indication that such patterns should be observed. One interesting possibility is that as one alloys along a column, the number of d-electrons given up may vary. We know that for alloys containing Cu, Ag or Au the tendency is for these solutes to form divalent, univalent and trivalent compounds respectively. Perhaps this is the case with the transitional impurities in Mn. The third period impurities could contribute a much smaller number of d-electrons or the second period could contribute a proportionally larger number of d-electrons. The important fact is that there is a precedent for anomalous behavior as one alloys down a transitional column.

Ternary Alloys

In this section, we turn our attention to ternary alloys. These alloys contain two impurities dissolved in the Mn lattice. These alloys are important in that they allow one to test the rigid band model approximation as well as some ideas of the type of AFM ordering. We report here the results from three such studies. We have looked at Mn-Fe-Cr,

Mn-Fe-Ni and Mn-Cr-Ti. These were selected for several reasons. The Mn-Fe-Cr alloys were studies to check on the rigid band approximation, while the other two were studied in connection with the apparent differences in the shift in the Neel temperature on going from the first two near-neighbor column impurities to the third. Whether these alloys behave like pseudo next-nearest-neighbor impurities or completely different would provide information on which models can be ruled out and which models may offer some explanation of the AFM ordering.

Mn-Fe-Cr alloys Several alloys were investigated in this series of alloys. The alloys studied are summarized in Table X and Figure 41. These alloys would provide a check on the suggestive pattern of variation of the Neel temperature for Mn-Fe and Mn-Cr alloys (see Figures 22 and 23). These figures imply that only the number of d-electrons that a solute bring to the Mn-crystal is important. Thus, one extra or one less electron has an equivalent absolute effect on the change in the Neel temperature. The first indication of this was reported by Bellau and Coles (1) where they determined the Neel temperature of a Mn-5%Fe-5%Cr sample from resistivity data. They note a Neel temperature of about 100 K, which is comparable to that of the pure metal (95 K). Later NMR studies of the spin-spin relaxation time for a similar alloy by Masuda et al. (24) also reported a Neel tem-

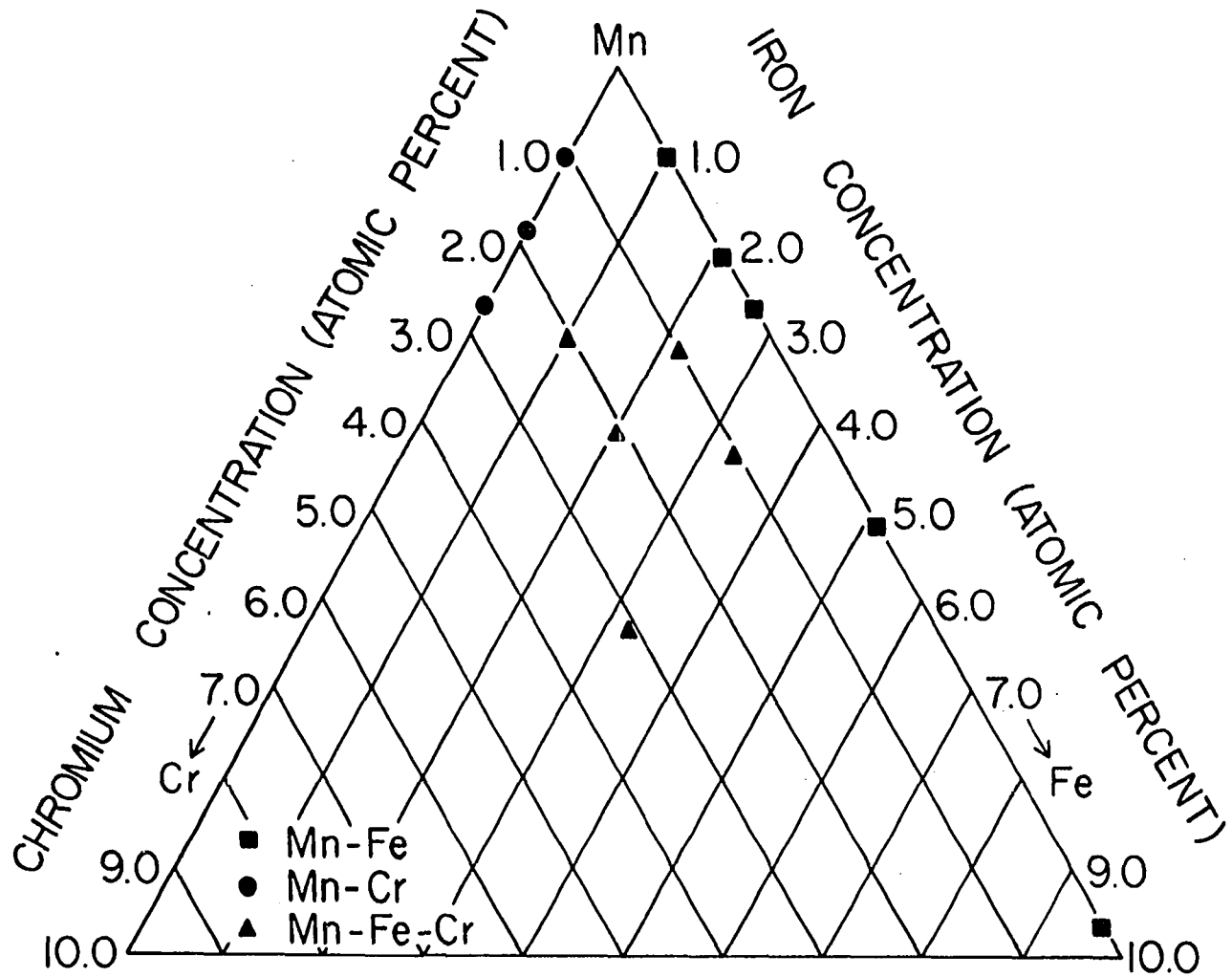

Figure 41. Chemical compositions of the specimens for Mn-Fe-Cr, Mn-Fe and Mn-Cr alloys

Table X. Summary of the Mn-Fe-Cr alloys.

		Concentration		
		Fe	Cr	Effective
Mn-Fe	(1)	0.99	0.0	0.99
	(2)	2.10	0.0	2.10
	(3)	2.7	0.0	2.7
Mn-Cr	(1)	0.0	1.05	1.05
	(2)	0.0	1.85	1.85
	(3)	0.0	2.7	2.7
Mn-Fe-Cr	(1)	2.2	0.97	1.23
	(2)	1.05	2.05	-1.00
	(3)	3.36	1.10	2.26
	(4)	2.03	2.12	-0.04
	(5)	3.24	3.13	0.11

perature around 100 K.

The normalized electrical resistivity is shown in Figures 42 and 43. The data show the characteristic minimum with various degrees of resistivity maximum. It is expected that the high temperature resistivity will not be effected to a large extent. This is consistent with the observed results. The expected behavior of the low temperature resistivity is not quite as clear. Probably the effective controlling solute would dominate the pattern of resistivity. This does seem to be the case. However, we do see a certain dependence of the enhancement factor on the effective controlling solute. Those alloys with an effective Fe concentration tend to have a larger factor than those with effective Cr concentration.

The variation of the Neel temperature as a functions of the effective atomic percent (the amount of Fe solute minus the amount of Cr solute) is shown in Figure 44. The data are imposed over the results for the two binary alloys Mn-Fe and Mn-Cr. The fit is very good. This immediately verifies the rigid band approximation for the Mn-Cr and Mn-Fe alloys.. Moreover, it implies that the average number of d-electrons per atom is the most important factor in determining the AFM ordering in pure Mn (see Figure 45). The anomalous behavior for the next-next-nearest column impurities must be linked to a change in the effective number of d-electrons those impuri-

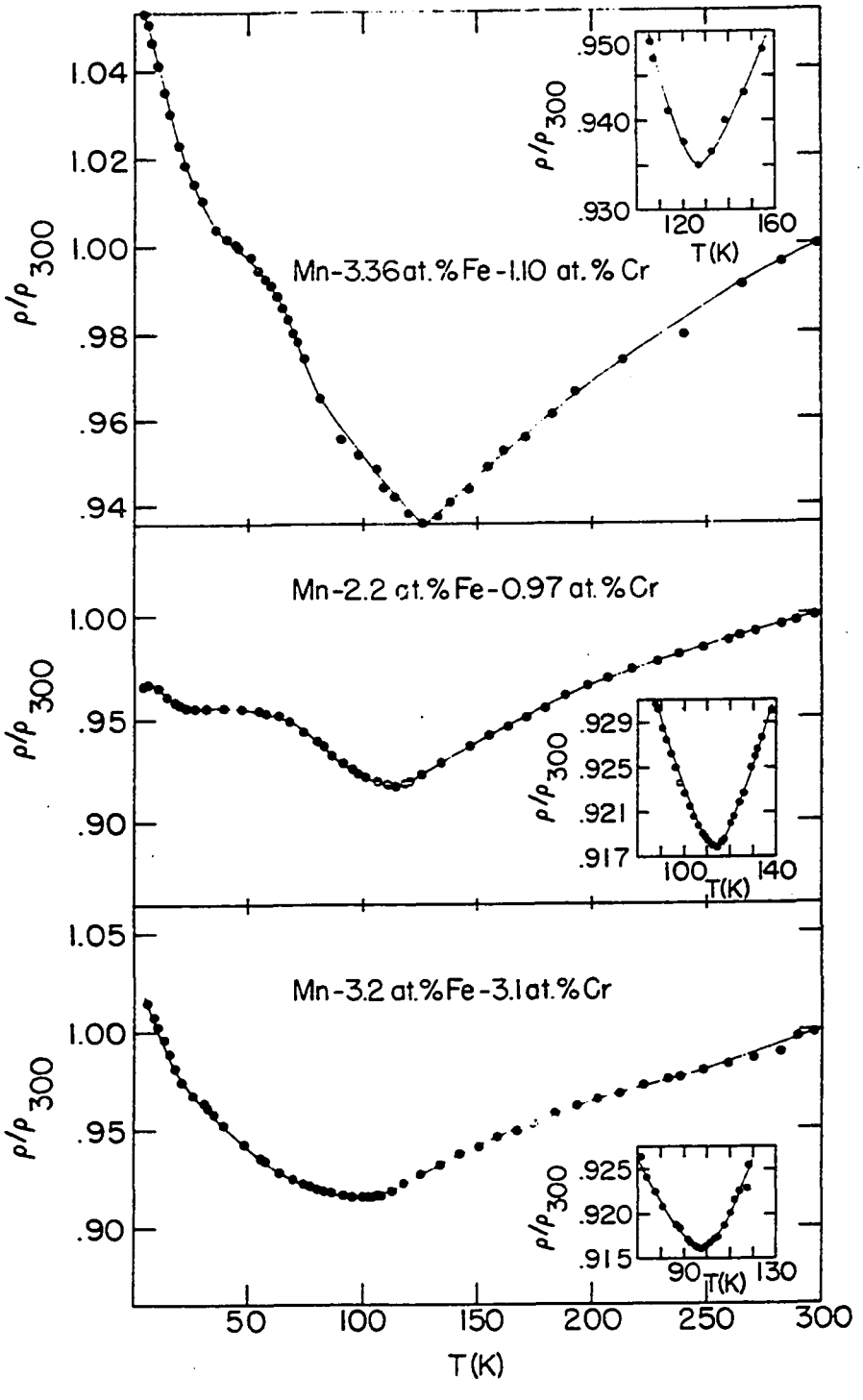

Figure 42. The normalized resistivity for several Mn-Fe-Cr alloys

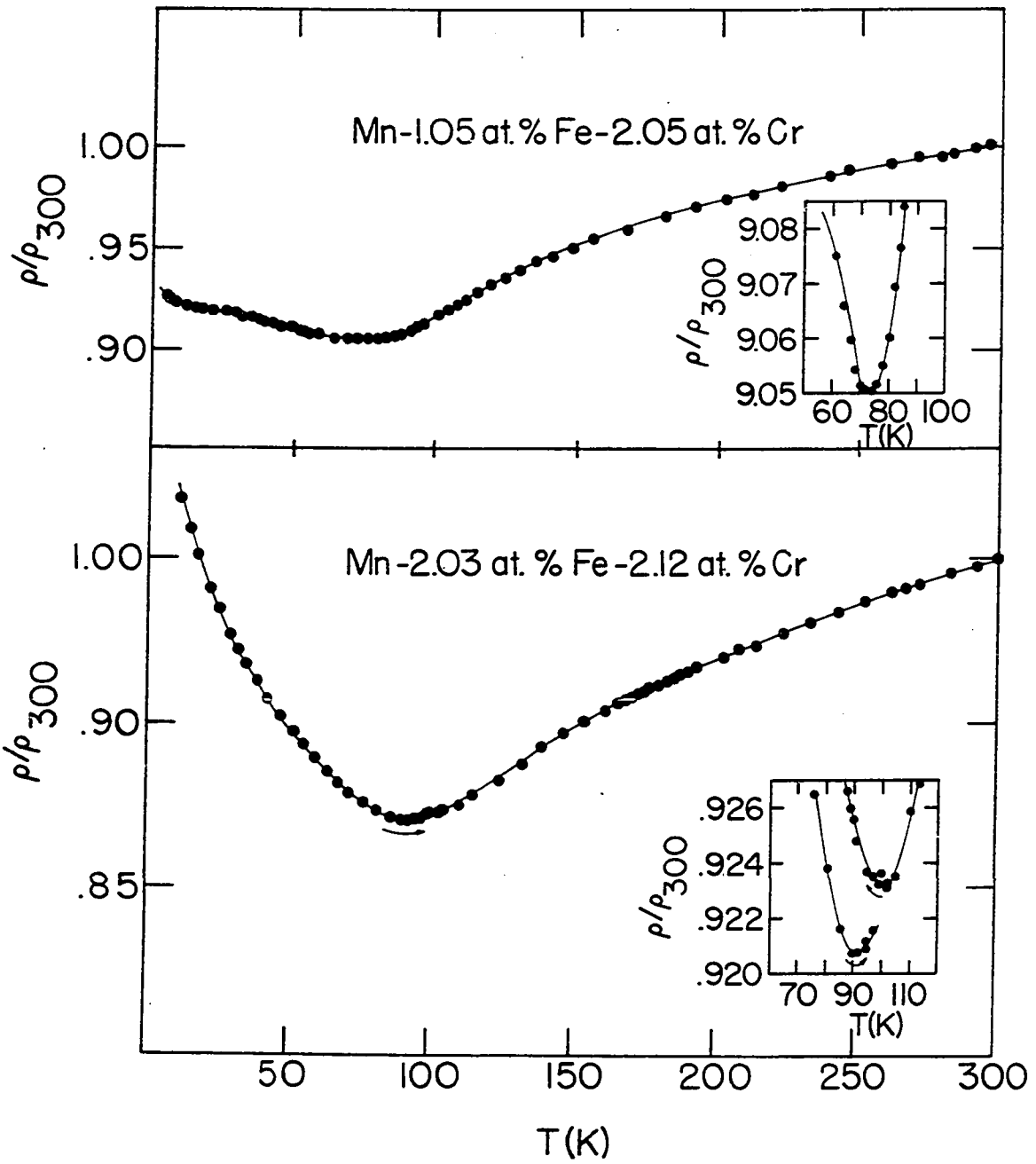

Figure 43. The normalized resistivity for two additional Mn-Fe-Cr alloys

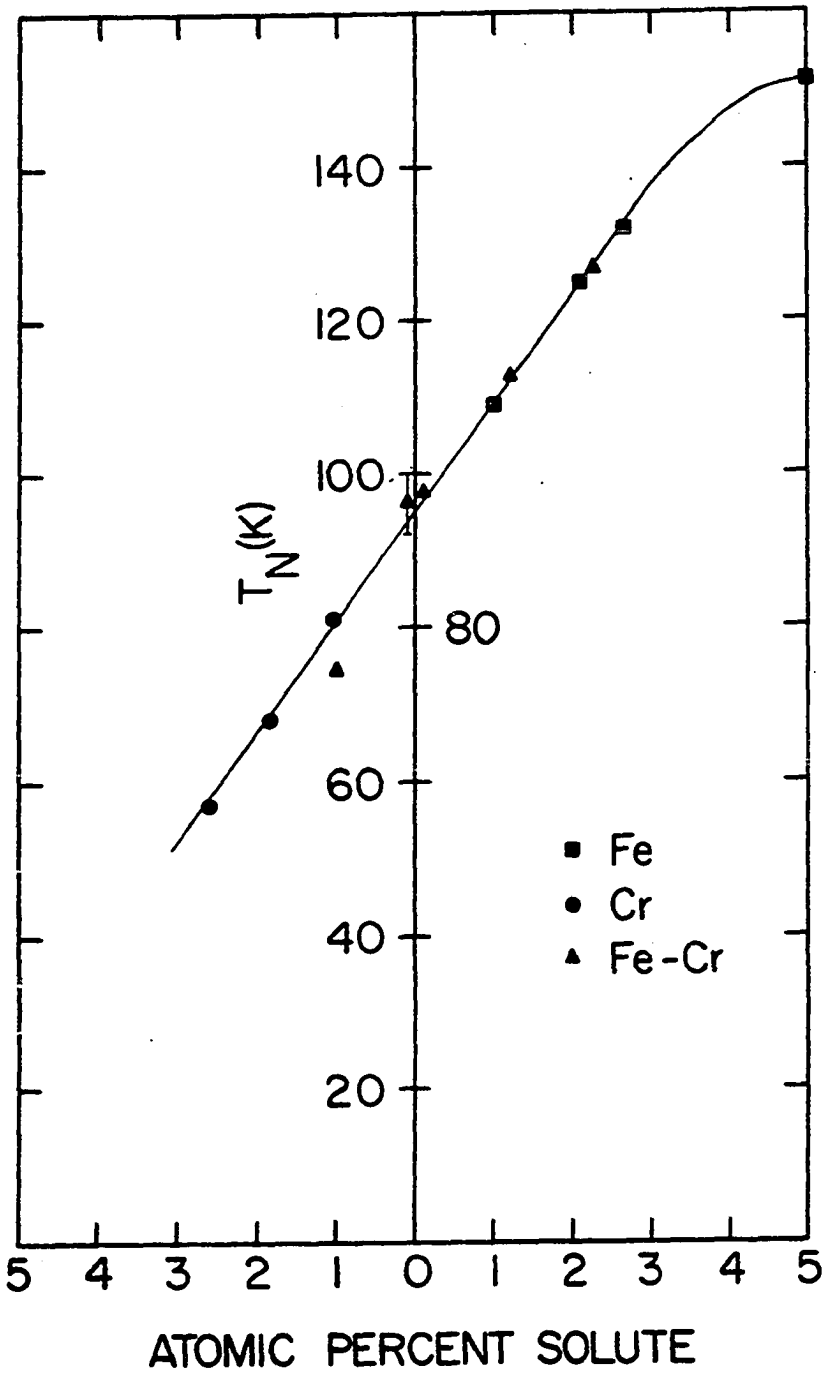

Figure 44. The variation of the Neel temperature as a function of the effective atomic percent solute (the amount of Fe solute minus the amount of Cr solute).

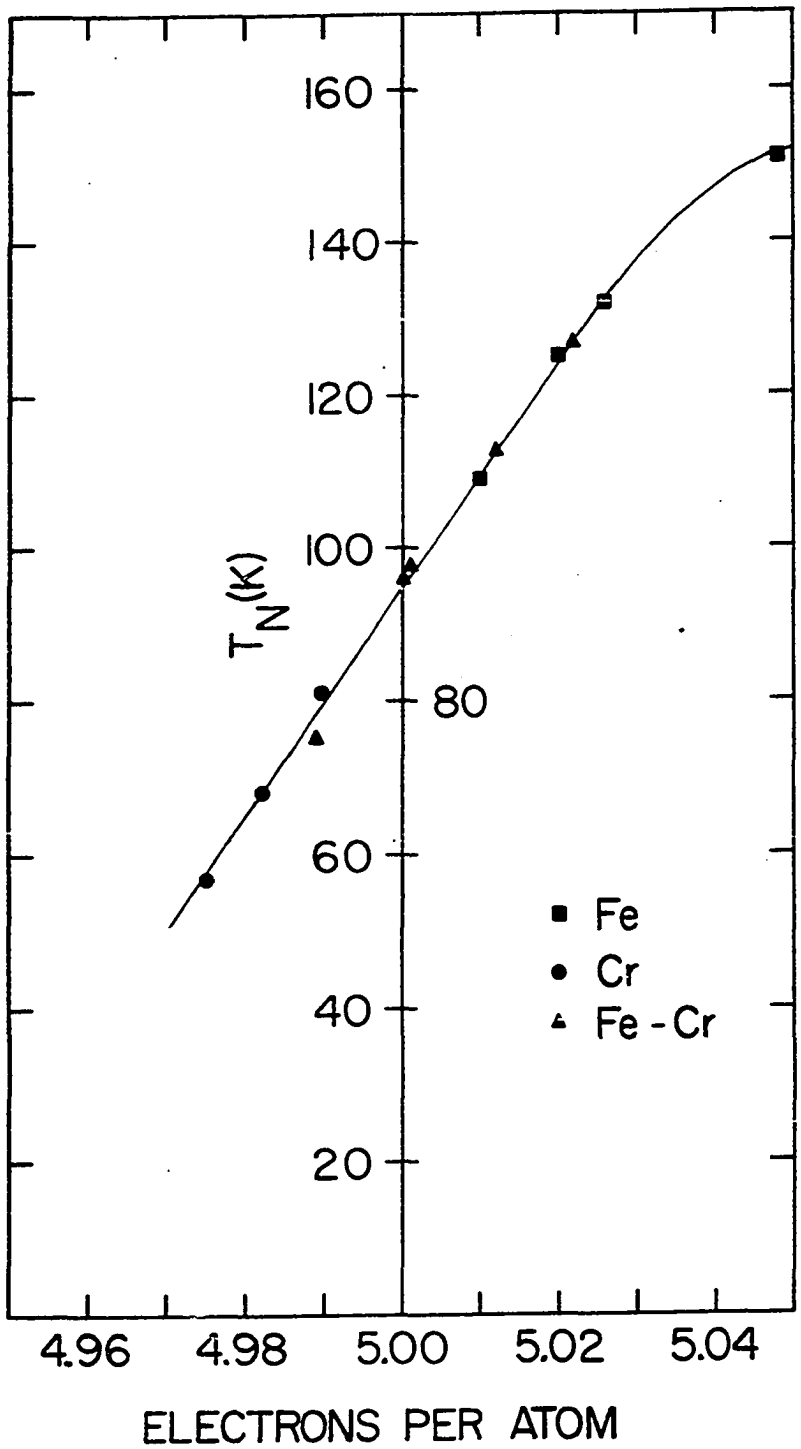

Figure 45. The variation of the Neel temperature as a function of the e/a ratio for the Mn-Fe-Cr alloys

ties contribute.

We may also infer several other conclusions. One is that the change in the lattice constant is not a determining consideration. Although it may reflect a need for the crystal to adjust the intra-atomic distances, this adjustment is most probably an effect rather than a cause. An increased or decreased moment may require a slightly different geometrical arrangement of the Mn atoms. However, this would be a direct result from the number of d-electrons associated with the impurity atoms. It follows that a increased or decreased moment results from the number of d-electrons associated with the impurity atoms and not as a result of a change in the lattice constant. We know that both Fe and Cr decrease the lattice constant, but have very opposite effects on the magnetic moment.

Mn-rich Fe-Ni Alloys Several alloys from this series were studied. They are summarized in Table XI and shown in Figure 46. These alloys were of interest because of the two separate lines that appear in the e/a versus T_N graph (see Figure 23). The determination of where the Neel temperature falls for these alloys should provide additional insight into the AFM ordering.

The normalized electrical resistivity is shown in Figures 47 and 48. The data shows a resistivity minimum after which there is a varying degree of enhancement. No

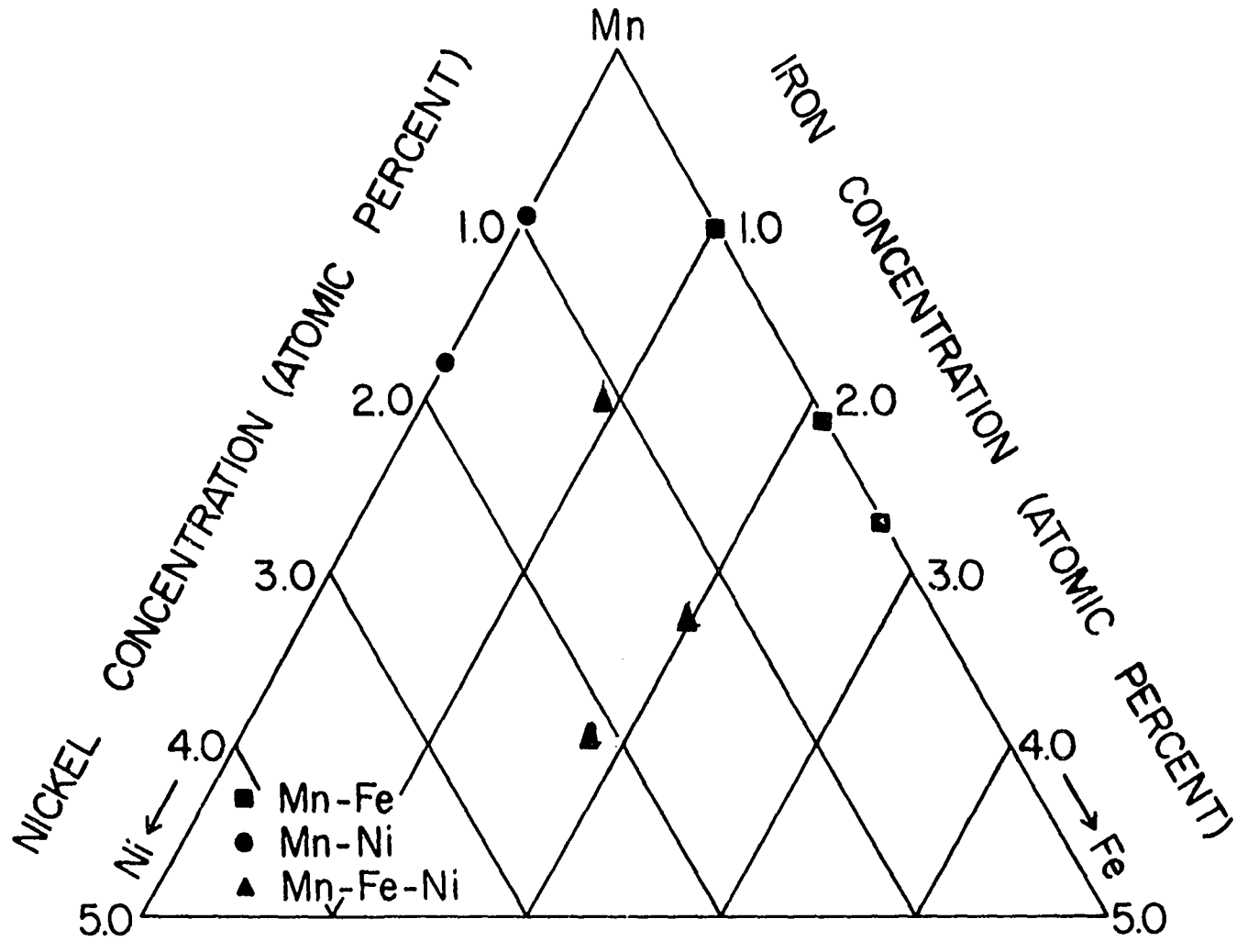

Figure 46. Chemical compositions of the specimens for Mn-Fe-Ni, Mn-Fe and Mn-Ni alloys

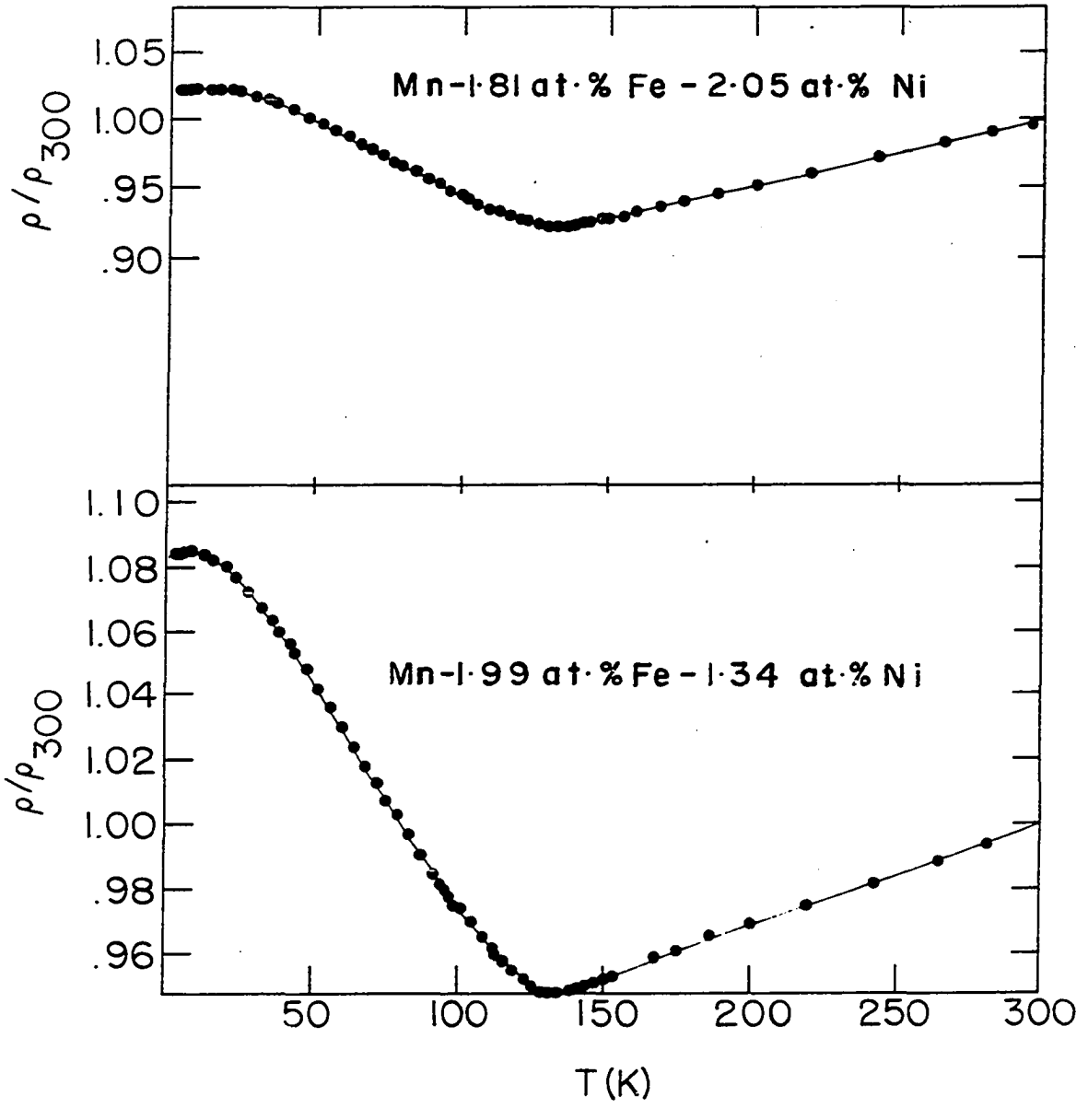

Figure 47. The normalized resistivity for several Mn-Fe-Ni alloys

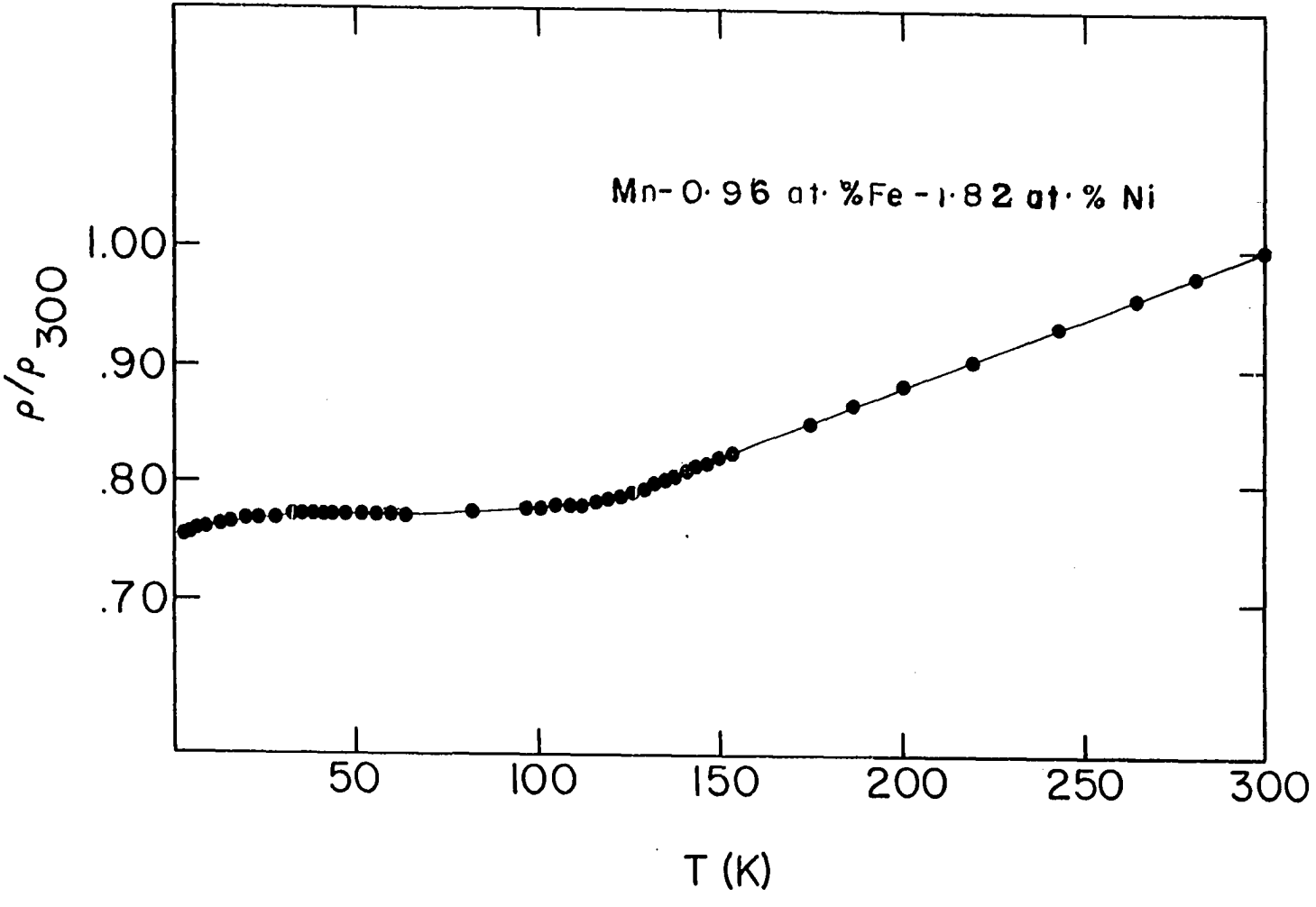

Figure 48. The normalized resistivity for one additional Mn-Fe-Ni alloy

Table XI. Summary of the Mn-Fe—Ni alloys.

		Concentration		
		Fe	Ni	Effective*
Mn-Fe	(1)	0.99	0.0	0.99
	(2)	2.10	0.0	2.10
	(3)	2.7	0.0	2.7
Mn-Ni	(1)	0.0	0.91	0.91
	(2)	0.0	1.78	1.78
Mn-Fe-Ni	(1)	0.96	1.82	2.78
	(2)	0.95	1.11	2.06
	(3)	1.99	1.34	3.33
	(4)	1.81	2.05	3.86

*The effective concentration is the sum total of solute (Fe solute plus Ni solute).

particular pattern of low temperature behavior was observed.

The variation of T_N with the e/a ratio is shown in Figure 49. The data appear to fall between the results for the binary alloys Mn-Fe and Mn-Ni. Moreover, the data do not fall on the curve for the Mn-Co alloys, which might be expected if only the average number of excess d-electrons (above the 5-d electrons of Mn) is important. In Figures 50 and 51 the atomic percent solute versus T_N is shown. It is interesting that the average atomic percent solute falls on the Mn-Co line, while the plot of a Pseudo-Co atomic percent falls close to the Mn-Ni line. Unfortunately, this behavior does not lend itself to any immediate explanation. We will, therefore, defer further comments to the theorists.

Mn-Rich Cr-Ti Alloys We looked at several alloys in this series. The preliminary results showed no tendency toward a resistivity minimum. It is not certain if this indicates that they do not order AFM.

We feel that the ternary alloys have provided some interesting results on the AFM ordering in Mn. With the exception of the Mn-Fe-Cr alloys, no consistent pattern is apparent. The Mn-Fe-Cr alloys have shown that T_N depends on the net number of excess d-electrons. Because this pattern is not followed for the Mn-Fe-Ni alloys, additional consideration must play a part.

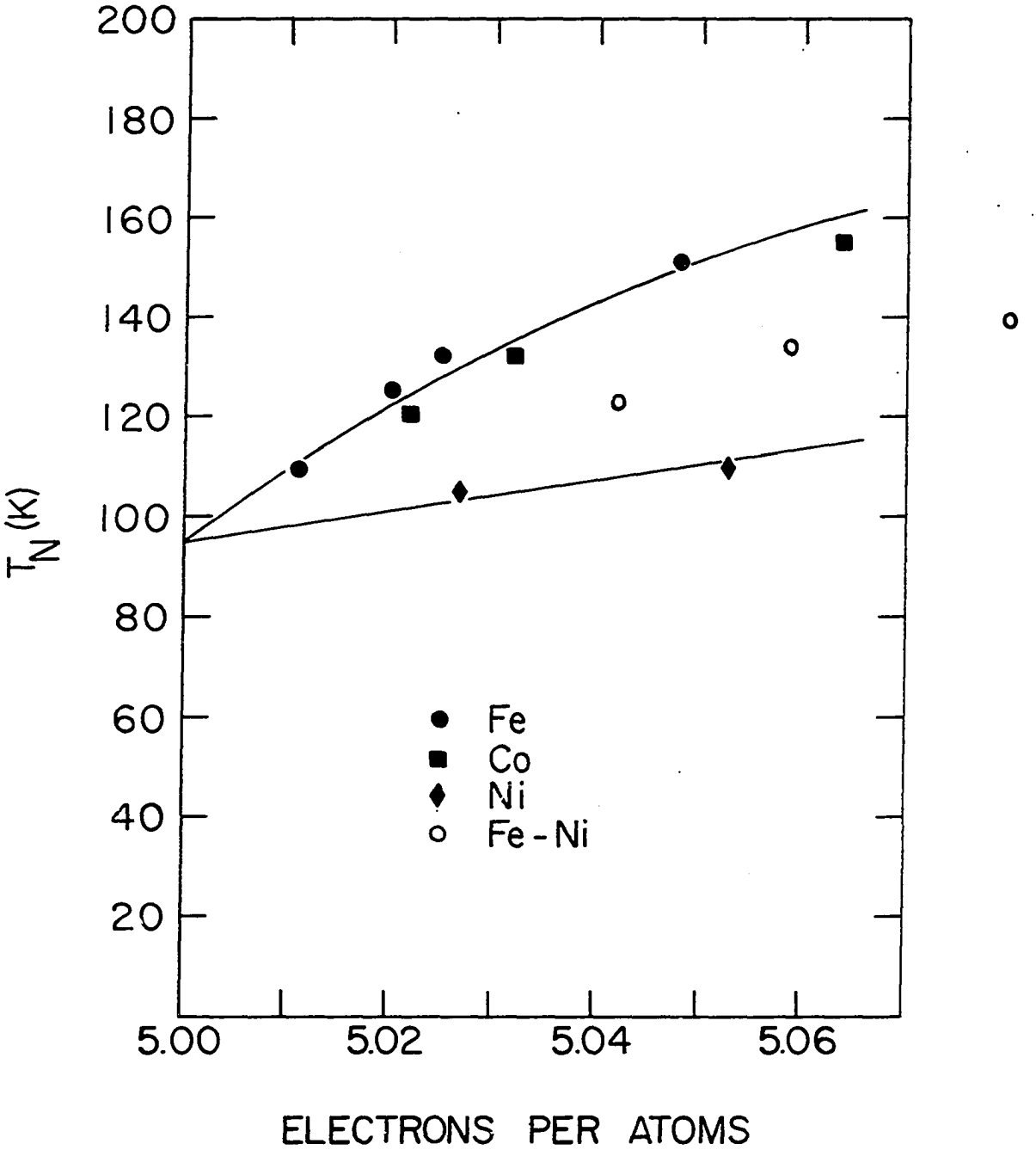

Figure 49. The variation of the Neel temperature as a function of the e/a ratio for the Mn-Fe-Ni alloys

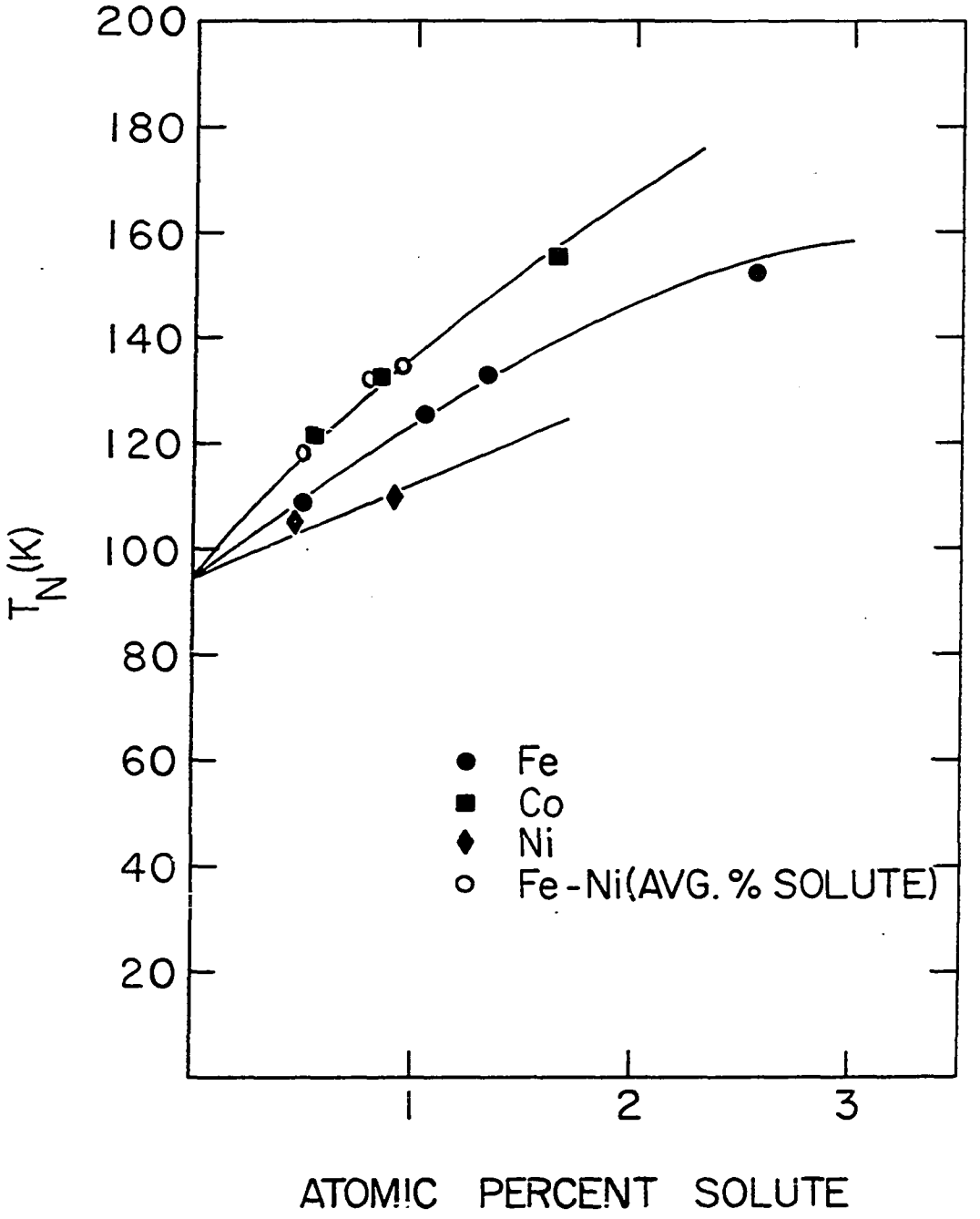

Figure 50. The variation of T_N as a function of atomic percent solute for the Mn-Fe-Ni alloys(avg. % solute)

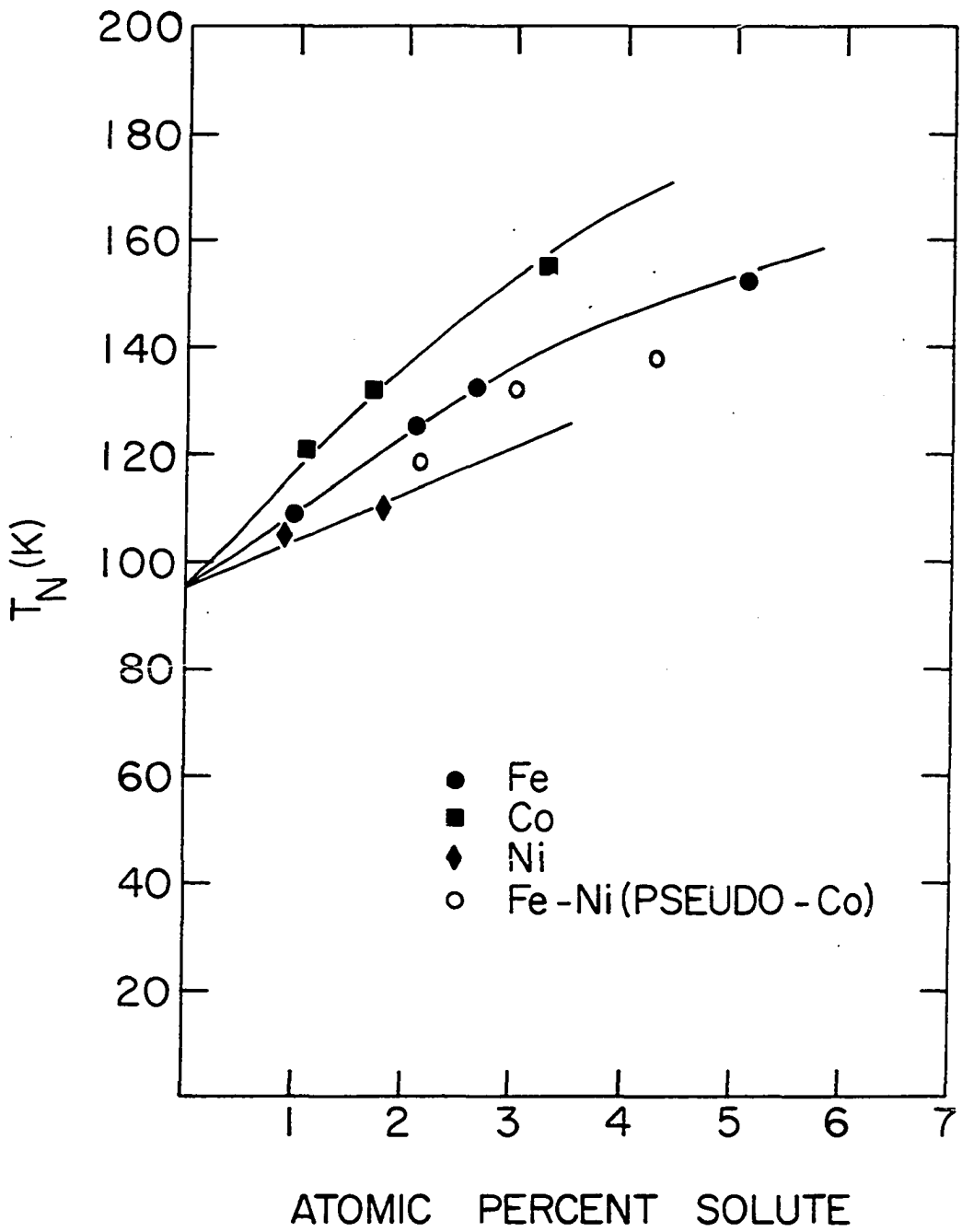

Figure 51. The variation of T_N as a function of atomic percent solute for the Mn-Fe-Ni alloys (pseudo-Co)

CONCLUSION

In this work, we have looked at several binary and ternary alloys of Mn. We observed the following trends:

(a) Impurity elements to the right of Mn with one or more d-electrons greater than Mn, all increased the Neel temperature, while those impurity elements to the left with one or fewer d-electrons, decreased the Neel temperature.

(b) Impurity elements from the second period have a larger change in T_N than elements from the other two periods. This was also true of next-nearest-neighbor impurities in all three periods.

The occurrence of AFM ordering in these alloys appears to be closely linked with the number d-electrons the impurity brings to the host lattice. This would suggest that the AFM ordering may depend on the conduction electrons as a mediator. Also, this behavior lends support to the idea of AFM ordering being determined by an interaction across two pieces of Fermi surfaces, as in the case of Cr. Whether this is the case or not will require additional experimental and theoretical work.

LITERATURE CITED

1. R. V. Bellau and B. R. Coles, Proc. Phys. Soc. (London) 82, 121 (1963).

2. W. Williams and J. Stanford, Phys. Rev. 7, 7 (1973).

3. T. Yamada, J. Phys. Soc. Japan 28,]499 (1970).

4. C. G. Shull and N. K. Wilkinson, Rev. Mod. Phys. 25, 100 (1953).

5. J. S. Kasper and B. W. Roberts, Phys. Rev. 101, 537 (1956).

6. A. Arrott and B. A. Coles, J. Appl. Phys. 32, 515 (1961).

7. A. H. Sully, Manganese, (Academic Press, New York, 1955).

8. R. J. Weiss and K. J. Tauer, J. Phys. Chem. Sol. 4, 135 (1958).

9. A. J. Bradley and J. Thewis, Proc. Roy. Soc. (London) A115, 456 (1927).

10. N. Kunitomi, T. Yamada, Y. Nakai and Y. Fujii, J. Appl. Phys. 40, 1265 (1969).

11. C. P. Gazzara, R. M. Middleton, R. J. Weiss and E. O. Hall, Acta. Cryst. 22, 859 (1967).

12. B. C. Phillips, J. Phys. Soc. Japan 34, 1285 (1973).

13. J. A. Oberteuffer, J. A. Marcus, L. H. Schwartz and G. P. Felcher, Phys. Rev. 2, 670 (1970).

14. T. Yamada, N. Kunitomi, Y. Nakai, D. E. Cox and G. Shirane, J. Phys. Soc. Japan 28, 615 (1970).

15. T. Yamada, J. Phys. Soc. Japan 28, 596 (1969).

16. H. Sato and A. Arrott, J. Phys. Soc. Japan 17, Supp. B-I, 147 (1962).

17. T. Yamada and S. Tazawa, J. Phys. Soc. Japan 28, 610 (1970).

18. V. A. Finkel, Sov. Phys. JEPT 27, 910 (1963).

19. J. A. C. Marples, Phys. Letters 24A, 207 (1967).

20. N. Mori and T. Mitsui, J. Phys. Soc. Japan 25, 82 (1968).

21. G. Ropke, Phys, Stat. Sol. 57, 571 (1973).

22. T. Kohara and K. Asayama, J. Phys. Soc. Japan 34, 670 (1973).

23. S. Itoh and Y. Masuda, J. Phys. Soc. Japan 18, 455 (1963).

24. Y. Masuda, K. Asayama, S. Kobayash and J. Itoh, J. Phys. Soc. Japan 19, 460 (1964).

25. V. Jaccarino and J. A. Seitchick, Bull. Amer. Phys. Soc. 10, 317 (1965).

26. Y. Masuda and T. Taki, J. Phys. Soc. Japan 22, 1645 (1967).

27. V. Jaccarino, M. Peter, and J. H. Wernick, Phys. Rev. Letters 5, 53 (1960).

28. R. G. Scurlock and W. W. R. Stevens, Proc. Intern. Conf. Low Temp. Phys. (London), 1962, P. 197.

29. P. N. Stetsenvo and Y. I. Arksenter, Sov. Phys. 26, 539 (1965).

30. C. W. Kimball, W. C. Phillips, M. V. Nevitt and R. S. Preston, Phys. Rev. 146, 375 (1966).

31. T. Kohara and K. Asayama, J. Phys. Soc. Japan 34, 1105 (1973).

32. J. S. Kasper, Theory of Alloy Phases, (American Society of Metals, Cleveland, Ohio 1956).

33. G. T. Meaden and R. Pelloux-Gervais, Cryogenics 7, 161 (1967).

34. S. Misawa, Phys. Letters 44A, 333 (1973).

35. N. Nagasawa and M. Vchinami, Phys. Letters 42A, 463 (1973).

36. J. Goodenough and S. Legvold, Private Communications.

37. A. Wilson, Theory of Metals (Cambridge University Press, London 1958).

38. K. K. Kelley, J. Amer. Chem. Phys. Soc. 61, 203 (1939).

39. C. H. Shomate, J. Chem. Phys. Soc. 13, 326 1945.

40. C. L. Booth, F. E. Hoare and B. T. Murphy, Proc. Phys. B68, 830 (1955).

41. K. S. Tauer and R. J. Weiss, J. Phys. Chem. Solids 2, 237 (1957).

42. J. C. Taylor, Cryogenics 7, 305 (1967).

43. M. Rosen, Phys. Rev. 165, 357 (1967).

44. D. Griffiths and B. R. Coles, Proc. Phys. Soc. (London) 83, 127 (1963).

45. G. T. Meaden and R. Pelloux-Gervais, Cryogenics, 5, 227 (1965).

46. K. C. Whittaker and P. A. Dziwornooh, J. Low Temp. Phys. 5, 447 (1971).

47. D. Finnemore, J. E. Ostenson and T. F. Stromberg, USAEC Report No. IS-1046, (Ames, Iowa 1964).

48. W. Seward and R. Rosebaum, University of Illinois Technical Report No. C00-1198-441 (1968) (unpublished).

49. H. W. Cooper, A. S. Arrott and H. W. Paxton, J. Appl. Phys. 32, 2506 (1961).

50. W. Williams, M. S. Thesis, Iowa State University (1972) (unpublished).

51. L. Patrick, Phys. Rev. 65, 370 (1953).

52. S. Arajs, Physica Scripta 8, 109 (1973).

53. M. Hansen, Constitution of Binary Alloys (McGraw-Hill Book Co., New York, 1958).

54. J. A. Oberteuffer and J. A. Marcus, Bull. Amer. Phys. 13, 58 (1968).

55. A. W. Overhauser, Phys. Rev. 128, 1437 (1962).

56. A. Blandin, E. Daniel and J. Friedel, Phil. Mag. 4, 180 (1959).

57. E. Daniel, J. Phys. Radium, 20, 769 (1959).

58. A. Blandin and E. Daniel, J. Phys. Chem. Solids 10, 126 (1959).

59. P. A. Fedders and P. C. Martin, Phys. Rev. 143, 245 (1966).

60. M. Shimizu, Private Communications.

61. Y. Suezaki and H. Mori, Progr. Theoret. Phys. 41, 1177 (1969).

ACKNOWLEDGEMENT

I wish to express my appreciation to Dr. John Stanford for his help and guidance during this work. Also to Mr. F. Schmidt, and other members of the Metal Development Division of Ames Lab for providing the alloys used in this study. A special thanks to Mr. R. Bachman, and members of his group for their efforts in determining the chemical analyses of these alloys.

Finally, I would like to express a special not of appreciation to my wife Lee, without whose efforts in typing this manuscript, as well as her aid in preparing some of the figures, this work would not have been completed.